



# THE UNIVERSITY *of* EDINBURGH

This thesis has been submitted in fulfilment of the requirements for a postgraduate degree (e.g. PhD, MPhil, DClinPsychol) at the University of Edinburgh. Please note the following terms and conditions of use:

This work is protected by copyright and other intellectual property rights, which are retained by the thesis author, unless otherwise stated.

A copy can be downloaded for personal non-commercial research or study, without prior permission or charge.

This thesis cannot be reproduced or quoted extensively from without first obtaining permission in writing from the author.

The content must not be changed in any way or sold commercially in any format or medium without the formal permission of the author.

When referring to this work, full bibliographic details including the author, title, awarding institution and date of the thesis must be given.

**Understanding interactions between  
*Ramularia collo-cygni* and barley leaf  
physiology to target improvements in  
host resistance and disease control  
strategy:**

**Effects of latent and symptomatic stages of  
*Ramularia* leaf spot disease development on  
leaf physiology and yield formation**

**Clarinda Molly Rose Burrell**

**Thesis submitted to the University of Edinburgh for  
the degree of Doctor of Philosophy**

**December 2021**



**THE UNIVERSITY  
*of* EDINBURGH**

## **Declaration**

I declare that this thesis was composed by myself and that the work contained herein is my own, except as acknowledged by means of references. This thesis has not been submitted for any other degree or professional qualification.

Clarinda Molly Rose Burrell

# Contents

List of figures .....	i
List of tables.....	vi
List of abbreviations .....	ix
Abstract .....	x
Lay summary .....	xiii
Acknowledgements .....	xv
<b>Chapter 1 General introduction .....</b>	<b>1</b>
Barley .....	1
Barley pests and diseases .....	2
Physiological responses of plants to fungal pathogens .....	3
Yield formation in barley .....	7
<i>Ramularia collo-cygni</i> .....	8
Project rationale and objectives .....	16
<b>Chapter 2 Physiological responses of barley seedlings to infection with</b>	
<b><i>R. collo-cygni</i> fungus .....</b>	<b>20</b>
Introduction.....	20
Photosynthetic responses of plants to pathogens.....	21
Chlorophyll fluorescence .....	23
Chapter objectives .....	26
Materials and methods .....	27
Overview.....	27
Plant material and growth conditions .....	28
Inoculation of plants with <i>R. collo-cygni</i> .....	29
Experimental design .....	30
Experimental series 1 .....	31
Chlorophyll fluorescence imaging .....	31
Visual assessment of disease progress .....	33
DNA extraction and quantification .....	33
Experimental series 2 .....	34
Chlorophyll fluorescence imaging .....	34
Transect analysis .....	35

Infra-red gas analysis .....	36
Data and statistical analysis.....	37
Results .....	38
Experimental series 1 .....	38
Fungal growth <i>in planta</i> .....	38
Visible symptom development and green leaf area.....	39
Chlorophyll fluorescence imaging .....	43
Experimental series 2 .....	53
Visible symptom development and green leaf area.....	53
Chlorophyll fluorescence imaging .....	55
Combined Infra-red gas analysis and chlorophyll fluorescence .....	65
Analysis of transects across leaves .....	67
Discussion .....	73
<b>Chapter 3 Relative impact of different <i>R. collo-cygni</i> life phases on barley yield .....</b>	<b>79</b>
Introduction.....	79
Effects of fungal pathogens on crop growth and yield .....	79
Chapter objectives .....	82
Materials and methods .....	83
Site and experimental design.....	83
Measurements .....	85
Calculations and statistical analysis.....	89
Results .....	92
Disease severity and % green area .....	92
Fungal growth <i>in planta</i> .....	96
Crop biomass.....	98
Chlorophyll fluorescence .....	100
Healthy area light interception .....	101
Crop yield.....	103
Yield components.....	103
Radiation use efficiency .....	103
Predicted and observed yield loss.....	104

Discussion .....	106
<b>Chapter 4 Effects of varying rates of leaf senescence on RLS disease development.....</b>	<b>112</b>
Introduction.....	112
Chapter objectives .....	114
Materials and methods .....	115
Overview.....	115
Preparation and foliar application of pH 6.5 cytokinin (6-Benzylaminopurine) solution.....	116
Measurement of relative leaf-chlorophyll content.....	117
Data and statistical analysis.....	117
Results .....	119
Senescence and visible symptom progression .....	119
Relative chlorophyll content .....	119
Green Leaf Area.....	120
RLS symptoms.....	121
Fungal growth <i>in planta</i> .....	124
<i>R. collo-cygni</i> DNA levels in leaves during the experiment .....	124
<i>R. collo-cygni</i> DNA levels in leaves at the end of the experiment ...	126
Discussion .....	128
<b>Chapter 5 General discussion .....</b>	<b>133</b>
References .....	139
Appendix 1 .....	157

## List of figures

Figure 1 Photomicrograph of a conidiophore of <i>R. collo-cygni</i> . Extracted from Walters et al. (2008).....	9
Figure 2 Typical RLS symptoms. Extracted from Havis <i>et al.</i> , 2015. ....	10
Figure 3 Global distribution of RLS. Countries identified by date of first report of the disease (Spencer et al., 2019). Licensed under CC BY.....	12
Figure 4 Lifecycle of <i>R. collo-cygni</i> on barley. Adapted from Havis et al. (2015). ....	13
Figure 5 Diagram of an example protocol for chlorophyll fluorescence quenching analysis during photosynthetic induction and steady state photosynthesis. Adapted from Scholes & Rolfe (2009).....	24
Figure 6 Clear plastic tubes used to keep plants upright and avoid damage during sampling.....	30
Figure 7 Light regime for chlorophyll fluorescence measurements in experimental series 1. PAR = Photosynthetically active radiation ( $\mu\text{mol m}^{-2} \text{s}^{-1}$ ). ....	32
Figure 8 Light regime for chlorophyll fluorescence measurements in experimental series 2. PAR = Photosynthetically active radiation ( $\mu\text{mol m}^{-2} \text{s}^{-1}$ ). ....	35
Figure 9 <i>R. collo-cygni</i> DNA in second leaves of barley seedlings cv. Concerto during disease development. Rcc = plants inoculated with <i>R. collo-cygni</i> mycelial suspension grown in Potato Dextrose Broth (PDB). Broth = plants inoculated with a control treatment of PDB. Water = plants inoculated with a control treatment of sterile distilled water. Black vertical line to the right of the graph represents the least significant difference (l.s.d., $P=0.05$ ) for Treatment. Days after inoculation from a two-way ANOVA with inoculation treatment and time as factors. Note that symbols for Broth treatment are hidden by those for Water. ....	39
Figure 10 Visual disease progress over time. A) RLS lesion development and B) Green leaf area (both as percentages of total measured leaf area). Second leaves of barley cv. Concerto seedlings inoculated with <i>R. collo-cygni</i> (Rcc) and control leaves sprayed with water or potato dextrose broth. Black	

vertical lines to the right of the graphs represent the least significant difference (l.s.d., $P=0.05$ ) for Treatment.Days after inoculation from a two-way ANOVA with inoculation and time as factors. Symbols for Broth are hidden by those for Water. ....	40
Figure 11 Photographs of second leaves of barley cv. Concerto seedlings inoculated with <i>R. collo-cygni</i> (Rcc) and control leaves sprayed with water or potato dextrose broth. Photographs taken at 8, 13 and 25 days post inoculation (d.p.i.).....	42
Figure 12 Chlorophyll fluorescence parameters: A) Maximal efficiency of PSII (Fv/Fm); B) Non-photochemical quenching (NPQ); C) Operating efficiency of PSII ( $\phi$ PSII); D) Electron Transport Rate (ETR) at steady state photosynthesis ( $230 \mu\text{mol m}^{-2}\text{s}^{-1}$ PAR), measured in second leaves of barley seedlings over an infection time course. ....	45
Figure 13 Photosynthetic operating efficiency ( $\Phi$ PSII) measured during photosynthetic induction of dark-adapted leaves with an actinic irradiance of $230 \mu\text{mol m}^{-2} \text{s}^{-1}$ PAR. Each point is the mean of 4 (8 dpi), 5 (13 dpi) and 3 (25 dpi) replicates. Black vertical lines to the right of the graphs represent the least significant difference (l.s.d., $P=0.05$ ) for Time.Treatment from a repeated measures ANOVA.....	49
Figure 14 Non-photochemical quenching (NPQ) measured during photosynthetic induction of dark-adapted leaves with an actinic irradiance of $230 \mu\text{mol m}^{-2} \text{s}^{-1}$ PAR. Each point is the mean of 4 (8 dpi), 5 (13 dpi) and 3 (25 dpi) replicates. Black vertical lines to the right of the graphs represent the least significant difference (l.s.d., $P=0.05$ ) for Time.Treatment from a repeated measures ANOVA.....	50
Figure 15 Electron transport rate (ETR) measured during photosynthetic induction of dark-adapted leaves with an actinic irradiance of $230 \mu\text{mol m}^{-2} \text{s}^{-1}$ PAR. Each point is the mean of 4 (8 dpi), 5 (13 dpi) and 3 (25 dpi) replicates. Black vertical lines to the right of the graphs represent the least significant difference (l.s.d., $P=0.05$ ) for Time.Treatment from a repeated measures ANOVA.....	51

Figure 16 <i>Ramularia</i> leaf spot severity (%) and % green leaf area (GLA) of second leaves of barley seedlings cv. Fairing over the time course of an infection. Values are means $\pm$ SEM of 6 replicates. Treatments: Rcc = plants inoculated with <i>R. collo-cygni</i> mycelial suspension grown in Potato Dextrose Broth (PDB). Broth = plants inoculated with a control treatment of PDB. Water = plants inoculated with a control treatment of sterile distilled water. Symbols for broth treated plants are hidden by those for water controls. ....	54
Figure 17 Maximal efficiency of PSII (Fv/Fm). N = at least 5. ....	56
Figure 18 $\Phi$ PSII at steady state photosynthesis. At 10 d.p.i. n = at least 4. At 18 d.p.i. n = 6 for both light intensities. At 26 d.p.i. n = at least 5 for 230 $\mu\text{mol m}^{-2} \text{s}^{-1}$ and at least 4 for 530 $\mu\text{mol m}^{-2} \text{s}^{-1}$ . ....	58
Figure 19 NPQ at steady state photosynthesis. At 10 d.p.i. n = at least 4. At 18 d.p.i. n = 6 for both light intensities. At 26 d.p.i. n = at least 5 for 230 $\mu\text{mol m}^{-2} \text{s}^{-1}$ and at least 4 for 530 $\mu\text{mol m}^{-2} \text{s}^{-1}$ . ....	59
Figure 20 ETR at steady state photosynthesis. At 10 d.p.i. n = at least 4. At 18 d.p.i. n = 6 for both light intensities. At 26 d.p.i. n = at least 5 for 230 $\mu\text{mol m}^{-2} \text{s}^{-1}$ and at least 4 for 530 $\mu\text{mol m}^{-2} \text{s}^{-1}$ . ....	60
Figure 21 Operating efficiency of PSII ( $\Phi$ PSII). Actinic light applied at 230 $\mu\text{mol m}^{-2} \text{s}^{-1}$ for 1507 seconds, then increased to 530 $\mu\text{mol m}^{-2} \text{s}^{-1}$ . Black vertical lines to the right of the graphs represent the least significant difference (l.s.d., $P=0.05$ ) for Time.Treatment from a repeated measures ANOVA (displayed for each light intensity where applicable). ....	62
Figure 22 Experimental series 2. Quenching. NPQ. Actinic light applied at 230 $\mu\text{mol m}^{-2} \text{s}^{-1}$ for 1507 seconds, then increased to 530 $\mu\text{mol m}^{-2} \text{s}^{-1}$ . Black vertical lines to the right of the graphs represent the least significant difference (l.s.d., $P=0.05$ ) for Time.Treatment from a repeated measures ANOVA (displayed for each light intensity where applicable). ....	63
Figure 23 Experimental series 2. Quenching. ETR. Actinic light applied at 230 $\mu\text{mol m}^{-2} \text{s}^{-1}$ for 1507 seconds, then increased to 530 $\mu\text{mol m}^{-2} \text{s}^{-1}$ . Black vertical lines to the right of the graphs represent the least significant difference (l.s.d., $P=0.05$ ) for Time.Treatment from a repeated measures ANOVA (displayed for each light intensity where applicable). ....	64

Figure 24 Leaves showing positions of upper and lower transects at 18 days and 26 days post-inoculation (d.p.i.).	68
Figure 25 Chlorophyll fluorescence measured across leaf transects. Exemplary figure. Full data is presented in Appendix 1. The photographs show the location of upper and lower leaf transects. The graphs show chlorophyll fluorescence parameter values along the transects. The left-hand panels show parameters for transects across lesions and across nearby non-symptomatic areas of infected leaves. The right-hand panels show parameters for transects across lesions and across equivalent areas of control leaves. Measurements were taken at 18 and 26 days after inoculation. Replicates categorised as group A = small, developing lesion. Replicates categorised as Group B = lesion at more advanced stage of development.	71
Figure 26 Diagrammatic representation of areas in each plot sampled for measurements of biomass, absolute area and % green area (GA). The three colours represent individual sampling dates. Each line represents a 0.5 m length of plants from rows 3 and 4.	86
Figure 27 Diagram showing the fractions of barley shoots used for determination of absolute area and % green area (GA).	87
Figure 28 RLS symptom development and green leaf area in field grown barley cv Concerto.	94
Figure 29 <i>R. collo-cygni</i> DNA (ng) in F-1 leaves of field-grown barley cv Concerto. Each point represents the mean of 4 replicates for fungicide treated and inoculated plots and 3 replicates for untreated plots (10 plants per replicate). The black bar to the right of the graph represents the l.s.d. for Treatment.Days after sowing from an analysis of variance.	97
Figure 30 Canopy biomass of field-grown barley cv Concerto. Each point represents the mean of 4 replicates for fungicide treated and inoculated plots and 3 replicates for untreated plots. The black line to the right of the graph represents the l.s.d. (5% level) for the Treatment.Days after sowing interaction from an analysis of variance.	99

Figure 31 Maximal efficiency of PSII (Fv/Fm) measured on F-1 leaves of field-grown barley. Each point represents the mean of 4 replicates for fungicide treated and inoculated plots and 3 replicates for untreated plots (5 plants per replicate). .....	100
Figure 32 Reduction in yield of inoculated and untreated plots relative to fungicide treated plots. Blue columns = observed reduction. Red columns = reduction predicted from the loss of green leaf area and healthy area PAR interception. Each column represents the average of 4 replicates (inoculated) and 3 replicates (untreated). Error bars are $\pm$ SEM. ....	105
Figure 33 Effects of cytokinin and additional fertiliser treatments on leaf senescence and RLS symptom development on barley cv Fairing seedlings over time (days after inoculation). <b>A</b> ) Relative leaf chlorophyll content (SPAD units): average value of measurements taken in distal and basal leaf sections. <b>B</b> ) Green Leaf Area (%) <b>C</b> ) Leaf area covered by RLS lesions (%). Points are means of 5 replicates. All data is from second leaves of barley seedlings. Vertical black lines to the right of the graphs represent the least significant difference (l.s.d. 5%) value for the interaction between cytokinin, fertiliser treatment, and time (days after inoculation) from a repeated measures ANOVA.....	123
Figure 34 <i>R. collo-cygni</i> DNA (ng) in second leaves of barley seedlings cv Fairing over time. From an experiment to compare the effects of cytokinin and fertiliser treatments on green leaf area retention and RLS disease development. Each point shows the average of 5 replicates. The black, vertical bar to the right of the graph represents the least significant difference (l.s.d. 5%) for the interaction between cytokinin treatment, fertiliser treatment and time from an analysis of variance.....	125
Figure 35 <i>R. collo-cygni</i> DNA (ng) in second leaves of barley seedlings Cv Fairing at 33 days after inoculation. Bars show average of 5 replicates. The black, vertical line to the right of the graph represents the l.s.d. (3.39) for Cytokinin.Fertiliser from a two-way ANOVA. The star above treatment group 1 (no cytokinin or fertiliser treatment) indicates that the plants in this treatment group had significantly higher <i>R. collo-cygni</i> DNA levels than those	

in any of the other treatment groups ( $P = 0.025$ ), when analysed using one-way ANOVA. ....	127
---	-----

## List of tables

Table 1 Chlorophyll fluorescence parameters used in this project .....	25
Table 2 Mean values for <i>R. collo-cygni</i> DNA quantity (ng/μl) in second leaves of barley seedlings during disease development. ....	38
Table 3 ANOVA analysis results from a two-way ANOVA with inoculation treatment and time after inoculation as factors for <i>R. collo-cygni</i> DNA quantity in second leaves of barley seedlings during disease development. ....	38
Table 4 Mean % leaf area covered by lesions and mean % green leaf area (GLA) over an infection time course. ....	41
Table 5 Mean values for chlorophyll fluorescence parameters at steady state ( $230 \mu\text{mol m}^{-2} \text{s}^{-1}$ ), measured in second leaves of barley seedlings over an infection time course. ....	43
Table 6 ANOVA results for comparison of chlorophyll fluorescence at steady state. ....	46
Table 7 P values from repeated measures ANOVA during photosynthetic induction of dark-adapted plants over an infection time course. ....	48
Table 8 P values for chlorophyll fluorescence parameters at steady state photosynthesis. ....	55
Table 9 ANOVA table repeated measures experiment 2. ....	61
Table 10. CO <sub>2</sub> flux. Ramularia leaf spot symptom severity (% of measured leaf area) and net CO <sub>2</sub> flux ( $\mu\text{mol CO}_2 \text{m}^{-2} \text{s}^{-1}$ ) with days after inoculation and measurement irradiance ( $\mu\text{mol PAR m}^{-2} \text{s}^{-1}$ ). ....	66
Table 11 ETR. Means and P values from one-way ANOVA at each time point. Ramularia leaf spot symptom severity (% of measured leaf area) and ETR with days after inoculation and measurement irradiance ( $\mu\text{mol PAR m}^{-2} \text{s}^{-1}$ ). ....	66
Table 12 ΦPSII. Means and P values from one-way ANOVA at each time point. Ramularia leaf spot symptom severity (% of measured leaf area) and	

$\Phi$ PSII with days after inoculation and measurement irradiance ( $\mu\text{mol PAR m}^{-2} \text{ s}^{-1}$ ). .....	67
Table 13 Lesion categories .....	69
Table 14 Direction and scale of change in fluorescence variables within the visible lesions on infected leaves compared to regions outside the lesion on the same leaves. Variables decreased ( $\downarrow$ ) or increased ( $\uparrow$ ) with the number of arrows indicating the relative scale from small ( $\downarrow$ ) to major ( $\downarrow\downarrow\downarrow$ ) change. $\sim$ indicates a possible marginal or uncertain effect. Where no effect was observed the cell has been left empty. Lesions are identified by leaf replicate number (R1, R2 etc) and whether the lesion was on the upper (U) or lower (L) transect. Variables are: Fv/Fm, maximal photochemical efficiency; NPQ, non-photochemical quenching; $\Phi$ PSII, operating photochemical efficiency; ETR, Electron Transport Rate.....	71
Table 15 Field experiment treatments.....	84
Table 16 Analysis of variance results for disease severity and % green area. P values and l.s.d. values from analysis of variance at each time point.....	95
Table 17 Analysis of Variance results for an analysis of the quantity of <i>R. collo-cygni</i> DNA in F-1 leaves of field-grown barley cv Concerto. L.s.d at 5% level. ....	98
Table 18 Analysis of variance results for above-ground biomass of field-grown barley cv Concerto. ....	99
Table 19 Analysis of variance results for maximal efficiency of PSII (Fv/Fm) measured on F-1 leaves of field-grown barley. ....	101
Table 20 Treatment means and analysis of variance results for the fraction of incident PAR that was intercepted by healthy (green) tissue of field grown barley plants cv Concerto at 3 time points during grain filling. ....	102
Table 21 Treatment means and analysis of variance results for total PAR ( $\text{MJ m}^{-2}$ ) intercepted by healthy (green) tissue of field grown barley plants cv Concerto during grain filling. ....	102
Table 22 Yield components. l.s.d. values are for 5% level.....	103
Table 23 Senescence experiment treatments.....	118

Table 24 P values from repeated measures ANOVA of effects of cytokinin treatment (yes or no), fertiliser treatment (yes or no) and time (days after inoculation) on the relative chlorophyll content (SPAD readings), % Green Leaf Area, and % area of leaf covered by RLS lesions of second leaves of barley seedlings N = 5. ....	123
Table 25 ANOVA results for fungal growth <i>in planta</i> . P values and l.s.d. values from ANOVA with cytokinin treatment (yes or no, fertiliser treatment (yes or no) and time (days after inoculation) as factors. N = 5. From an experiment to compare the effects of cytokinin and fertiliser treatments on green leaf area retention and RLS disease development. ....	126
Table 26 ANOVA results for fungal DNA in plants at the end of the experiment. P values from a two-way ANOVA including interaction between fertiliser and cytokinin treatment. N = 5.....	128

## List of abbreviations

Abbreviation	Definition
ATP	Adenosine triphosphate
ETR	The rate of photosynthetic electron transport
Fv/Fm	The maximal efficiency of PSII, or maximum quantum yield of PSII
MGW	Mean grain weight
MLO	Mildew resistance locus O
NADPH	Reduced nicotinamide adenine dinucleotide phosphate
NPQ	Nonphotochemical quenching
PSII	Photosystem II
RI	Radiation interception
RLS	Ramularia leaf spot
RUE	Radiation use efficiency
$\Phi$ PSII	The operating efficiency of Photosystem II (PSII)

## Abstract

Ramularia Leaf Spot (RLS) is an increasingly problematic disease of barley. Control options are limited as the causal fungus, *Ramularia collo-cygni*, has developed resistance to several of the major fungicide groups. Developing new methods for controlling this disease is therefore a priority. *R. collo-cygni* can grow systemically in barley plants from infected seed, without inducing visible symptoms. In the field, visible symptoms normally only appear after flowering. The relative contribution of the latent and symptomatic stages of the fungal lifecycle to reduction in barley yield is not currently known with any certainty. Two possibilities are that the effect of asymptomatic infection on pre-flowering photosynthetic activity, and the development of grain sink capacity, plays an important role; or that reduction in photosynthetic activity during grain filling, resulting from lesion development and loss of green leaf area, is the predominant factor. This research aimed to increase our understanding of the impact of different phases of the fungal lifecycle on barley photosynthesis and yield formation, to better target host resistance and disease control strategies.

Controlled environment and field experiments were used to determine the relative effects of asymptomatic and symptom-expressing phases of *R. collo-cygni* infection on photosynthesis and yield formation in spring barley. In controlled environment experiments leaf photosynthetic activity was measured in seedlings inoculated with suspensions of *R. collo-cygni* mycelia. Measurements were made before and after visible symptom development using Infra-Red Gas Analysis (IRGA), chlorophyll fluorescence analysis and chlorophyll fluorescence imaging. No reduction in photosynthetic activity was observed in leaves infected with *R. collo-cygni*, compared to those of non-

infected leaves, during the latent phase of infection. After the appearance of visible symptoms, photosynthetic activity within lesions reduced as the lesions developed. However, this did not lead to reductions in photosynthetic activity when measured across the whole leaf area, suggesting that for there to be a significant effect of disease on whole leaf photosynthetic activity, visible symptoms must develop into mature lesions and coalesce to cover larger areas of the leaf surface.

In field experiments plots were treated with a full fungicide regime, left untreated, or inoculated with *R. collo-cygni* and treated with fungicide to which *R. collo-cygni* is resistant (the latter as a precaution against lack of natural RLS disease that year and/or other diseases developing on untreated plots). RLS was the only disease of significance that developed in untreated or inoculated plots. Symptoms first appeared after flowering, around Zadoks Growth Stage 72. Fungicide-treated plots remained free of disease.

Chlorophyll fluorescence analysis of field plants showed no effect of infection on the maximum quantum efficiency of Photosystem II ( $F_v/F_m$ ) before visible symptom development, consistent with results from controlled environment experiments. Grain yield of untreated and fungicide-treated plots was predicted from fixed common values of radiation use efficiency (RUE) and utilisation of soluble sugar reserves, and measured values of post-flowering healthy (green) leaf area light interception. Grain yields predicted from the difference in post-flowering light interception between fungicide-treated plants and untreated or inoculated plants displaying symptoms of RLS were comparable with the measured yield response to fungicide. This suggests that yield loss to RLS is primarily associated with a reduction in light capture during grain filling, resulting from lesion development and loss of green leaf area.

Results from controlled environment and field experiments suggested that symptom expression was associated with leaf senescence. Further controlled environment experiments tested this relationship by using treatments to vary the onset and rate of leaf senescence. Seedlings that were treated with

cytokinin to delay senescence after inoculation with suspensions of *R. collo-cygni* mycelia developed fewer lesions than control plants. Fungal growth, as measured by quantification of *R. collo-cygni* DNA in leaves, was also restricted in plants treated with cytokinin.

Collectively these results suggest that prevention of visible symptom development, rather than prevention of asymptomatic growth, is the most important target for management of this disease. Control methods targeted at delaying senescence could be a useful avenue for further investigation.

## Lay summary

Ramularia leaf spot is a plant disease that causes damage to barley plants. It is caused by a fungus called *Ramularia collo-cygni*. The damage caused by this disease can reduce the amount and quality of barley grain at harvest, lowering the value of the crop. Ramularia leaf spot disease has become a serious problem particularly over the last 20 years or so as it has spread around the world.

*Ramularia collo-cygni* fungus can live inside barley plants for most of the growing season without any visible disease symptoms appearing on plant leaves, then visible symptoms (dark spots and lesions on the leaves) can appear later in the season after barley plants have flowered. It was not known whether *Ramularia collo-cygni* causes unseen damage inside barley plants during the long period before visible disease symptoms appear, or whether the damage is only caused once they appear. One way in which the fungus could possibly cause unseen damage is by interfering with radiation use efficiency (the ways in which plants use the energy from sunlight which they process via photosynthesis for growth or grain development). Otherwise, the damage cause by ramularia leaf spot could be due to interference in radiation interception (physical blocking of sunlight caused by the spots and lesions on the leaf once visible symptoms appear).

The experiments conducted in this project did not find any evidence to indicate that *Ramularia collo-cygni* affects barley photosynthesis during the period before visible disease symptoms appear. Field experiments used a technique to predict what the expected yield loss (damage) to barley grains

would be if the main cause of damage were interference in radiation interception because of visible disease symptoms, and then compared this with the actual yield loss. These results showed that the period after visible symptoms appear on leaves is likely to be the biggest contributor to yield loss, so this is the most important stage of disease development to try and control.

Based on these results, the last part of the project looked at whether it might be possible to delay the appearance, or reduce the amount, of visible disease symptoms on barley leaves without using fungicides. Plants were sprayed with a plant hormone called cytokinin that has the effect of delaying leaf senescence (keeping leaves green for longer by slowing down the process of dying). The results of these experiments showed that plants that were sprayed with cytokinin developed fewer disease symptoms and symptom appearance was also delayed in these plants in comparison to plants that were not sprayed with cytokinin.

# Acknowledgements

Thank you to AHDB and SRUC for funding this research.

Thank you to my supervisors Ian Bingham, Neil Havis and Steven Spoel, and to everyone else at SRUC, the University of Edinburgh and beyond who provided advice and support. I am especially grateful to all the technical and field staff at SRUC, without whom this work would not have been possible, particularly Colin Crawford, Kalina Parkinson, Linda Paterson, Maria Stanisz-Migal and Clare Macdonald. Thanks also to Steven Kildea and Steve Hoad for examining this thesis.

Thank you to everyone involved in the Gatsby Plant Science Network for invaluable support over many years, including the Gatsby Plant Science Summer School, training weekends and networking meetings.

I would like to thank the University of Edinburgh Student Disability and Counselling Services for their excellent support that allowed me to complete this research and Mairead Rae, Postgraduate Programme Administrator for the University of Edinburgh Graduate School of Biological Sciences, for helping me to navigate through some choppy waters.

I am grateful to my friends and family, and most of all to my partner Greg for his unwavering belief, support and encouragement.

# Chapter 1 General introduction

## Barley

Barley (*Hordeum vulgare*) is an ancient crop with a wide geographic range and a reputation for resilience. It has been part of human diets since its domestication in the Middle East and central Asia more than 10,000 years ago, and is now grown around the world (Von Bothmer and Komatsuda, 2011). The total worldwide harvested area of barley has fallen from around 80 million hectares in the late 1970s and early 1980s to just under 50 million hectares today. Global annual production currently stands at around 145 million tonnes (FAOSTAT, 2020). Barley is still grown as a basic food crop, particularly in areas where resources are limited or the climate less suitable for other cereal crops, as barley yield is generally less variable than that of other major cereals and it can be grown successfully across an extensive range of altitudes and climates (Newton *et al.*, 2011). In richer countries with milder climates, despite experiencing a small renaissance as a health food (Hecker *et al.*, 1998), barley is now grown mainly for use in animal feed or alcohol production.

In Scotland, where whisky is one of the nation's most valuable export commodities, 53% of the 2019 barley harvest was sold to the malting industry (The Scottish Government, 2020). Barley is the most widely grown crop in Scotland, accounting for 65% of total crop production in 2020; with spring barley alone accounting for 55% (The Scottish Government, 2020).

## Barley pests and diseases

Barley can be affected by a range of biotic stresses. Free-living nematodes, bacterial pathogens such as *Pseudomonas syringae*, birds such as crows (particularly during crop establishment) and viral pathogens such as Barley yellow dwarf virus (vectored by aphids) are all causes for concern for growers. However, fungal pathogens are responsible for some of the most economically important diseases of barley.

*Rhynchosporium commune*, the causal agent of barley leaf blotch (or scald), is the most significant foliar disease of barley in northern Europe. Net blotch and brown rust, two more damaging foliar diseases of barley, are caused by the fungal pathogens *Pyrenophora teres* and *Puccinia hordei*, respectively. Fusarium species, including *Fusarium graminearum*, contribute to seedling wilt and Fusarium head blight (Bottalico and Perrone, 2002).

Powdery mildew (*Blumeria graminis* f. sp. *hordei*) has historically been a problematic disease for barley growers. However, resistant spring barley varieties are now widely grown. Loss of function mutations at the *Mildew resistance locus O* (*MLO*) were found to confer resistance to powdery mildew (Piffanelli *et al.*, 2002), leading breeders to develop *mlo*-mediated resistant spring barley cultivars.

Widespread adoption of spring barley varieties with *mlo*-mediated resistance to powdery mildew has been suggested as a contributing factor in the emergence of Ramularia leaf spot (RLS), an increasingly problematic disease of barley caused by the fungus *Ramularia collo-cygni*. Spring barley varieties carrying the mutant *mlo* allele have been found to be more susceptible to RLS (Pinnschmidt *et al.*, 2006; Pinnschmidt and Sindberg, 2009; McGrann *et al.*, 2014), although the strength of this observed effect appears to vary across different locations, environments and genetic backgrounds (Hofer *et al.*, 2014; Havis *et al.*, 2015).

## Physiological responses of plants to fungal pathogens

Fungal pathogens of plants utilise varied strategies to obtain sufficient nutrition for growth and development from host plants. The way in which they obtain their nutrition has commonly been used to categorise them as biotrophs, necrotrophs or hemibiotrophs. Biotrophs gain nourishment from living plant tissue, necrotrophs kill plant cells and gain nourishment from dead plant tissue, and hemibiotrophs have an initial biotrophic stage, followed by a switch to necrotrophy.

Some crop pathogens, including *Zymoseptoria tritici* (Septoria leaf blotch of wheat), *Rhynchosporium commune* (Barley leaf blotch/scald), *Cladosporium fulvum* (Tomato leaf mould) and *Ramularia collo-cygni* (Ramularia leaf spot of barley), exhibit lifestyles characterised by a period of asymptomatic growth within the host plant, followed by a switch to causing necrotic lesions. These fungi grow intercellularly during the asymptomatic period of growth, and do not produce specialised feeding structures, thus the first phase of their lifecycle, prior to the necrotrophic phase, does not fit so neatly into the classification of biotrophy. *R. collo-cygni* has sometimes been described as growing endophytically in barley prior to the appearance of visible foliar disease symptoms, and Salamati and Reitan (2006) hypothesised that it may have been an endophyte that subsequently evolved to be capable of pathogenicity. Although *R. collo-cygni* presumably obtains nourishment from barley plants in the apoplast where fungal hyphae grow for extended periods, the precise form of this and mechanisms of uptake are not yet certain.

Negative effects on host plants of being used as a source of nourishment by pests can arise from direct physical damage or from indirect impacts on plant functions. Localised responses, for example at individual leaf level, can add up to impact the yield or quality of a crop if circumstances are conducive. Boote *et al.* (1983), in a paper coupling plant pests and their effects on plants

to carbon flow processes in crop growth simulators, suggested classifying pests into seven groups according to the nature of their impact on plants: tissue consumers, leaf senescence accelerators, stand reducers, light stealers, photosynthetic rate reducers, assimilate sappers, and turgor reducers. Johnson (1987) suggested a further, broader classification into pests mainly affecting solar radiation interception (RI) and those mainly affecting radiation use efficiency (RUE). Effects of fungal pathogens on plants such as the development of necrotic lesions, accelerated leaf senescence, or defoliation can therefore be thought of as impacting RI, and effects such as a reduction in photosynthetic rate, or changes caused by the redirection of host soluble assimilates for fungal nutrition, can be thought of as impacting RUE. Clearly, single pathogens can have effects on both RI and RUE, particularly those that change between different trophic states during their lifecycle.

Biotrophic growth of fungal pathogens in plants can lead to an extensive reprogramming of host primary metabolism. Source-sink balance is often affected, creating sinks for assimilate at infection sites, resulting in an increase in import of photosynthetic products to infected areas and/or a decrease in export away from them (Biemelt and Sonnewald, 2006). The nutrition obtained by biotrophic fungi from living plant tissue is thought to be mainly in the form of hexoses and amino acids. Studies using the biotrophic rust *Uromyces fabae* identified hexose and amino acid transporters expressed specifically in haustoria (Hahn *et al.*, 1997; Voegelé *et al.*, 2001) and another amino acid transporter expressed in both haustoria and intercellular hyphae (Struck *et al.*, 2002). Increased expression of host and/or fungal cell-wall invertases, necessary to cleave apoplastic sucrose into hexoses, has been shown to occur in response to infection by several biotrophic or hemibiotrophic fungal pathogens (Heisterüber *et al.*, 1994; Chou *et al.*, 2000; Fotopoulos *et al.*, 2003; Behr *et al.*, 2010). Increased invertase activity, and accumulation of hexoses, has been linked to the down-regulation of photosynthesis which is also frequently observed in association with infection by biotrophic and hemibiotrophic plant pathogens. Scholes *et*

*al.* (1994) proposed that accumulation of hexoses functions together with changes to carbohydrate translocation patterns to downregulate photosynthetic gene expression via a transduction pathway or pathways, leading to a reduction in photosynthetic rate. Increased cell-wall invertase activity and accumulation of hexoses in the apoplast may benefit fungi by providing nutrition, however, hexose accumulation can also serve as a signal for triggering plant defence responses (Koch, 1996; Ehness *et al.*, 1997; Chou *et al.*, 2000; Bilgin *et al.*, 2010).

While photosynthesis is often reduced in plants infected with biotrophic or hemibiotrophic fungal pathogens, respiration is frequently increased, including in incompatible interactions. A comparison of the respiratory reactions of barley to inoculation with virulent and avirulent strains of powdery mildew (Smedegaard-Petersen and Stolen, 1981) found that respiration in resistant plants increased rapidly in the first 16 hours after inoculation, before declining again after a few days, whereas respiration in susceptible plants only began to increase after 72 hours and then remained high until the onset of senescence. Although resistant plants remained free of symptoms, grain yield and quality were reduced, suggesting that mobilisation of the defence response may have come at a cost to other processes via a reduction in available energy, reductant or precursor molecules for biosynthesis.

Biotrophic pathogens can cause significant reductions in growth and yield despite the fact that they do not directly kill plant cells. Effects on carbohydrate partitioning may play an important role in this. Using  $^{14}\text{CO}_2$  feeding, Livne and Daly (1966) found that infection of mature French bean leaves with the rust fungus *Uromyces appendiculatus* led to a substantial increase in both retention and import of assimilate in these leaves, with consequent reductions in translocations of assimilate to roots and younger, developing leaves. Similar work in barley leaves infected with brown-rust showed increased retention of assimilate in infected leaves (Owera *et al.*, 1983). Increased cell-wall invertase activity has been linked to the sink-

capacity of infected leaves through downregulation of photosynthesis, as discussed above, and is also thought to catalyse phloem unloading of sucrose due to the creation of a sucrose gradient (Roitsch *et al.*, 2003).

In contrast to biotrophic pathogens, necrotrophs directly kill plant cells. Agricultural yield losses may occur due to direct damage to the parts of the plant used as produce, for example direct damage to fruit or grain, or due to damage to other parts of a plant which are severe enough to interfere with plant functions, for example foliar necrotic lesions reducing solar radiation interception sufficiently to limit the availability of assimilates for yield-forming processes.

Disease severity, timing, duration and location within the plant can all affect the outcome of pathogen infection on crop yield (Gaunt, 1995). The timing of pathogen infection in relation to crop growth stage is an important factor in both the degree of yield loss, and the yield components which are primarily affected. For example early-season infection of barley with powdery mildew (up to stem elongation) has been found to reduce the number of fertile tillers produced (Scott and Griffiths, 1980), therefore early infection can have a compounding effect on the reduction in grain size normally associated with infection later in the season. Some fungal diseases of barley still have the potential to cause significant yield loss when infection occurs late in the season, particularly if they attack the ear or the flag and upper leaves (Jordan *et al.*, 1985; Jebbouj and El Yousfi, 2009). *R. collo-cygni* infection of barley typically leads to the appearance of late-season, post-anthesis foliar disease symptoms, therefore yield loss to this disease may be due to a reduction in assimilates from post-anthesis photosynthesis during grain filling. However, *R. collo-cygni* can grow within barley plants for an extended period prior to the appearance of visible symptoms (Frei *et al.*, 2007; Havis *et al.*, 2014). Whether this asymptomatic growth period can affect yield formation processes, and, if so, the relative impact on yield of asymptomatic and symptomatic growth periods, is not yet known.

## Yield formation in barley

Grain yield of barley and other cereals is a function of both the number of grains produced per unit ground area and the mean grain weight (MGW), but yield formation is an extended process, occurring over the course of the growing season, and influenced by multiple genetic and environmental factors (Reynolds *et al.*, 2005; Bingham *et al.*, 2007a; Bingham *et al.*, 2007b; Slafer *et al.*, 2014; Distelfeld *et al.*, 2014).

In barley, canopy size and grain sink capacity are already largely established by the time of flowering. Grain sink capacity is influenced by the individual storage capacity of grain sites, and also the number and survival of tillers and spikelets. Therefore, yield formation processes that occur during the pre-flowering growth period have a significant effect on the eventual number of grains produced per unit ground area. During grain filling, carbon assimilates from both post-anthesis photosynthesis and from the remobilisation of stored carbohydrate reserves may be utilised by barley plants, contributing to eventual mean grain weight.

Yield formation in non-diseased barley in the UK is considered to be primarily sink-limited (Bingham *et al.*, 2007a; Bingham *et al.*, 2007b; Kennedy *et al.*, 2017). Therefore, it could be argued that factors resulting in a reduction in radiation interception during grain filling, for example foliar disease symptoms of a late season disease, might not be predicted to significantly influence yield of spring barley provided that this reduction was not sufficient to reduce the availability of carbon assimilate below that needed to meet the grain sink capacity established earlier in the growing season. Indeed, Bingham *et al.*, 2019 demonstrated that light interception by green canopy does not need protection against foliar disease for the entire duration of grain filling in sink-limited spring barley crops.

However, as discussed above, pathogen infection can in some cases result in subtle effects on plants, such as a reduction in photosynthetic rate, that are

not immediately apparent to the observer but have the potential to affect yield formation over time. For example, an extended reduction in photosynthetic rate of spring barley plants throughout the pre-flowering growth period could potentially impact multiple factors such as canopy size, tiller number, number of grains per ear, potential grain weight and availability of soluble carbohydrate reserves. This highlights the importance of considering potential impacts of pathogens on barley yield in the context of the physiological processes of yield formation that are underway during the lifecycle of the pathogen.

In the case of *R. collo-cygni*, the extended, visually asymptomatic growth period of this fungus in barley typically occurs during the pre-flowering growth period, while visible foliar symptoms typically occur during grain filling. Therefore, assessing the impact of this fungus during both these barley life stages is essential to understand the ways in which it may affect yield formation.

### ***Ramularia collo-cygni***

Fungal structures associated with the foliar symptoms in barley now known as Ramularia leaf spot (RLS) were first identified in Italy in the 1890s. The fungus was originally named *Ophiocladium hordei* (Cavara, 1893), then subsequently renamed *Ramularia collo-cygni* (Sutton and Waller, 1988). The name refers to a perceived resemblance of the tortuose conidiophores to a swan's neck (Figure 1).

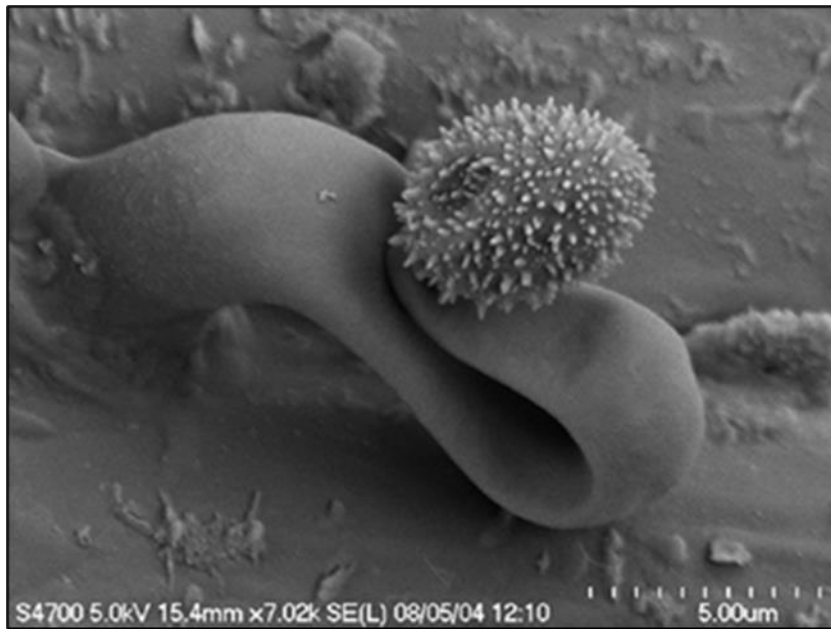


Figure 1 Photomicrograph of a conidiophore of *R. collo-cygni*.  
Extracted from Walters et al. (2008)

More recent molecular studies have confirmed that *R. collo-cygni* belongs to the class of Dothidiomycetes, in the Mycosphaerellaceae family, and the genus *Ramularia* (Crous *et al.*, 2000; Crous *et al.*, 2001; Crous *et al.*, 2009). The development of molecular diagnostic techniques has enabled rapid and accurate detection of *R. collo-cygni* even at low levels and early stages of infection (Havis *et al.*, 2006; Frei *et al.*, 2007; Taylor *et al.*, 2010), and sequencing of the first *R. collo-cygni* genome in 2016 allowed further clarification by phylogenetic analysis of the relationships between *R. collo-cygni* and other plant pathogens (McGrann *et al.*, 2016). *R. collo-cygni* was found to be closely related to *Zymoseptoria tritici*, the causal agent of the most damaging wheat disease in Europe, septoria tritici blotch (STB). Other close relatives included the tomato pathogen *Cladosporium fulvum*, the banana pathogen *Pseudocercospora fijiensis*, and the pine pathogen *Dothistroma septosporum*.

Typical symptoms of RLS found on plants in the field are dark, reddish-brown, rectangular lesions on leaves, surrounded by a 'halo' of chlorotic

tissue, restricted by leaf veins (Figure 2). Symptoms are not usually observed until after flowering has occurred (Walters *et al.*, 2008).



Figure 2 Typical RLS symptoms. Extracted from Havis *et al.*, 2015.

The development of necrotic symptoms of RLS on barley leaves is thought to be associated with the production of secondary metabolites by the fungus. Heiser *et al.* (2003) identified one of a number of coloured metabolites produced by *R. collo-cygni* as the anthraquinoid phytotoxin rubellin D, which produces light- and concentration-dependent necrosis when applied to barley leaves. The authors used a model system to demonstrate photodynamic activity of rubellin D, triggering the light-dependent production of reactive oxygen species (ROS) and peroxidation of  $\alpha$ -linolenic acid. *R. collo-cygni* can also produce different isomers of rubellin that exhibit similar photodynamic activity (Miethbauer *et al.*, 2003; Heiser *et al.*, 2004; Miethbauer *et al.*, 2006). Heiser *et al.*, (2004) proposed that rubellins produced by *R. collo-cygni* could act as pathogenicity factors, causing or exacerbating oxidative stress in barley and leading to the formation of necrotic symptoms. A similar mechanism of pathogenicity to that hypothesised for *R. collo-cygni* by Heiser *et al.*, (2004) has been shown for *Cercospora* species, plant pathogenic fungi which produce the light-activated phytotoxin cercosporin (Daub and Ehrenshaft, 2000). However, Dussart *et al.*, (2018), in experiments infiltrating

barley leaves with rubellin D, found that RLS susceptibility did not correspond with rubellin D sensitivity. The *R. collo-cygni* genome contains several clusters of genes associated with secondary metabolism, indicating that the fungus may be capable of producing a wide range of secondary metabolites (Dussart *et al.*, 2018b), and co-expression of secondary metabolism core genes and their predicted transcriptional regulators has been demonstrated in the early stages of RLS symptom development in barley seedlings (Dussart *et al.*, 2018a).

Abiotic stress factors such as high light levels can cause physiological leaf spotting on barley leaves that is similar in appearance to early RLS symptoms (Wu and Von Tiedemann, 2002), however RLS lesions are distinguishable as they 'go right through' the leaf i.e. a developed lesion will be clearly visible on both the adaxial and abaxial leaf surface. RLS symptoms are also relatively easily confused with those of some other fungal pathogens of barley, particularly *Pyrenophora teres* (net blotch) in its spot form (*P. teres* f. *maculata*).

Recorded yield losses to RLS are typically around 5 – 10%, although losses as high as 70% have been reported in South America, and grain quality can also be affected (Havis *et al.*, 2015). A higher proportion of small grains (screenings), often observed in grain from barley affected by RLS, can reduce the value of a crop as it may then not meet criteria for the malting market, such as an even germination of seed.

Over the last two decades, RLS has become more prevalent globally (Figure 3).

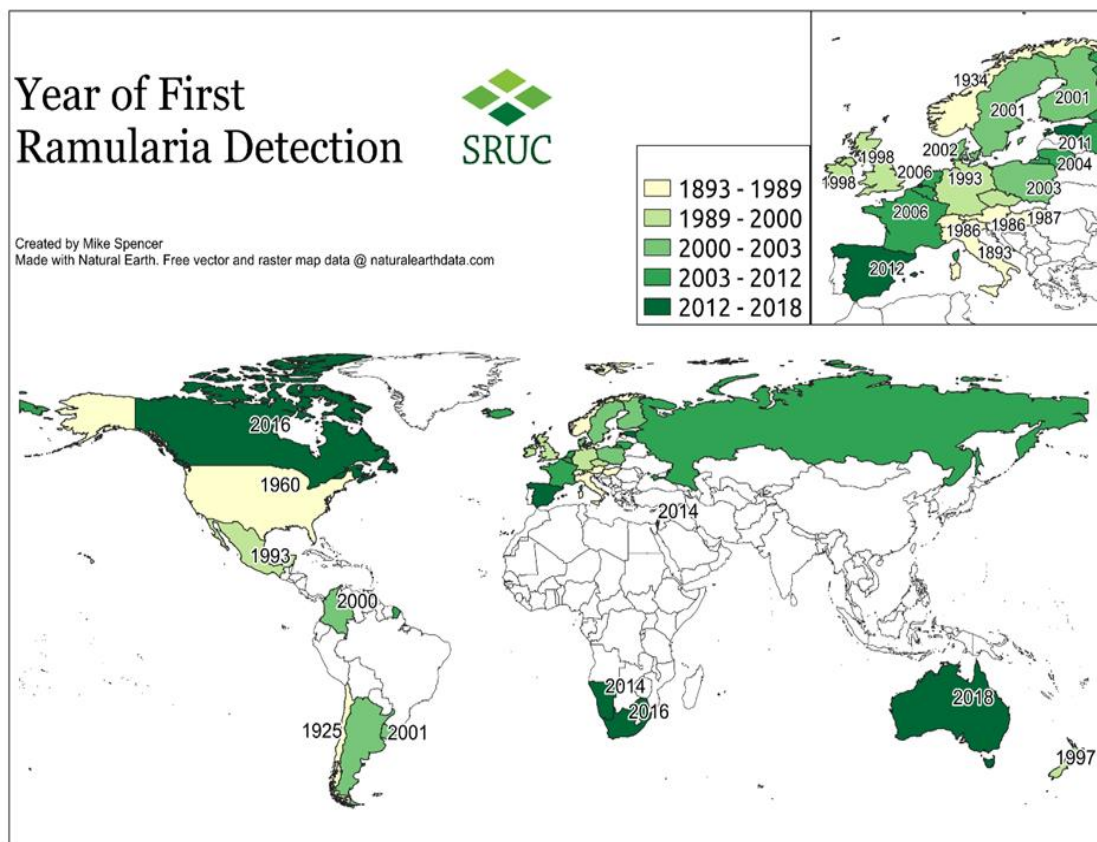


Figure 3 Global distribution of RLS. Countries identified by date of first report of the disease (Spencer et al., 2019). Licensed under CC BY.

Multiple factors may have contributed to this, including increased global trade, climatic changes, agricultural practices, or genetic changes in *R. collo-cygni* or barley. Susceptibility of barley lines with *mlo*-mediated resistance to powdery mildew, the possibility of historic misidentification of RLS symptoms, and human movement of infected seed have all been suggested as contributors to the global spread of RLS. Population structure analyses of *R. collo-cygni* isolates from two northern European barley populations (Hjortshøj et al., 2012) and from diverse hosts across several European locations (Stam et al., 2019) found high genetic diversity within local sub-populations rather than distinctions between countries (Hjortshøj et al., 2012) and revealed little evidence of global clustering or host specification (Stam et al., 2019). These

studies suggest that human movement of infected seed is likely to play an important role in dispersal.

*R. collo-cygni* is a commercially important pathogen of barley, however it can also infect a wide range of other hosts, including wheat (*Triticum aestivum*), oat (*Avena sativa*), maize (*Zea mays*) and rye (*Secale cereale*) (Huss, 2004), as well as several wild grasses (Huss, 2004; Frei and Gindro, 2015; Kaczmarek *et al.*, 2017) and the model grass species *Brachypodium distachyon* (Peraldi *et al.*, 2014). *R. collo-cygni* in barley (Figure 4) can be seed-borne and grow internally through plants, moving into new leaf layers as they emerge, without displaying any visible symptoms (Frei *et al.*, 2007; Havis *et al.*, 2014).

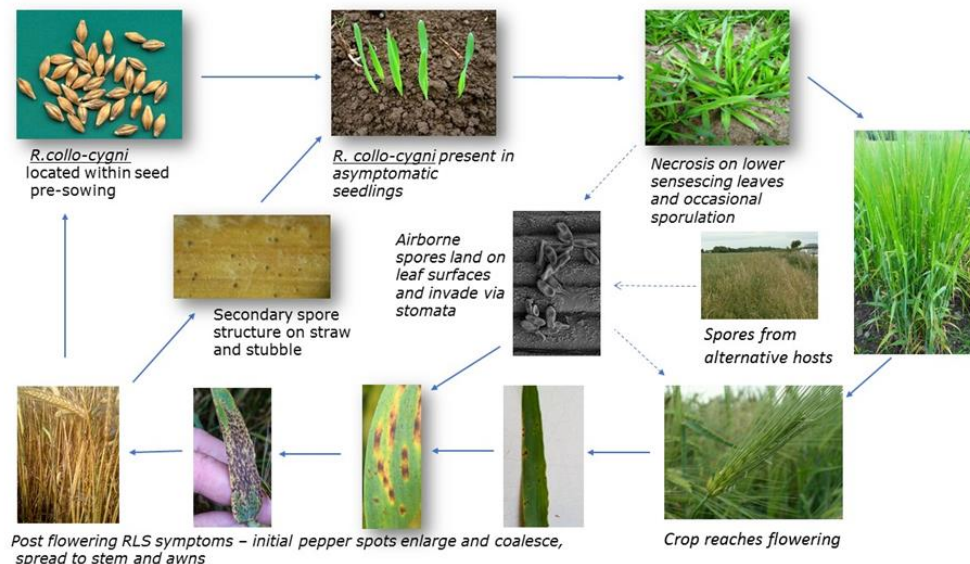


Figure 4 Lifecycle of *R. collo-cygni* on barley. Adapted from Havis *et al.* (2015).

Symptoms are sometimes observed on lower leaves of young plants early in the growing season, particularly when plants have experienced adverse environmental conditions such as waterlogging (McGrann and Havis, 2017). However, typically *R. collo-cygni* has a long period of asymptomatic growth

and symptoms only appear after flowering. Spotting and lesions appear on upper leaves, and can spread to other leaves, stems and awns as the disease develops. Lesions often multiply and coalesce, accompanied by chlorosis and necrosis of leaves (Walters *et al.*, 2008).

The role of spores in *R. collo-cygni* epidemics is less clear, but infection from spores overwintering on straw and stubble, from senescing lower leaves during the growing season, or from alternative hosts may be significant in some years and locations (Mäe *et al.*, 2018), although further research is needed on the role of alternative hosts to establish evidence for spore movement. Spore germination occurs on the barley leaf surface in moist conditions. Fungal hyphae enter leaves through stomata and grow intercellularly in the mesophyll. After symptom appearance fungal sporulation can occur in necrotic tissue, with conidiophores emerging through stomata (Sutton and Waller, 1988; Stabenheimer *et al.*, 2009; Thirugnanasambandam *et al.*, 2011; Kaczmarek *et al.*, 2017) and also directly through the mesophyll (Kaczmarek *et al.*, 2017). There is evidence that *R. collo-cygni* can reproduce sexually (Piotrowska *et al.*, 2016) so spread may also occur through sexual ascospores, but this has yet to be confirmed.

RLS is a concern for barley growers as it is now widespread globally and can, in some years, cause severe yield losses. The genetic similarity of *R. collo-cygni* to other damaging pathogens like *Zymoseptoria tritici*, its broad host range, and its suspected ability to reproduce sexually all contribute to concern about possible future developments. Prophylactic fungicide applications are currently widely used to control RLS disease by preventing *R. collo-cygni* survival in barley. However, methods for suppression of disease symptom severity, rather than prevention of *R. collo-cygni* survival per se are also the subject of ongoing research efforts.

### **Control of RLS: disease prevention**

Control of RLS in barley is currently heavily reliant on the use of fungicides, applied prophylactically with the aim of preventing disease by killing any *R.*

*collo-cygni* fungus present in plants. However, *R. collo-cygni* has developed resistance to strobilurin (Quinone outside inhibitor: QOI) fungicides and resistance to succinate dehydrogenase inhibitor (SDHI) fungicides is increasing (Piotrowska *et al.*, 2017). The multisite fungicide chlorothalonil remains an effective control, but EU approval for this product has been withdrawn and it is no longer in use in the EU as of May 2020. These factors, along with more widespread calls to reduce pesticide usage due to environmental concerns, have increased the urgency of research aimed at developing alternative methods of disease control such as breeding barley varieties for resistance to RLS and understanding the effects of environment on disease expression.

### **Control of RLS: disease suppression**

A key target of research aimed at limiting the damage caused to barley by RLS is the identification of genetic traits associated with reduced disease severity. However, breeding barley varieties for resistance to RLS is complicated by the effects of environment on disease expression. Prolonged leaf wetness during stem extension has been reported as a key factor in RLS development and symptom severity (Formayer *et al.*, 2004; Huss, 2004; Salamati and Reitan, 2006), however, multi-year analysis of data from an investigation in to the potential for a period of leaf wetness for 14 days at GS30/31 to act as a risk predictor for RLS in barley found that disease levels could not be predicted using this parameter alone, despite some observed within-season correlation between leaf wetness and eventual disease levels (Havis *et al.*, 2018). Light intensity has also been associated with RLS symptom severity, however, reports of this affect vary. Unpublished results from E. Sachs, published in Heiser *et al.*, (2003), suggested that light intensity can influence RLS symptom levels on barley leaves. Subsequently, Makepeace (2006) reported higher levels of RLS symptoms on barley plants exposed to high light intensity prior to inoculation with *R. collo-cygni* than on barley plants grown under low light intensity. Makepeace (2006) also found that plants grown in high light intensity after inoculation with *R. collo-cygni*

developed fewer RLS symptoms than plants grown under lower light intensity, suggesting that the timing of exposure to high light intensity is an important factor, possibly negatively affecting pathogenicity later in the life cycle of *R. collo-cygni* in barley. Increased RLS symptoms were reported in barley seedlings exposed to abiotic stress (either waterlogging or high light intensity) prior to inoculation with *R. collo-cygni*, by McGrann and Brown (2018), but this response was found to differ across barley varieties. Formayer *et al.*, (2004) reported that humidity, but not light intensity, affected RLS symptom development in experiments in Austria, and Mařík *et al.*, (2011) found that increased RLS symptom severity in the Czech Republic was associated with a greater number of rainy days during the three weeks post-heading, and lower rainfall and higher temperatures after flowering was associated with reduced symptom severity. More work is still needed to fully understand the effects of individual or combinations of environmental factors on the incidence and severity of RLS in barley, and how these may interact with host or fungal genotype. Advances in this area could potentially lead to the development of varieties exhibiting heritable resistance to RLS under multiple environmental conditions, or to improved prediction tools to inform decisions about targeting control methods such as fungicide application according to environmental risk factors.

## **Project rationale and objectives**

*R. collo-cygni* infection of barley is characterised by a long period of latent growth, i.e. no visible disease symptoms apparent on plants, followed (sometimes, but not always) by a 'lifestyle switch' to necrotrophic growth and visible symptom expression. Understanding the effects of *R. collo-cygni* on barley physiology during asymptomatic growth and the switch to symptomatic growth is therefore important to target improvements in host resistance and disease control strategies. Infected seed is an important source of *R. collo-*

*cygni* infection in barley, and the fungus can be present in plants from the earliest stages of their development (Havis *et al.*, 2014). Although *R. collo-cygni* has sometimes been described as leading an endophytic lifestyle in barley prior to visible symptom appearance on leaves late in the growing season (McGrann *et al.*, 2016), gaps in our knowledge remain about what impact this long latent stage of infection may have on host plants.

It is possible that the latent stage of *R. collo-cygni* infection in barley could be a contributor to eventual yield loss, as in the field asymptomatic infection coincides with processes contributing to the establishment of grain sink capacity, such as the development of tillers, ears and spikelets. In the UK, and other countries with similar climates, yield formation in non-diseased barley crops is thought to be predominantly sink-limited (Bingham *et al.*, 2007a; Bingham *et al.*, 2019). Therefore, the latent phase of *R. collo-cygni* infection could potentially contribute to reduction in barley yield due to effects on the development of grain sink capacity, for example due to reduced carbon assimilation from pre-anthesis photosynthesis, or changes to pre-anthesis resource allocation within the plant. Alternatively, reduction in photosynthetic activity during grain filling, due to necrotic lesion development and loss of green leaf area, or post-anthesis effects on resource allocation, could be significant contributing factors to the yield reduction associated with RLS.

The work described in Chapters 2 and 3 of this thesis was designed to investigate whether the visually asymptomatic period of *R. collo-cygni* growth in barley impacts host photosynthesis, in order to increase our understanding of the relative importance of different *R. collo-cygni* life stages in yield loss to RLS.

The following hypotheses were tested in Chapters 2 and 3:

- Infection of barley seedlings with *R. collo-cygni* does not impact leaf photosynthesis prior to the appearance of visible RLS symptoms.

- Net leaf photosynthesis is reduced after the appearance of visible RLS symptoms on leaves of barley seedlings infected with *R. collo-cygni*.
- Infection of field grown barley plants with *R. collo-cygni* does not impact leaf photosynthesis prior to the appearance of visible RLS symptoms.
- Yield loss to RLS in barley is due to post-anthesis reduction in PAR interception due to visible RLS symptom expression.

The factors involved in triggering the *R. collo-cygni* switch to necrotrophic growth in barley and the appearance of RLS symptoms are not yet fully understood. It has been linked to adverse environmental conditions, and differences in varietal responses to these, as described above. Transgenic barley plants exhibiting delayed leaf senescence due to overexpression of a *Stress-induced NAC1* transcription factor, also linked to drought tolerance, were found to have increased resistance to RLS (McGrann *et al.*, 2015), and there is some evidence to suggest that changes in host reactive oxygen species (ROS) status that can lead to senescence are involved in the transition to necrotrophic growth (McGrann and Brown, 2018; McGrann *et al.*, 2020). It is possible, therefore, that treatments designed to delay the onset of senescence could interfere with processes affecting the *R. collo-cygni* switch to necrotrophic growth.

The work described in Chapter 4 of this thesis investigated the effect of delaying foliar senescence of barley seedlings on *R. collo-cygni* growth *in planta* and RLS symptom development.

The following hypotheses were tested in Chapter 4:

- Delaying foliar senescence in barley seedlings infected with *R. collo-cygni* reduces visible RLS symptom severity.

Delaying foliar senescence in barley seedlings infected with *R. collo-cygni* reduces fungal growth *in planta*.

# Chapter 2 Physiological responses of barley seedlings to infection with *R. collo-cygni* fungus

## Introduction

The relationship between visible disease severity and crop yield loss is not simple, and factors such as host genotype and timing of disease development can lead to different outcomes (Gaunt, 1995; Bingham *et al.*, 2009; Bingham *et al.*, 2019). An assumption of eventual yield loss directly proportionate to visible disease severity will not always be accurate, so insight into the quantitative relationship between physiological processes affected by the presence of a pathogen and visible symptoms is useful (Robert *et al.*, 2004).

Quantification of the relationship between plant physiological processes, presence of the fungus, and development of visible symptoms might be of particular relevance for *R. collo-cygni*, as the fungus can grow asymptotically for extended periods, and the processes involved in the switch to necrotrophic growth and symptom development in barley are not yet clear. The work described in chapter 2 focused on quantifying this relationship at leaf level, particularly looking at photosynthetic responses to infection across the leaf surface before and during visible symptom development.

## Photosynthetic responses of plants to pathogens

Host responses to infection with biotrophic or hemibiotrophic fungi can often involve a decrease in the rate of photosynthesis and an increase in respiration rate, as discussed in Chapter 1. However, there is extensive variation in the reported dynamics of these responses.

Effects of pathogens on photosynthesis are not always confined to visibly symptomatic tissue. Some studies in leaves of crops showing visible disease symptoms have found decreases in photosynthetic rate in symptomless areas of infected leaves (Martin, 1986; Scholes and Farrar, 1986; Bastiaans, 1991). Others, though, have found increases in photosynthetic rate in symptomless areas (Habeshaw, 1984; Last, 1963; Scholes and Rolfe, 2009).

Bastiaans (1991) used the idea of a virtual lesion to describe how effects of pathogen infection on leaf photosynthesis can extend beyond visible lesions; a virtual lesion consisting of a visible lesion and surrounding leaf area in which photosynthesis is negligible. In this model the parameter  $\beta$  is used to represent the ratio of virtual to visible lesion area, indicating whether the effect of disease on photosynthesis is greater ( $\beta > 1$ ), lower ( $\beta < 1$ ), or equal ( $\beta = 1$ ) to the proportion of visible symptom area.

Two studies (Robert *et al.*, 2005 and Robert *et al.*, 2006) used Bastiaan's virtual lesion model to analyse the relationship between foliar disease symptoms and leaf photosynthesis for leaf rust (*Puccinia triticina*) and Septoria leaf blotch (*Septoria tritici*) in wheat, finding that the type of symptom included in the analysis and the stage of symptom development affected  $\beta$  values. For leaf rust, analyses including areas of disease-induced chlorosis, in contrast to those using areas of fungal sporulation only or areas of fungal sporulation plus areas of disease-induced necrosis, were found to have low  $\beta$  values ( $\beta < 1$ ) (Robert *et al.*, 2005). The authors of this study concluded that leaf rust does not have a global effect on the photosynthesis of symptomless areas of wheat leaves if disease-induced chlorosis is

included in interpretation of the symptomatic area. For Septoria leaf blotch, noting that symptoms progress from chlorotic to necrotic damage, analysis of chlorotic symptoms again found  $\beta$  values of  $<1$ , but  $>1$  for necrotic symptoms, suggesting that the stage of symptom development is an important factor in the global effect of this disease on leaf net photosynthetic rate, and that some photosynthetic capacity is retained in chlorotic tissue (Robert *et al.*, 2006). Studies of other foliar diseases of cereals have found evidence of reduced rates of photosynthesis in green, asymptomatic tissue of infected leaves, for example powdery mildew in barley (Coughlan and Walters, 1992) and crown rust (*Puccinia coronata*) in oats (Scholes and Rolfe, 1996).

It is clear, therefore, that we cannot make assumptions about the effects of pathogen infection on whole-leaf photosynthesis based on the presence or extent of visible symptoms. The impact on host plants may be more severe than expected, as limitations to photosynthesis can extend beyond symptomatic areas. Equally so, the impact may be lower than expected, as heterogeneous responses to infection across a leaf can lead to no net change in photosynthesis when averaged over the whole leaf surface, at least for a period during the progress of a disease. Scholes and Farrar (1986) found the rate of photosynthesis in areas between brown rust (*Puccinia hordei*) pustules on barley was reduced compared to control plants, however within pustules it was increased. Scholes and Rolfe (2009) found that photosynthesis in wheat as measured by whole leaf  $\text{CO}_2$  assimilation did not differ significantly between control leaves and leaves infected with *Zymoseptoria tritici* (and displaying necrotic lesions). Chlorophyll fluorescence imaging analysis revealed that photosynthesis as measured by the rate of photosynthetic electron transport was greatly reduced within lesions, however in the surrounding green areas it was higher than that of control leaves. The authors hypothesised that this could be a compensatory reaction to loss of green area, or a response to an increase in sink demand in infected leaves.

Plant pathogens can have multiple impacts on plant physiology, for example on water relations or nitrogen dynamics. This project sought to assess the potential impact of *R. collo-cygni* on barley growth and development processes involved in yield formation. Photosynthesis is the key driver of plant growth and development, thus assessment of physiological responses to infection focused on photosynthetic responses. Photosynthesis can be measured directly by measurement of gas exchange, and photosynthetic activity can also be assessed indirectly by measurement of chlorophyll fluorescence emitted from leaves. Both infra-red gas analysis and chlorophyll fluorescence analysis were used to assess photosynthetic responses of barley to *R. collo-cygni* infection, to build a detailed and robust picture of the impact of *R. collo-cygni* on barley photosynthesis. These techniques provide more sensitive measurements of carbon metabolism than could be achieved through traditional growth analysis.

## **Chlorophyll fluorescence**

Chlorophyll fluorescence analysis can be used to monitor the effects of pathogen infection on host photosynthetic metabolism (Scholes and Rolfe, 2009). It is a non-destructive method that can be used to indirectly measure photosynthetic activity in live plants.

The basic premise behind chlorophyll fluorescence analysis is as follows; light energy is converted to chemical energy by the photosystems in the thylakoid reactions of photosynthesis. Light energy absorbed by chlorophyll molecules is used to power the processes that lead to the production of ATP and NADPH. All the energy must be used (quenched) if photo-damage to leaves is to be avoided. Light energy can be used to drive photosynthetic electron transport (photochemical quenching), dissipated as heat (non-photochemical quenching) or re-emitted as fluorescence. The competition between these processes varies fluorescence yield and this information can

be used to detect changes in the operation of the photosynthetic apparatus. Imaging fluorometers can detect heterogenous changes in photosynthetic activity across a leaf surface (Murchie and Lawson, 2013).

A typical protocol for examining photosynthetic responses in leaves using chlorophyll fluorescence quenching analysis during photosynthetic induction and steady-state photosynthesis is described below, and a diagrammatic representation is shown in Figure 5, adapted from Scholes and Rolfe (2009).

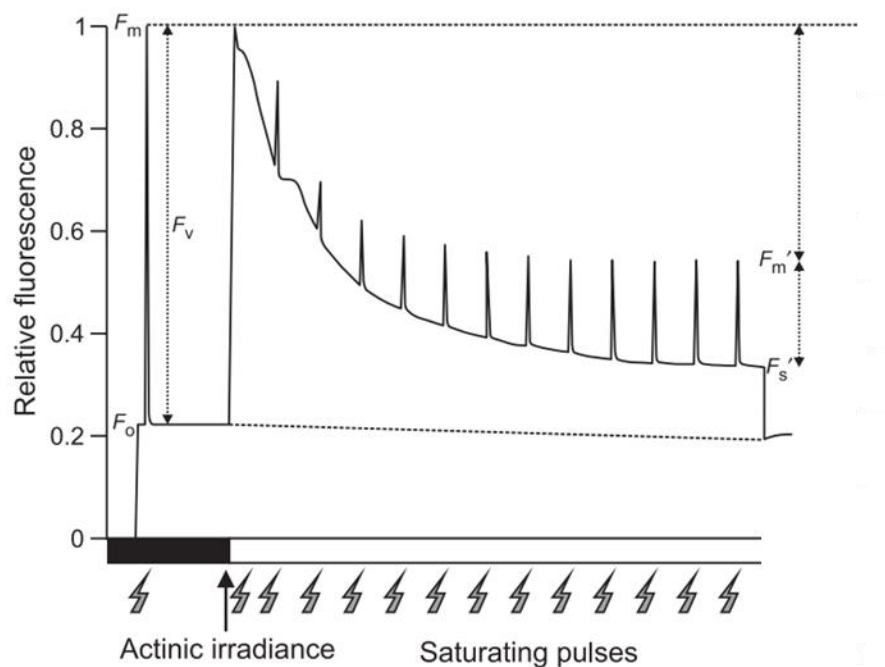


Figure 5 Diagram of an example protocol for chlorophyll fluorescence quenching analysis during photosynthetic induction and steady state photosynthesis. Adapted from Scholes & Rolfe (2009).

Plants are first placed in darkness for a period, during which photochemical and non-photochemical energy dissipation processes relax so all Photosystem II (PSII) reaction centres should be fully oxidised. Minimal fluorescence of dark-adapted plants is measured using a weak measuring beam ( $<1 \text{ mmol m}^{-2} \text{ s}^{-1}$ ). The excitation light intensity of the measuring beam is enough to detect minimal fluorescence, but not high enough to drive photosynthesis.

Plants are then exposed to a high intensity saturating flash of light to measure maximal fluorescence ( $F_m$ ), at which point all PSII reaction centres should be transiently fully reduced.

Maximal efficiency of PSII ( $F_v/F_m$ ) (Table 1) can be calculated from the minimal and maximal fluorescence values ( $F_m - F_o$ )/ $F_m$ . Reduction of  $F_v/F_m$  values can indicate damage to the photosynthetic apparatus (Denmig and Bjorkman, 1987) and this parameter is widely used as an indicator of plant stress.

Table 1 Chlorophyll fluorescence parameters used in this project

<b><math>\Phi_{PSII}</math></b>	The operating efficiency of Photosystem II (PSII), or the proportion of absorbed quanta that are converted into chemically fixed energy by the photochemical charge separation at PSII reaction centres
<b>NPQ</b>	A measure of nonphotochemical quenching
<b>ETR</b>	The rate of photosynthetic electron transport
<b><math>F_v/F_m</math></b>	The maximal efficiency of PSII, or maximum quantum yield of PSII

Plants are then exposed to actinic light (level dependent on the particulars of the analysis), causing fluorescence to rapidly increase and then decline due to the activation of photochemical and non-photochemical energy dissipation (quenching) processes until steady state photosynthesis ( $F_s'$ ) is achieved.

The relative contribution of photochemical and non-photochemical processes to fluorescence quenching is revealed by regularly exposing plants to flashes of saturating light throughout. This transiently closes PSII reaction centres, so at these points only non-photochemical quenching (NPQ) (Table 1) should be evident. NPQ is calculated as  $(F_m - F_m')/F_m'$ .

The operating efficiency of PSII ( $\Phi_{PSII}$ ) (Table 1) is calculated as  $(F_m' - F_s')/F_m'$ . Electron Transport Rate (Table 1) is calculated as  $\Phi_{PSII} \times$  absorbed irradiance  $\times 0.5$ .

## Chapter objectives

The appearance of *Ramularia* leaf spot symptoms on barley leaves can be preceded by an extended phase during which *R. collo-cygni* grows asymptotically within hosts plants. The effect of this asymptomatic phase on barley is not well understood.

We have seen that infection of plants with pathogens is often, but not always, associated with reduced rates of photosynthesis, and that effects of infection on photosynthesis are frequently not directly related to visible symptom severity. Studies of some pathosystems have indicated that entirely asymptomatic phases of infection do not have an effect on host plant photosynthesis (van Oijen, 1990; Robert *et al.*, 2006) while others have detected pre-symptomatic changes (Berger *et al.*, 2004; Pérez-Bueno *et al.*, 2006; Pineda *et al.*, 2008; Granum *et al.*, 2015).

Should *R. collo-cygni* reduce (or increase) photosynthesis during the long asymptomatic period common in field-grown barley, this could impact assimilate availability and/or resource partitioning with potential implications for yield forming processes such as tiller growth or spikelet formation. Combined with an understanding of how the extent of visible symptom area

relates to the extent of any effect on photosynthesis, this knowledge could be informative in relation to timing of targeted disease control efforts.

Using a model system of spring barley seedlings inoculated with *R. collo-cygni* mycelium and grown in controlled environment chambers, the objective of this chapter was to determine the relative effects of asymptomatic and symptom-expressing phases of *R. collo-cygni* infection on leaf photosynthesis, analysing the relationship between photosynthesis, fungal growth *in planta* and the development of visible symptoms.

The specific hypotheses tested in Chapter 2 were:

- Infection of barley seedlings with *R. collo-cygni* does not impact leaf photosynthesis prior to the appearance of visible RLS symptoms.
- Net leaf photosynthesis is reduced after the appearance of visible RLS symptoms on leaves of barley seedlings infected with *R. collo-cygni*.

## Materials and methods

### Overview

Leaf photosynthetic activity and quantity of *R. collo-cygni* DNA in inoculated and control plants were measured throughout the time-course of disease development. Infra-red gas analysis and chlorophyll fluorescence imaging were used as non-invasive ways to probe photosynthetic performance. Quantitative polymerase chain reaction analysis (qPCR) was used to quantify the amount of *R. collo-cygni* DNA present in leaves.

## Plant material and growth conditions

All experiments were conducted on spring barley (*Hordeum vulgare* L.) varieties Concerto or Fairing. Both these varieties contained the loss of function mutation at the *Mildew resistance locus O (MLO)* conferring resistance to powdery mildew. There was little difference in disease resistance ratings for *Ramularia* between the varieties (both varieties were scored as 6 in the 2016 AHDB Recommended List, and Concerto and Fairing were scored as 6 and 7, respectively, in 2017). The AHDB Recommended List 2016/17 Barley and Oat Pocketbook reported the pedigree of Concerto as Minstrel x Westminster and the pedigree of Fairing as Titouan x 144-02-4. Seeds were germinated by placing them in a Petri-dish lined with Whatman filter paper (GE Healthcare Life Sciences, Buckinghamshire, UK) soaked in tap water. The Petri-dishes were wrapped in aluminium foil to exclude light and left at room temperature for two to four days until the seeds had germinated. The germinated seeds were then planted in plastic pots with a volume of 147 cm<sup>3</sup> and placed in trays in a controlled environment growth chamber. The growth medium used was Levington M3 high nutrient pot and bedding compost (ICL, Suffolk, UK).

The growth cabinets used were the JUMO IMAGO F3000 model (Snijders Labs, Tilburg, The Netherlands). The cabinet conditions were set to 18.0 °C during the light period and 12°C during the dark period, 90 % Relative Humidity, photoperiod 16 h light and 8 h dark, and Photosynthetically Active Radiation (PAR) was supplied by fluorescent lamps (TLD-90 36W/950 6K, Philips, Amsterdam, Netherlands) giving a photon flux density of 230  $\mu\text{mol m}^{-2} \text{s}^{-1}$  at initial plant height. The compost was kept moist, but not water-logged, by inspecting daily and watering as required. The seedlings were inoculated with *R. collo-cygni* 14 days after sowing at growth stage 12 of the Zadoks decimal code for cereals (Tottman et al., 1979) when plants had two fully emerged leaves.

## Inoculation of plants with *R. collo-cygni*

The inoculation protocol was adapted from Makepeace et al. (2008). Five 1 cm<sup>2</sup> blocks of fungal mycelium were cut from a Petri-dish containing *R. collo-cygni* isolate DK05 Rcc 001, isolated from susceptible spring barley cv Braemar in Denmark in 2005, which had been growing on potato dextrose agar (PDA) for two weeks. These blocks were then placed in 250 ml of potato dextrose broth (PDB) and incubated in the dark on a shaker at 125 rpm at 18°C for a further two weeks.

The PDA was prepared with 39.0 g l<sup>-1</sup> PDA powder (Sigma-Aldrich, Dorset, UK) in sterile distilled water (SDW). This solution was autoclaved, then 0.1 % streptomycin was added to give a concentration of 1 ml l<sup>-1</sup>. The PDB was prepared with 24.0 g l<sup>-1</sup> PDB powder (Sigma-Aldrich, Dorset, UK) in SDW. This solution was autoclaved, then 0.1 % streptomycin was added to give a concentration of 1 ml l<sup>-1</sup>.

Two controls were made using five 1 cm<sup>2</sup> blocks of PDA with no fungus in 250 ml of either PDB or SDW, with streptomycin added at the same concentration as above. The controls were also incubated in the dark on a shaker at 125 rpm at 18°C. After two weeks of incubation, the *R. collo-cygni* culture and controls were used to inoculate the plants. The fungal cultures and controls were each blended until smooth in a clean kitchen blender, in three runs of 30 seconds each. Polyoxyethylene-sorbitan monolaurate (Tween 20) (Sigma-Aldrich, Dorset, UK) was added at a concentration of 0.01% (or approximately 1 drop per 50 ml) to all three treatments to break the surface tension of the spray droplets on the leaf surface. The inoculum was then sprayed onto the barley plants using an air brush (Clarke Wiz Air®, Clarke International, Essex, UK) at an application rate of 0.5 ml per plant. The plants were sprayed evenly from different directions to ensure the inoculum was uniformly distributed over them.

The plants were placed in propagators, which were then sealed with microporous tape. Each treatment group was in a separate propagator to avoid cross contamination. The propagators were each placed inside two black plastic bags to exclude light and sealed with microporous tape. After two days the bags were removed. This process created favourable conditions for fungal growth and infection by facilitating a period of high humidity. After a further three days the lids of the propagators were removed. The three treatment groups were kept separate until the leaves were completely dry. Once the plants had dried, they were arranged into randomised blocks in the cabinet. Open-ended clear plastic tubes were used to keep the plants upright and avoid damage during sampling (Figure 6).

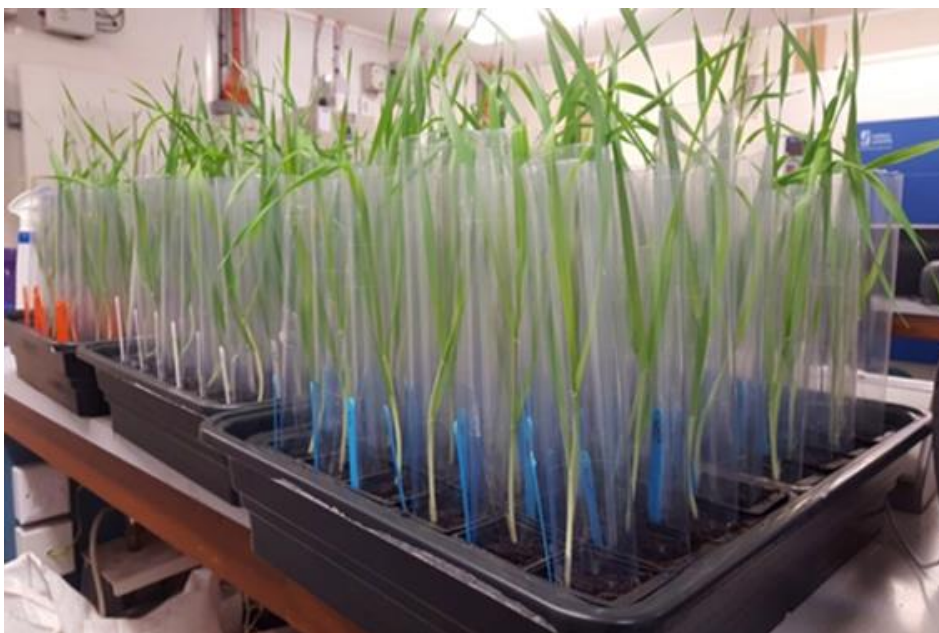


Figure 6 Clear plastic tubes used to keep plants upright and avoid damage during sampling.

## **Experimental design**

Two series of experiments were conducted. The first series was conducted on cv. Concerto and the second on cv. Fairing. In each series, chlorophyll

fluorescence images were captured on leaf 2 of intact plants (the youngest fully emerged leaf at the time of inoculation) using the MAXI-head version of the IMAGING-PAM M-Series Chlorophyll Fluorescence System (Walz, Effeltrich, Germany), resolution 1392 x 1040 pixels, which utilises ImagingWin software. Depending on the experimental series, other supporting measurements of disease development and photosynthetic activity were made. In series 1, no supplementary mineral nutrients were given. In series 2 additional nutrients were supplied twenty-eight days after sowing (14 d.p.i.). 0.06 ml of Liquid Growmore fertiliser solution (Doff Portland Ltd., Nottingham, UK) was added to 10 ml of water, then this solution was pipetted directly onto the surface of the soil at the base of the plants (10 ml of solution applied to each plant). The undiluted fertiliser solution contained 7 % Nitrogen (N), 7 % Phosphorus Pentoxide ( $P_2O_5$ ), and 7 % Potassium Oxide ( $K_2O$ ).

## **Experimental series 1**

### **Chlorophyll fluorescence imaging**

Chlorophyll fluorescence measurements were taken at six time points: 6, 8, 10, 13, 16, and 25 days post inoculation (d.p.i.) during photosynthetic induction in dark-adapted plants. The general induction process and calculation of fluorescence parameters were as described by Baker (2008). Leaves (leaf 2) from a single replicate of each treatment were placed in the Imaging PAM leaf holder and covered with a black cloth to exclude light. The instrument was also located in a dark room with green safe light to guard against light straying around the edges of the cloth. This arrangement of leaves allowed measurements on all treatments to be made simultaneously. The position of a given treatment within the holder was randomised for each measurement occasion and replicate.

Leaves were left to dark adapt for 30 min after which they were exposed to a weak measuring beam for 8 seconds to capture minimal, or dark, fluorescence ( $F_o$ ), then a saturating pulse was applied to capture maximal fluorescence ( $F_m$ ) (Figure 7).

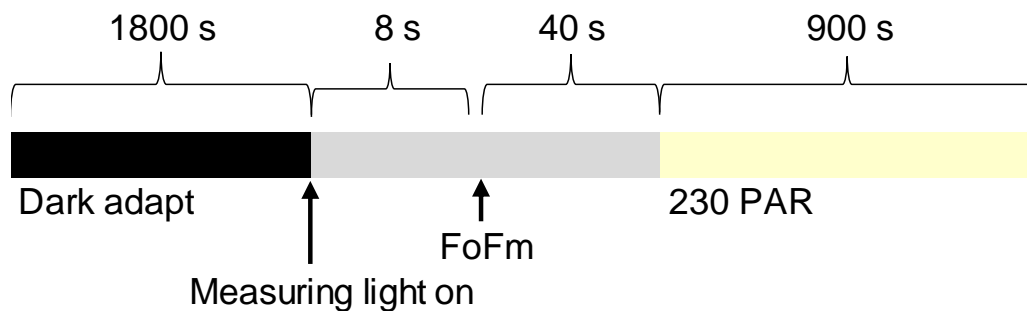


Figure 7 Light regime for chlorophyll fluorescence measurements in experimental series 1. PAR = Photosynthetically active radiation ( $\mu\text{mol m}^{-2} \text{s}^{-1}$ ).

Variable fluorescence ( $F_v$ ) was estimated as ( $F_m - F_o$ ). These values were used to calculate maximal efficiency of PSII ( $F_v/F_m$ ). Forty seconds after the measurement of minimal and maximal fluorescence (referred to here as the  $F_oF_m$  measurement), the actinic light was switched on at  $230 \mu\text{mol m}^{-2} \text{s}^{-1}$ . This light was provided by blue LED-lamps (450 nm). Over the next 15 minutes (940 s), as the plants adapted to the new light conditions, a saturating pulse was applied every 20 seconds to differentiate between non-photochemical quenching (NPQ) and photochemical quenching, or operating efficiency of PSII ( $\Phi\text{PSII}$ ). Electron transport rate (ETR) was given as  $0.5 \times \Phi\text{PSII} \times \text{PAR} \times \text{Leaf Absorptivity } \mu\text{equivalents m}^{-2} \text{s}^{-1}$ . The Absorptivity measurement was used as the common assumption of a PAR-Absorptivity of 0.84, i.e. that 84% of the incident photons of photosynthetically active radiation will be absorbed by a leaf, can be inaccurate in cases of diseased or senescing leaves. Red (660 nm) and near-infrared (780 nm) LED-lamps

were used to measure absorptivity. Leaves were illuminated with red, then near-infrared light. Absorptivity was then calculated pixel by pixel from the red and near-infrared light remission images captured by the camera, using this formula:

$$\text{Absorptivity of photosynthetically active light} = 1 - R/NIR$$

Where R = Red light remission: an inverse measure of the absorption of photosynthetically active radiation, and;

NIR = Near-infrared light remission: a measure of the remission of light that is not absorbed by photosynthetically active pigments.

## **Visual assessment of disease progress**

After completion of chlorophyll fluorescence imaging, a digital photograph of the leaves in the leaf holder was taken using a SONY® Cyber-shot DSC-HX9V camera. The visible disease severity (% area of leaf surface occupied by *Ramularia* leaf spot symptoms) was assessed visually for the section of leaf that had been used for chlorophyll fluorescence measurements. This was > 80% of the total leaf surface. The percentage of remaining green leaf area was also visually assessed.

## **DNA extraction and quantification**

The leaf was then excised from the plant, snap-frozen in liquid nitrogen directly, and stored at - 20°C to await analysis. Total DNA (leaf and pathogen) was extracted from leaf tissue using the Illustra Nucleon Phytopure Genomic DNA Extraction Kit (GE Healthcare Europe GmbH, Freiburg, Germany). Leaves were ground to a powder using liquid nitrogen in

a mortar and pestle. After DNA extraction, the quantity of DNA in each sample was measured using a Nanodrop. Samples were then diluted to 20 ng/μl. 5 μl of each diluted sample was used in a total reaction volume of 25 μl for Quantitative real-time PCR of *R. collo-cygni*, carried out using the method described in Taylor *et al.* (2010).

## Experimental series 2

These experiments were conducted using spring barley cv. Fairing. Growth conditions, and methodology for inoculations, DNA extraction and qPCR analysis were as described above.

### Chlorophyll fluorescence imaging

Chlorophyll fluorescence imaging measurements were taken at three time points: 10, 18, and 26 days post inoculation (d.p.i.). In order for photosynthetic characteristics to be investigated in relation to the development of specific lesions on the leaf, measurements were made non-destructively on the same set of leaves on each occasion. Leaves of a single replicate of each treatment were placed in the leaf holder and dark adapted as described for experimental series 1.  $F_v/F_m$  was then determined as described above and photosynthetic induction conducted over two levels of actinic irradiance; the first was  $230 \mu\text{mol m}^{-2} \text{s}^{-1}$  as before, and the second was  $530 \mu\text{mol m}^{-2} \text{s}^{-1}$  PAR (Figure 8). The Maxi head camera was set at a greater magnification than that in experimental series 1, giving a smaller field of view but greater resolution of events occurring around individual lesions (when present). After each full set of induction measurements, leaves were photographed, and plants were returned to the growth cabinet.

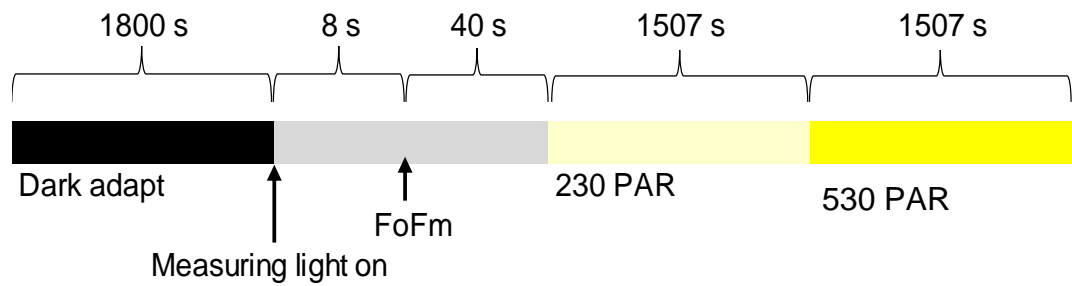


Figure 8 Light regime for chlorophyll fluorescence measurements in experimental series 2. PAR = Photosynthetically active radiation ( $\mu\text{mol m}^{-2} \text{s}^{-1}$ ).

## Transect analysis

Replicates from Experimental series 2 which had developed lesions on infected leaves by 18 or 26 days after inoculation were selected for use in this analysis. The chlorophyll fluorescence images used were those captured at steady state photosynthesis at  $230 \mu\text{mol m}^{-2} \text{s}^{-1}$  PAR, as described above. The ImagingWin software system was used to draw transects across the leaf images, allowing values for the chlorophyll fluorescence outputs of  $F_v/F_m$ , NPQ,  $\Phi\text{PSII}$  and ETR to be recorded pixel by pixel along each transect, thus capturing detailed, localised data on the pattern of photosynthetic activity across leaves at a single point in time. Transects were drawn across infected leaves, through one lesion in the upper leaf area (towards the leaf tip) and one lesion in the lower leaf area (towards the base), and in corresponding areas of control leaves. Transects were also drawn across areas of infected leaves which had no lesions, close to each transect through a lesion. Prior to analysis of chlorophyll fluorescence outputs, each lesion was visually

categorised as being either a small, developing lesion (category A) or a lesion at a more advanced stage of development (category B). Lesions that were selected for analysis at 18 days post inoculation were reanalysed at 26 days, and the direction and relative scale of the effects observed were summarised qualitatively for each lesion.

## **Infra-red gas analysis**

The same leaves were used on different measurement occasions for simultaneous measurement of leaf gas exchange (infra-red gas analysis) and light-adapted chlorophyll fluorescence (an area-averaged measure), using the LI-6400XT Portable Fluorescence System with the 6400-40 Leaf Chamber Fluorometer (LI-COR Biosciences, Lincoln, USA).

Net CO<sub>2</sub> uptake was measured using a flow rate of 300  $\mu\text{mol}$ , CO<sub>2</sub> concentration of 400 ppm and chamber air temperature of 18°C. A central section of leaf two was placed in the chamber and an irradiance of 260  $\mu\text{mol m}^{-2} \text{s}^{-1}$  provided at the leaf surface. The value of irradiance was selected because it was close to that used during the growth of plants in the growth cabinet. The leaf was allowed to acclimate for 20 minutes and the rate of CO<sub>2</sub> uptake to stabilise before readings commenced. Readings were then logged every minutes for a duration of five minutes.

The irradiance was then increased to 1500  $\mu\text{mol m}^{-2} \text{s}^{-1}$  to measure CO<sub>2</sub> uptake at light saturation. Readings were logged after allowing a further 20 minutes for leaves to adjust to the new light regime. The actinic light was then switched off and measurements of dark respiration logged over another five minute period. The measured chlorophyll fluorescence outputs were  $\Phi\text{PSII}$  and ETR. After gas exchange and fluorescence measurements had been completed the ramularia leaf spot severity and % green leaf area were

assessed visually on the upper surface of the section of leaf that was in the chamber.

## **Data and statistical analysis**

In experimental series 1, plants were organised into three randomised blocks in the growth cabinet, with each block containing 16 replicates (12 intended for use in the experiment, and four spare).

Leaves that had curled or twisted during measurements were excluded from the analysis. At 25 days after inoculation, leaf 2 of some individual replicates had completely senesced and become chlorotic. This included leaves of both control and *R. collo-cygni*-inoculated plants. As the primary objective was to measure the effects of *R. collo-cygni* on photosynthetic activity during the development of symptoms but prior to complete leaf senescence, any leaves that had no green area remaining were also excluded from the analysis. This accounted for three broth control leaves, two water control leaves and two infected leaves at day 25, but no leaves at earlier time points.

Data were analysed using either repeated measures or standard analysis of variance using GenStat software (19<sup>th</sup> Edition, VSN International, Hemel Hempstead, UK). Residuals were checked for normality of distribution and homogeneity of variance before analysis.

# Results

## Experimental series 1

### Fungal growth *in planta*

*R. collo-cygni* DNA was detected in plants inoculated with fungal mycelium throughout the experiment (Figure 9 and Table 2). A two-way ANOVA with time as a factor (Table 3) did not reveal a significant interaction between time and treatment. Fungal biomass in second leaves, as indicated by *R. collo-cygni* DNA, did not increase or decrease significantly during the experiment.

Table 2 Mean values for *R. collo-cygni* DNA quantity (ng/μl) in second leaves of barley seedlings during disease development.

	Days after inoculation				
	8	10	13	16	25
Broth	0.00	0.00	0.00	0.00	0.00
Rcc	0.20	0.17	0.11	0.15	0.14
Water	0.00	0.00	0.00	0.00	0.00

Table 3 ANOVA analysis results from a two-way ANOVA with inoculation treatment and time after inoculation as factors for *R. collo-cygni* DNA quantity in second leaves of barley seedlings during disease development.

	P value	I.s.d.
Treatment	<0.001	0.034
Days after inoculation	0.723	0.043
Treatment.Days after inoculation	0.839	0.075

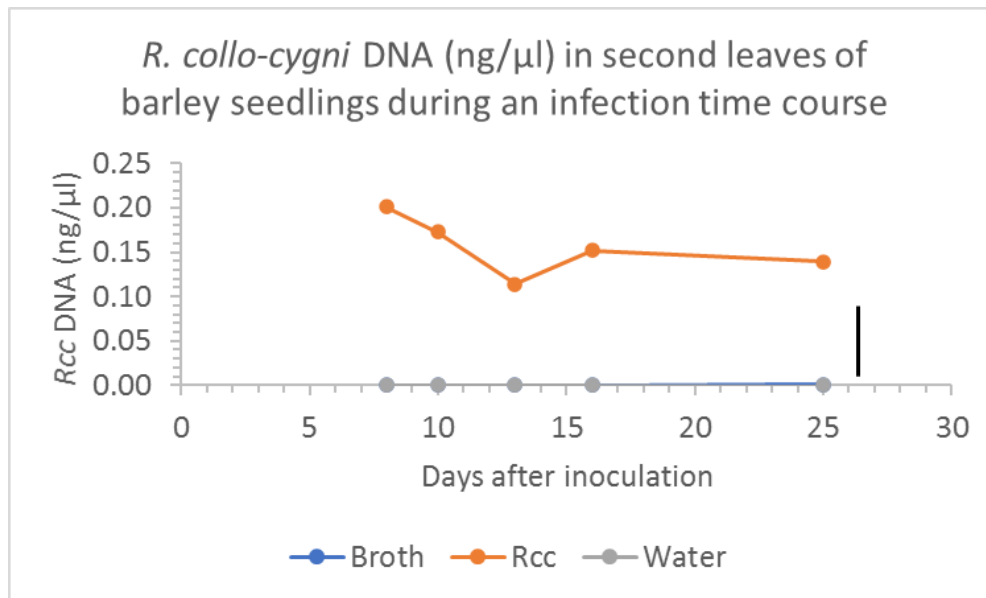


Figure 9 *R. collo-cygni* DNA in second leaves of barley seedlings cv. Concerto during disease development. Rcc = plants inoculated with *R. collo-cygni* mycelial suspension grown in Potato Dextrose Broth (PDB). Broth = plants inoculated with a control treatment of PDB. Water = plants inoculated with a control treatment of sterile distilled water. Black vertical line to the right of the graph represents the least significant difference (l.s.d.,  $P=0.05$ ) for Treatment.Days after inoculation from a two-way ANOVA with inoculation treatment and time as factors. Note that symbols for Broth treatment are hidden by those for Water.

## Visible symptom development and green leaf area

The first symptoms (lesions) were observed on one infected leaf around 10 days after inoculation (Figure 10 and Table 4).

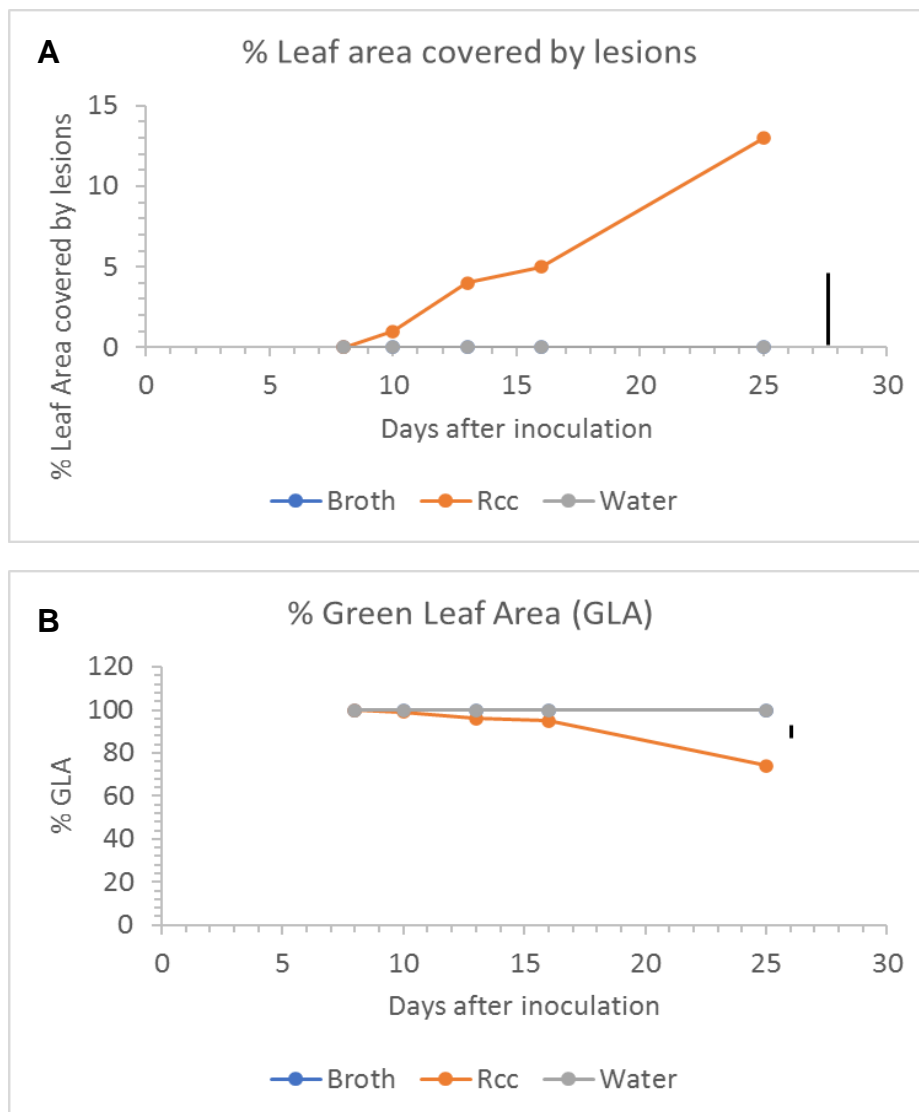


Figure 10 Visual disease progress over time. A) RLS lesion development and B) Green leaf area (both as percentages of total measured leaf area). Second leaves of barley cv. Concerto seedlings inoculated with *R. collo-cygni* (Rcc) and control leaves sprayed with water or potato dextrose broth. Black vertical lines to the right of the graphs represent the least significant difference (l.s.d.,  $P=0.05$ ) for Treatment.Days after inoculation from a two-way ANOVA with inoculation and time as factors. Symbols for Broth are hidden by those for Water.

Table 4 Mean % leaf area covered by lesions and mean % green leaf area (GLA) over an infection time course.

Treatment	Days after inoculation				
	8	10	13	16	25
% Lesions					
Broth	0.0	0.0	0.0	0.0	0.0
Rcc	0.0	0.8	4.2	4.8	12.5
Water	0.0	0.0	0.0	0.0	0.0
% GLA					
Broth	100.0	100.0	100.0	100.0	100.0
Rcc	100.0	99.2	95.8	95.2	73.8
Water	100.0	100.0	100.0	100.0	100.0

Symptoms had increased marginally on infected leaves by 16 days after inoculation, and by 25 days after inoculation an average of 13 % of the measured leaf area was covered by lesions in infected leaves. At both 13 and 16 days after inoculation, only one infected leaf (out of 5) displayed more advanced symptoms, with around 20 % of the measured leaf area covered by lesions. Other infected leaves at these time points had either no or very mild symptoms, with only 0 – 2 % of the measured leaf area covered by lesions. By 25 days after inoculation symptoms were more advanced in all infected leaves, however there was still some variation, with the percentage of measured leaf area covered by lesions ranging from 5 – 20 %. Water and broth controls remained free of any lesions throughout the experiment.

Control plants maintained 100 % green leaf area (GLA) within the measured area throughout the experiment (Figure 10 and Table 4). Infected leaves lost 5 % of GLA on average by 16 days after inoculation, then a further 20 % by 25 days after inoculation. The % GLA observed in infected leaves at 25 days after inoculation ranged from 60 – 95 %. GLA was reduced in infected leaves by a combination of lesions and, in some cases, areas of chlorotic tissue extending beyond the lesions (Figure 11).

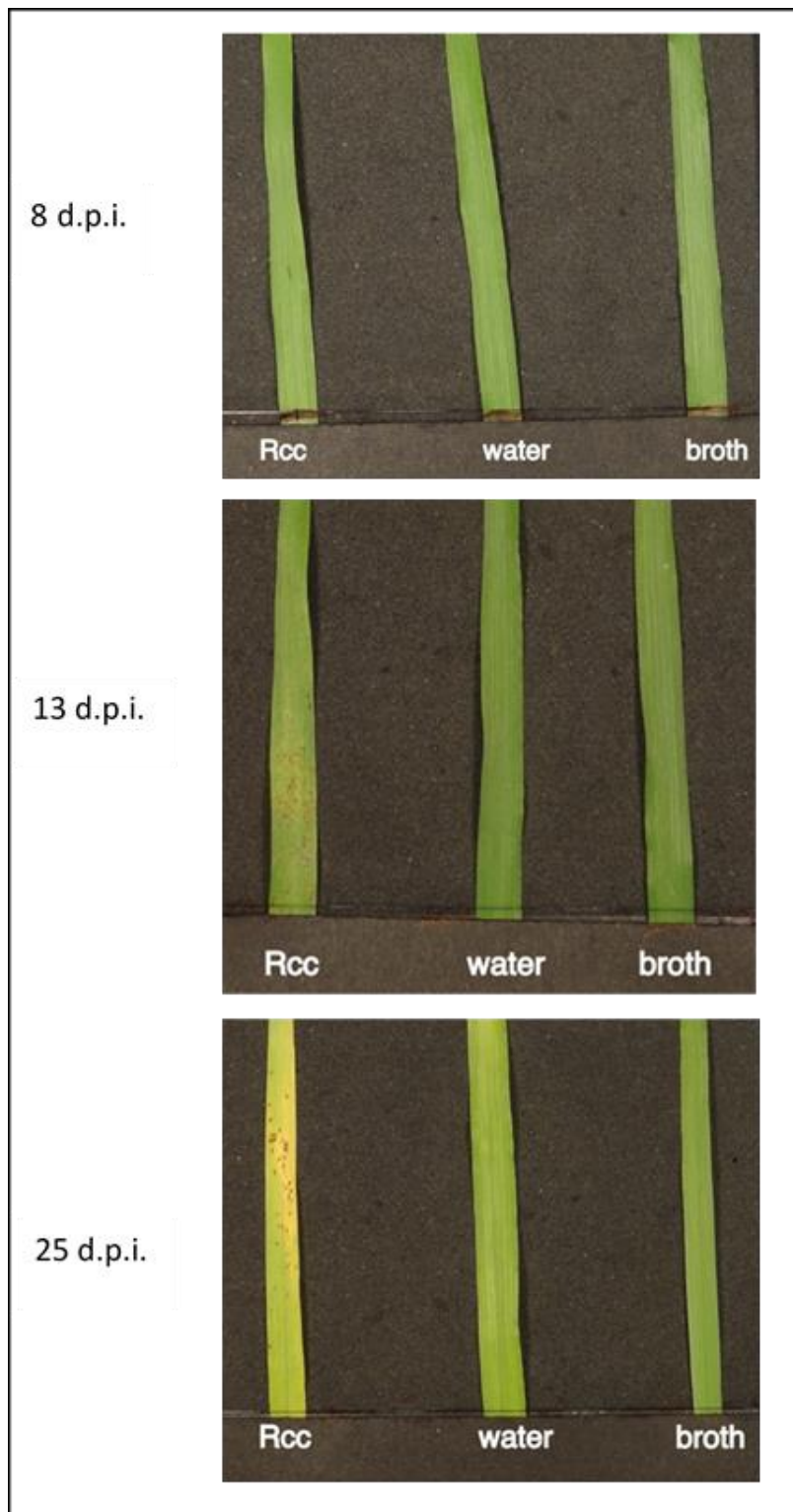


Figure 11 Photographs of second leaves of barley cv. Concerto seedlings inoculated with *R. collo-cygni* (Rcc) and control leaves sprayed with water or potato dextrose broth. Photographs taken at 8, 13 and 25 days post inoculation (d.p.i.).

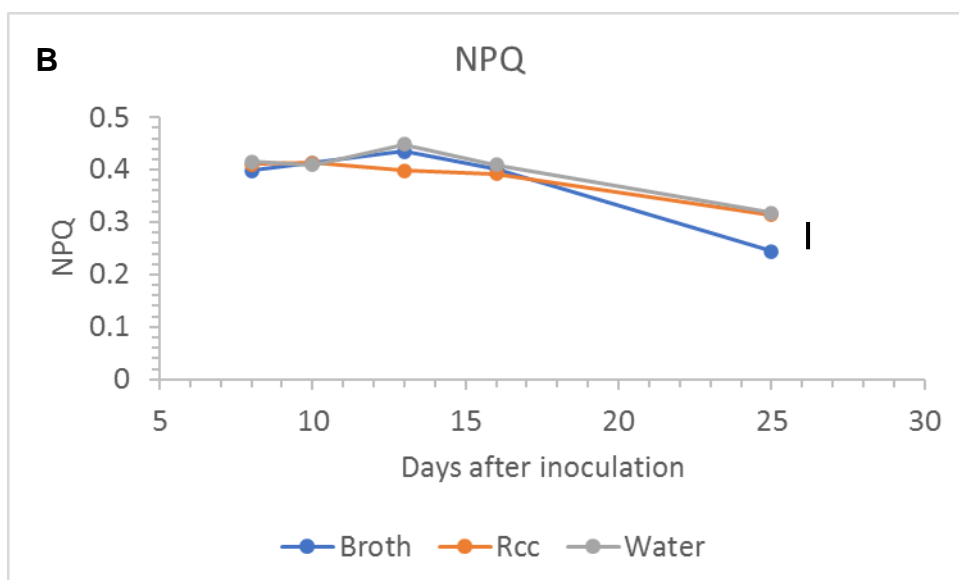
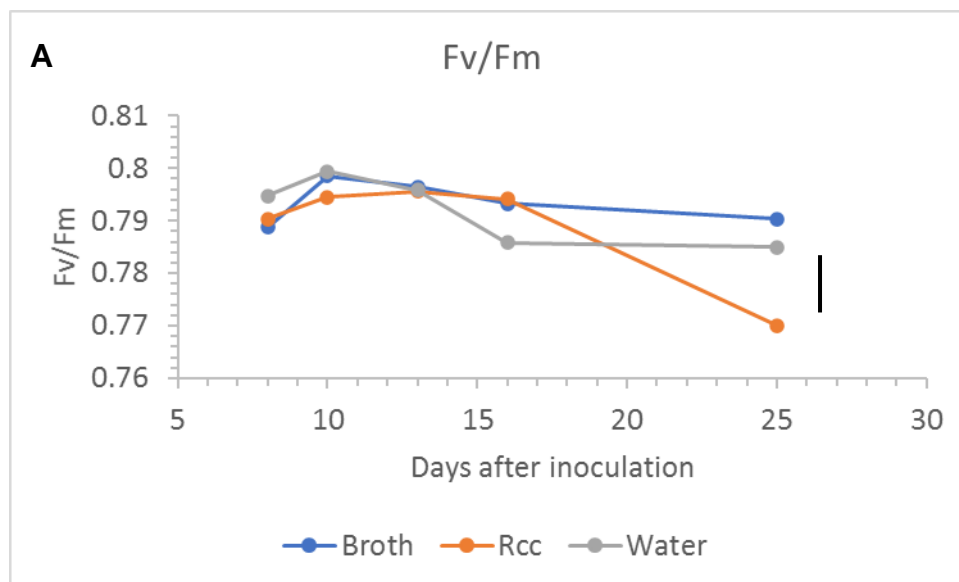
## Chlorophyll fluorescence imaging

### Chlorophyll fluorescence imaging – steady state photosynthesis

Maximal efficiency of PSII (Fv/Fm) (Figure 12 & Table 5) increased with leaf age for all treatments until 10 days after inoculation.

Table 5 Mean values for chlorophyll fluorescence parameters at steady state ( $230 \mu\text{mol m}^{-2} \text{s}^{-1}$ ), measured in second leaves of barley seedlings over an infection time course.

	Days after inoculation				
	8	10	13	16	25
Fv/Fm					
Broth	0.79	0.80	0.80	0.79	0.79
Rcc	0.79	0.79	0.80	0.79	0.77
Water	0.79	0.80	0.80	0.79	0.79
NPQ					
Broth	0.40	0.41	0.44	0.40	0.24
Rcc	0.41	0.41	0.40	0.39	0.31
Water	0.42	0.41	0.45	0.41	0.32
$\phi\text{PSII}$					
Broth	0.46	0.45	0.46	0.45	0.24
Rcc	0.44	0.45	0.46	0.43	0.30
Water	0.44	0.45	0.45	0.41	0.31
ETR					
Broth	45.61	44.91	45.71	44.52	22.69
Rcc	43.24	44.13	44.44	41.83	25.09
Water	43.82	44.32	44.96	40.44	30.03



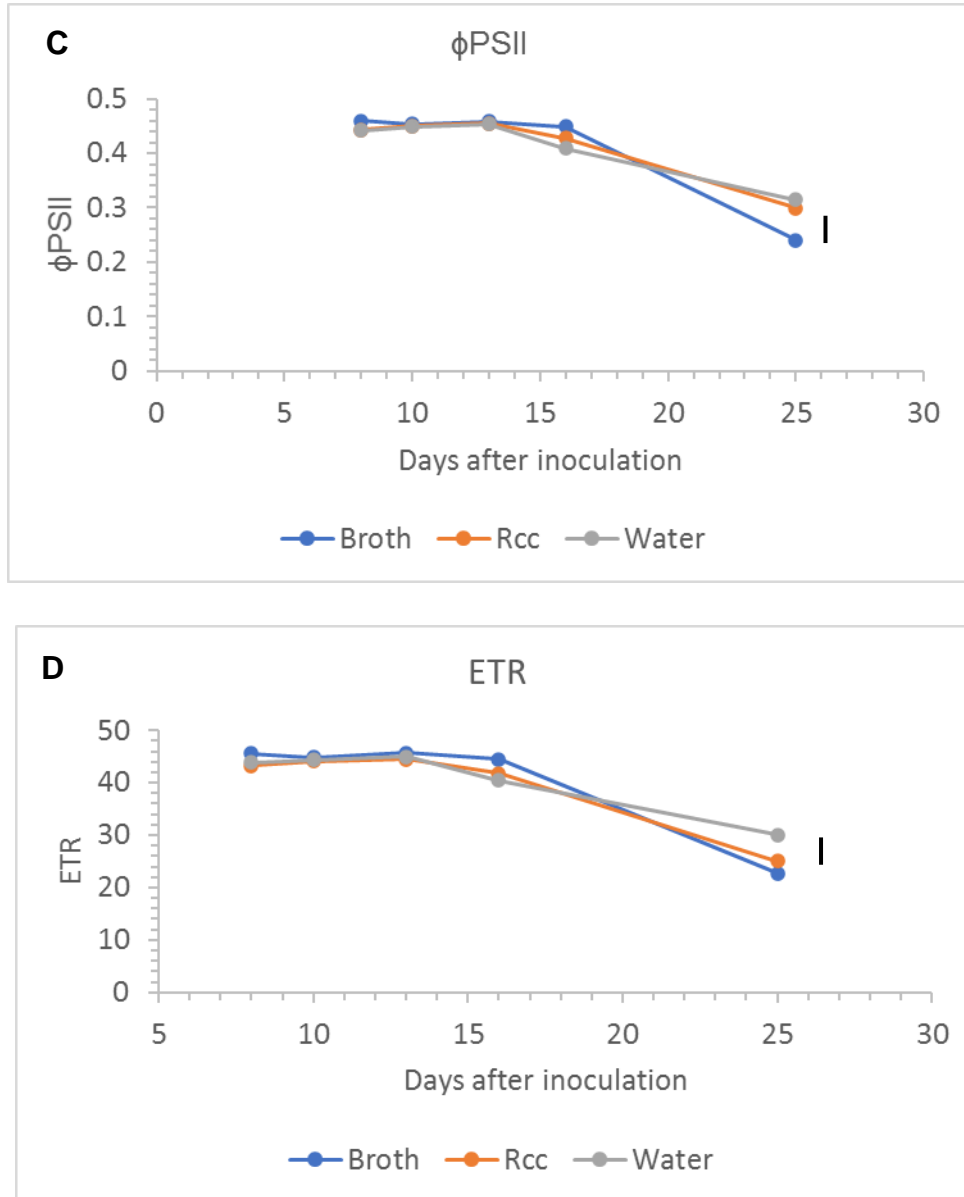


Figure 12 Chlorophyll fluorescence parameters: A) Maximal efficiency of PSII ( $F_v/F_m$ ); B) Non-photochemical quenching (NPQ); C) Operating efficiency of PSII ( $\phi\text{PSII}$ ); D) Electron Transport Rate (ETR) at steady state photosynthesis ( $230 \mu\text{mol m}^{-2}\text{s}^{-1}$  PAR), measured in second leaves of barley seedlings over an infection time course.

Values peaked by 10 days after inoculation for control plants, and by 13 days after inoculation for plants infected with *R. collo-cygni*. Fv/Fm values dropped between 13 and 16 days after inoculation for all treatments. Between 16 and 25 days after inoculation, values for control plants remained relatively stable, while values for infected plants dropped again, coinciding with increasing symptom severity. A two-way ANOVA (Table 6) found a close to significant ( $P = 0.053$ ) effect of treatment. The interaction between treatment and time had a  $P$  value of 0.069 indicating a weak effect.

Table 6 ANOVA results for comparison of chlorophyll fluorescence at steady state.

	P value	I.s.d.
Fv/Fm		
Treatment	0.053	0.005
Days after inoculation	<0.001	0.006
Treatment.Days after inoculation	0.069	0.010
NPQ		
Treatment	0.233	0.026
Days after inoculation	<0.001	0.033
Treatment.Days after inoculation	0.329	0.058
$\phi$ PSII		
Treatment	0.962	0.020
Days after inoculation	<0.001	0.026
Treatment.Days after inoculation	0.058	0.044
ETR		
Treatment	0.578	2.101
Days after inoculation	<0.001	2.712
Treatment.Days after inoculation	0.114	4.697

The effects of inoculation treatments on operating efficiency of PSII ( $\phi$ PSII), non-photochemical quenching (NPQ) and Electron Transport Rate (ETR) at the end of the induction period after the leaves had reached steady state are presented in Figure 12 and Table 5. A two-way ANOVA found no significant effect of treatment on steady state photosynthesis during this experiment but

photosynthetic parameters did change significantly ( $P < 0.001$ ) with time (Table 6).  $\Phi PSII$  values remained quite stable throughout the infection time course. By 25 days after inoculation  $\Phi PSII$  values had dropped in both infected and control plants. Steady state NPQ values rose for control plants between 8 and 13 days after inoculation, however no increase was observed in infected plants. There was a reduction in steady state NPQ values for both infected and control plants between 16 and 25 days after inoculation. Steady state ETR values remained quite stable until 16 days after inoculation. There was a reduction in steady state ETR values for both infected and control plants between 16 and 25 days after inoculation.

### **Chlorophyll fluorescence imaging – quenching analysis**

An analysis of the whole light induction curve was conducted at each sampling time (days after inoculation) to investigate whether inoculation treatments had any effect on chlorophyll fluorescence variables not observed after steady state had been reached. The analysis was by repeated measures ANOVA using time after the actinic light was switched on as the repeated measure factor. For each of the fluorescence variables,  $\Phi PSII$ , NPQ and ETR, there was a significant ( $P < 0.001$ ) effect of time, but no significant effect of treatment nor interaction between treatment and time for any of the sampling dates (Table 7). This indicates that the induction kinetics were similar across all treatments regardless of the date the leaves were sampled after inoculation. Mean induction curves for days 8, 13 and 25 are presented in Figure 13, Figure 14 and Figure 15 as examples. They illustrate changes in the induction kinetics with leaf ageing.

Table 7 P values from repeated measures ANOVA during photosynthetic induction of dark-adapted plants over an infection time course.

Number of reps	Days after inoculation	$\phi$ PSII P values			I.s.d. values for Time.Treatment
		Time	Treatment	Time.Treatment	
4	8	<0.001	0.941	0.469	0.048
6	10	<0.001	0.65	0.864	0.028
5	13	<0.001	0.981	0.955	0.066
4	16	<0.001	0.068	0.381	0.042
3	25	<0.001	0.602	0.497	0.046
Number of reps	Days after inoculation	NPQ P values			I.s.d. values for Time.Treatment
		Time	Treatment	Time.Treatment	
4	8	<0.001	0.876	0.838	0.064
6	10	<0.001	0.533	0.826	0.050
5	13	<0.001	0.51	0.666	0.066
4	16	<0.001	0.352	0.676	0.058
3	25	<0.001	0.578	0.750	0.060
Number of reps	Days after inoculation	ETR P values			I.s.d. values for Time.Treatment
		Time	Treatment	Time.Treatment	
4	8	<0.001	0.997	0.422	5.124
6	10	<0.001	0.916	0.771	3.804
5	13	<0.001	0.982	0.955	6.711
4	16	<0.001	0.066	0.386	5.770
3	25	<0.001	0.722	0.672	4.614

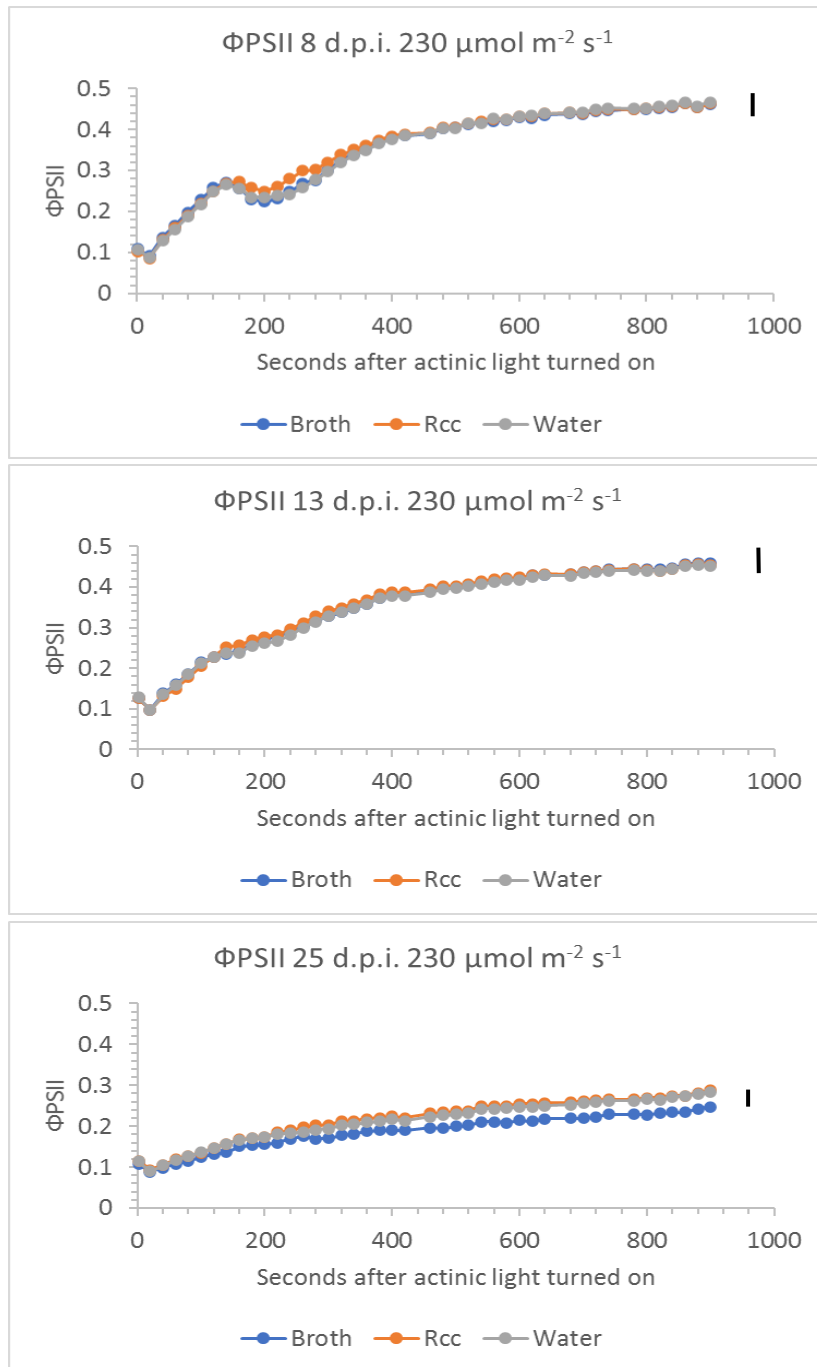


Figure 13 Photosynthetic operating efficiency ( $\Phi_{PSII}$ ) measured during photosynthetic induction of dark-adapted leaves with an actinic irradiance of  $230 \mu\text{mol m}^{-2} \text{s}^{-1}$  PAR. Each point is the mean of 4 (8 dpi), 5 (13 dpi) and 3 (25 dpi) replicates. Black vertical lines to the right of the graphs represent the least significant difference (l.s.d.,  $P=0.05$ ) for Time.Treatment from a repeated measures ANOVA.

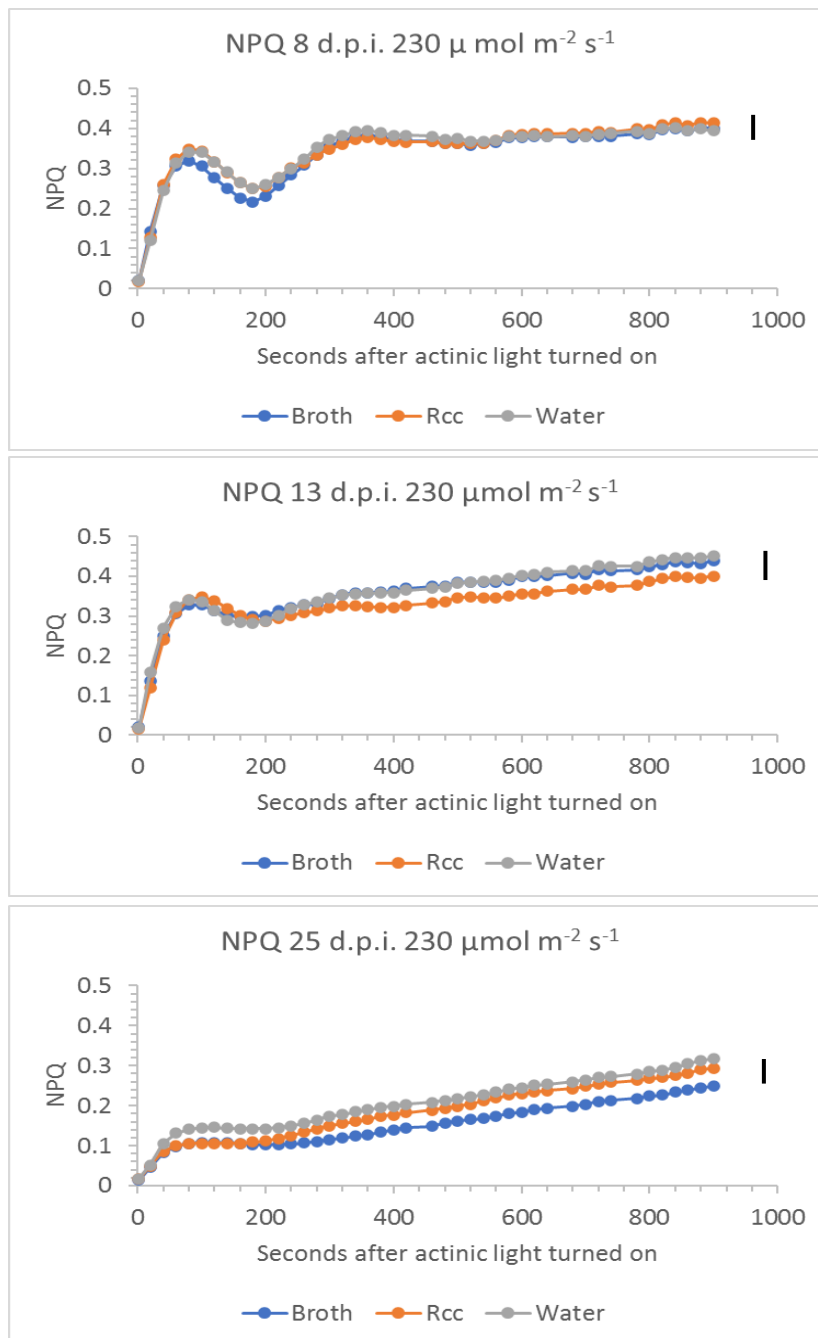


Figure 14 Non-photochemical quenching (NPQ) measured during photosynthetic induction of dark-adapted leaves with an actinic irradiance of  $230 \mu\text{mol m}^{-2} \text{s}^{-1}$  PAR. Each point is the mean of 4 (8 dpi), 5 (13 dpi) and 3 (25 dpi) replicates. Black vertical lines to the right of the graphs represent the least significant difference (l.s.d.,  $P=0.05$ ) for Time.Treatment from a repeated measures ANOVA.

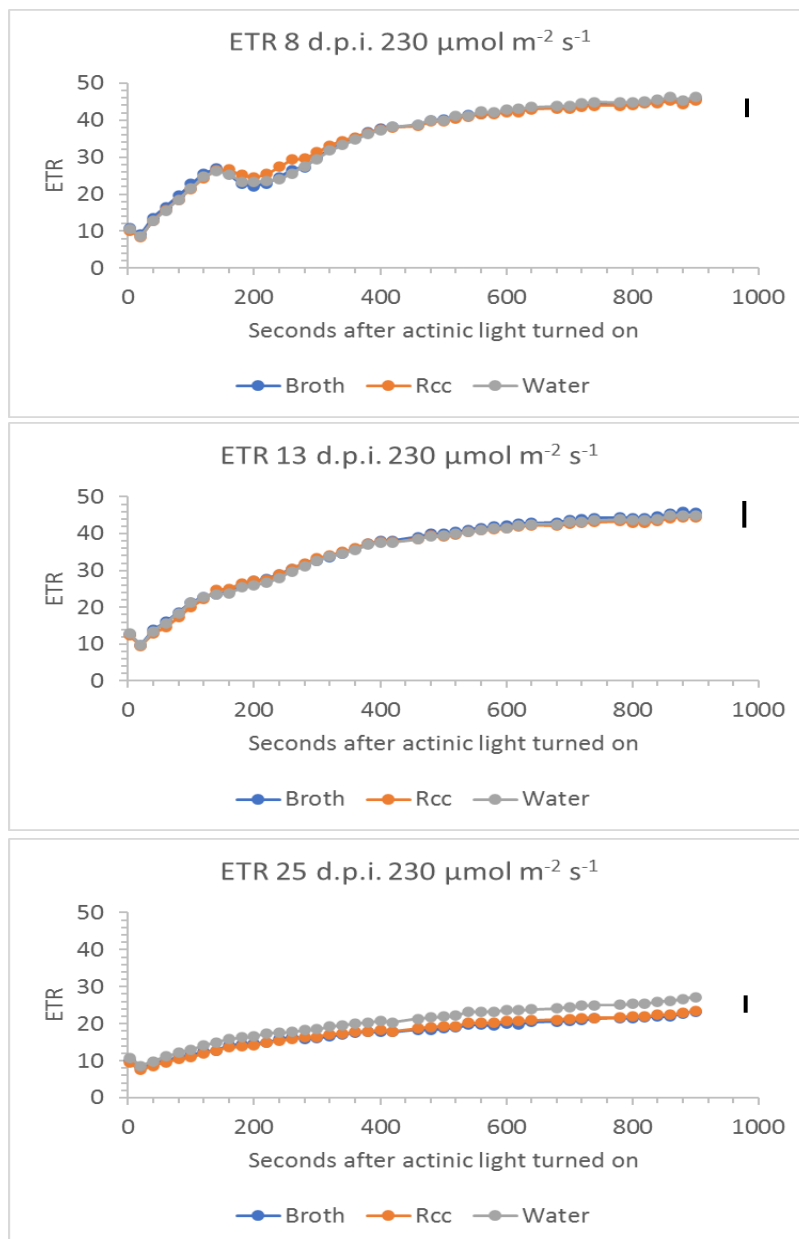


Figure 15 Electron transport rate (ETR) measured during photosynthetic induction of dark-adapted leaves with an actinic irradiance of  $230 \mu\text{mol m}^{-2} \text{s}^{-1}$  PAR. Each point is the mean of 4 (8 dpi), 5 (13 dpi) and 3 (25 dpi) replicates. Black vertical lines to the right of the graphs represent the least significant difference (l.s.d.,  $P=0.05$ ) for Time.Treatment from a repeated measures ANOVA.

In leaves sampled eight days after inoculation,  $\Phi$ PSII values rose steadily after the actinic light was switched on, before levelling out once steady state photosynthesis was reached (Figure 13). A slight dip in  $\Phi$ PSII values was observed for all treatments around 200 s. A similar pattern occurred at subsequent sampling points (13 and 25 dai), although no dip was observed during the induction period. By 25 days after inoculation,  $\Phi$ PSII values increased less rapidly through the induction period and the final values were substantially lower than at previous sampling points in both infected and control plants.

Eight days after inoculation NPQ values rose rapidly for all treatments until around 80 s after the actinic light was switched on, at which point a transient drop to lower values was observed, before values rose again more slowly until steady state was achieved (Figure 14). Steady state was reached at around 320 s after the actinic light was switched on. As leaves aged this pattern of NPQ changed. The initial peak and transient drop in NPQ between 80 and 180 s was less pronounced and the slow rise in NPQ after 180 s continued for the entire measurement period suggesting a steady state was not achieved for NPQ in the older leaves. By 25 days after inoculation, NPQ values throughout the induction curve were lower than at previous sampling points in both infected and control plants.

The induction kinetics for ETR followed the same pattern as  $\Phi$ PSII (Figure 15). Thus, there was an initial peak at 140 s followed by a transient dip at 200s before the rise to steady state by the end of the measurement period. As leaves aged, the transient changes were lost and the increase in ETR was less rapid.

## **Experimental series 2**

Experimental series 2 used barley seedlings cv. Fairing. In this experimental series, the same set of leaves were measured at each time point. Chlorophyll fluorescence imaging and infra-red gas analysis were both used to measure the same set of leaves. A higher actinic light intensity period was included in the chlorophyll fluorescence imaging protocol, in addition to the PAR 230  $\mu\text{mol m}^{-2} \text{s}^{-1}$  used in experimental series 1, and an additional analysis was conducted on transects taken across chlorophyll fluorescence images of leaves.

### **Visible symptom development and green leaf area**

In Experimental series 2, the first symptoms were observed on infected leaves around 18 days after inoculation (Figure 16). Between 18 and 26 days after inoculation, the mean percentage of the infected leaves covered by lesions increased from 2 % to 5 %. The mean % green leaf area of infected leaves fell from 100 % to 86 %, between 18 and 26 days after inoculation. The control treatments did not develop any symptoms. Overall, visible symptom expression was quite low in this experiment.

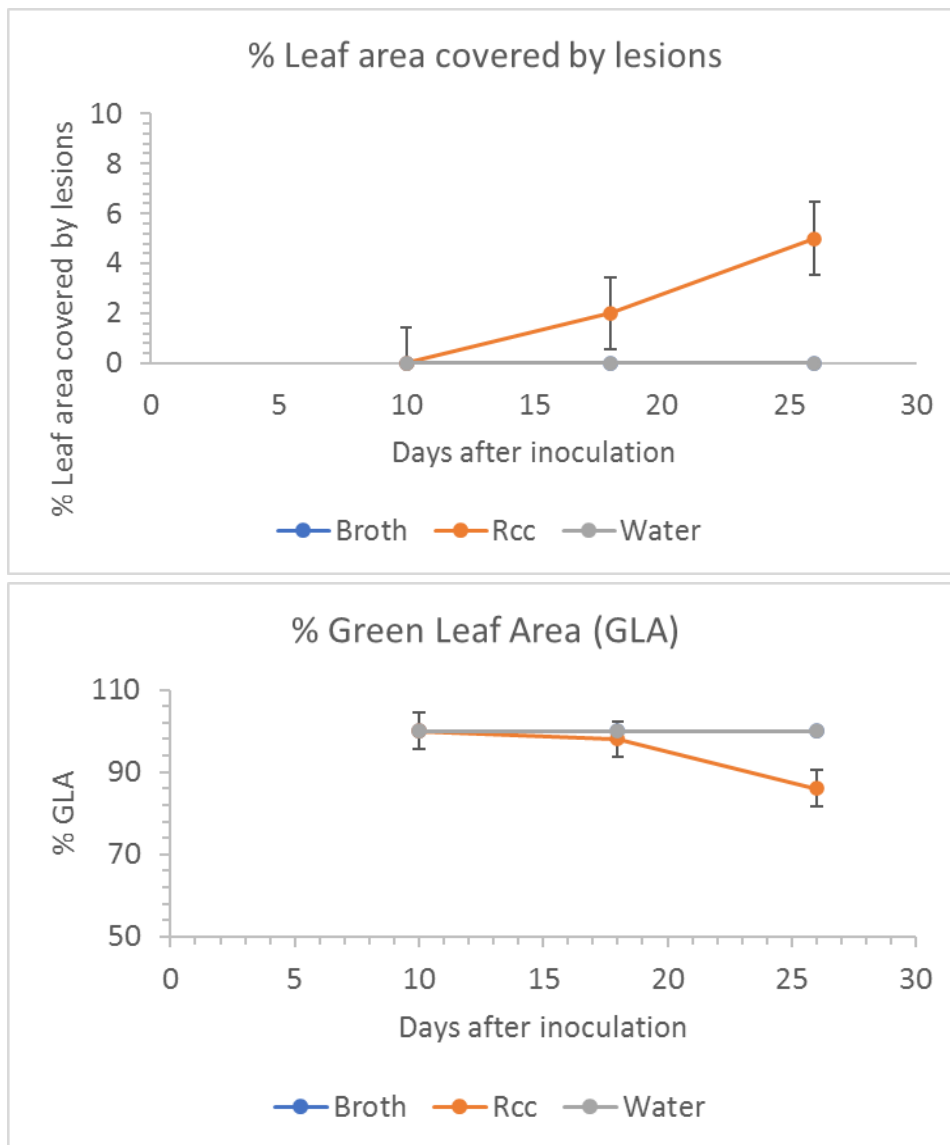


Figure 16 *Ramularia* leaf spot severity (%) and % green leaf area (GLA) of second leaves of barley seedlings cv. Fairing over the time course of an infection. Values are means  $\pm$  SEM of 6 replicates. Treatments: Rcc = plants inoculated with *R. collo-cygni* mycelial suspension grown in Potato Dextrose Broth (PDB). Broth = plants inoculated with a control treatment of PDB. Water = plants inoculated with a control treatment of sterile distilled water. Symbols for broth treated plants are hidden by those for water controls.

## Chlorophyll fluorescence imaging

Results from 10 d.p.i do not include measurements taken at the higher light level, as leaf movement during the time these measurements were being taken rendered them invalid. Fv/Fm value averages for all treatments decreased slightly over time, although none dropped below 0.801, and the treatments did not differ significantly ( $P>0.05$ ) from each other at any of the three time points when measurements were taken (Figure 17 and Table 8). There was a greater decrease in Fv/Fm value for infected leaves between 18 and 26 d.p.i., after symptom appearance, than for control treatments. Fv/Fm values decreased by 0.009, 0.002 and 0.001 for infected, broth-control, and water-control treatments respectively between 18 and 26 d.p.i.

Table 8 P values for chlorophyll fluorescence parameters at steady state photosynthesis.

Days after inoculation	Minimum number of reps	Actinic light intensity ( $\mu\text{mol m}^{-2} \text{s}^{-1}$ )	Variable	P value
10	4	230	Fv/Fm	0.614
10	4	230	$\Phi\text{PSII}$	0.704
10	4	230	NPQ	0.376
10	4	230	ETR	0.584
18	6	230	Fv/Fm	0.697
18	6	230	$\Phi\text{PSII}$	0.355
18	6	230	NPQ	0.466
18	6	230	ETR	0.412
18	6	<b>530</b>	$\Phi\text{PSII}$	0.386
18	6	<b>530</b>	NPQ	0.604
18	6	<b>530</b>	ETR	0.443
26	5	230	Fv/Fm	0.530
26	5	230	$\Phi\text{PSII}$	0.789
26	5	230	NPQ	0.402
26	5	230	ETR	0.465
26	4	<b>530</b>	$\Phi\text{PSII}$	0.647
26	4	<b>530</b>	NPQ	0.070
26	4	<b>530</b>	ETR	0.501

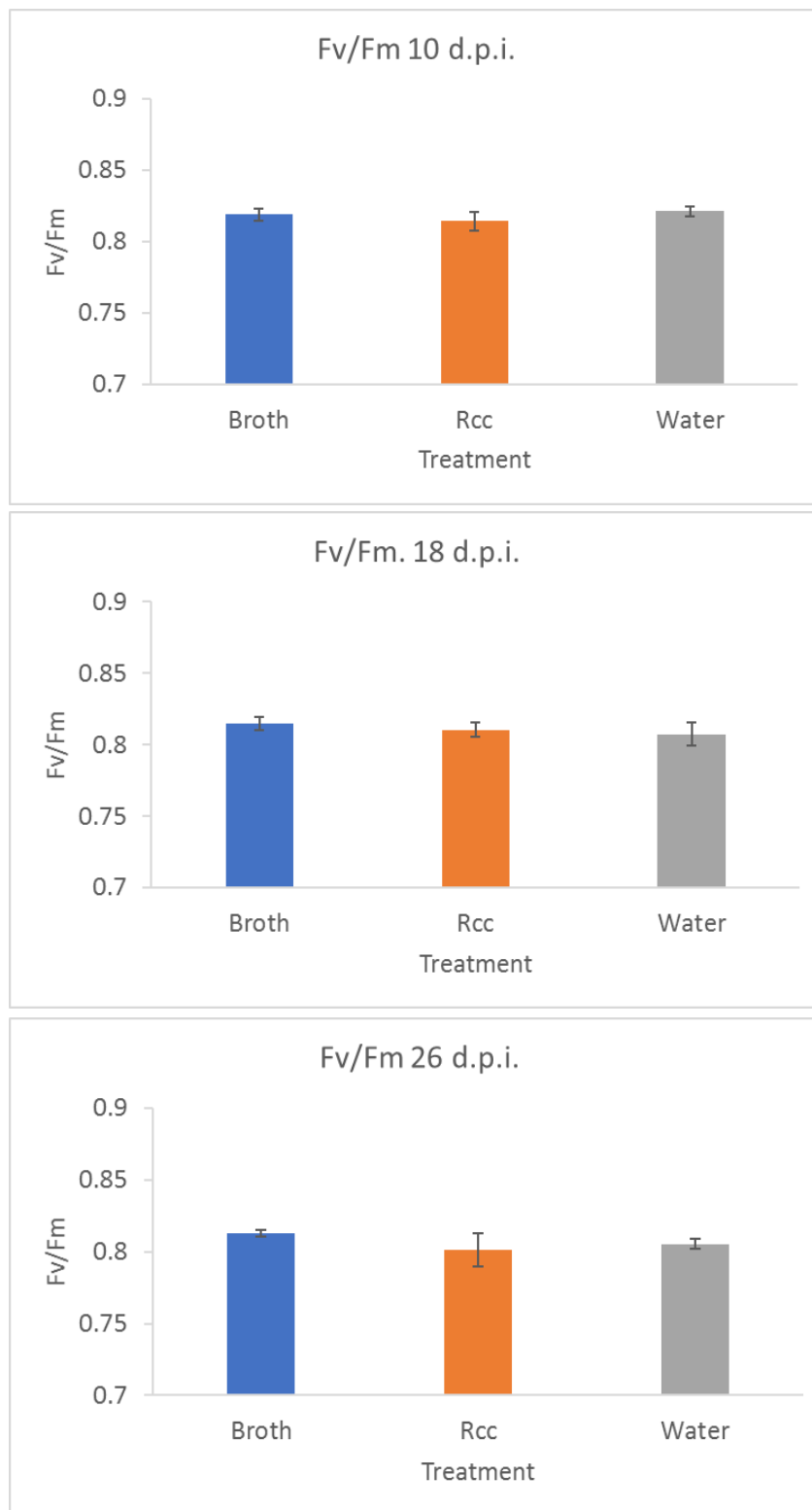


Figure 17 Maximal efficiency of PSII (Fv/Fm). N = at least 5.

## Chlorophyll fluorescence imaging – steady state

Steady state  $\Phi_{PSII}$  values did not differ ( $P>0.05$ ) between treatments at either actinic irradiance or measurement occasion (Figure 18 and Table 8). The operating efficiency ( $\Phi_{PSII}$ ) was greater at the growth irradiance of  $230 \mu\text{mol m}^{-2} \text{s}^{-1}$  PAR than  $530 \mu\text{mol m}^{-2} \text{s}^{-1}$  PAR. For all treatments  $\Phi_{PSII}$  also decreased over time.

Steady state NPQ values did not differ ( $P>0.05$ ) between treatments at either actinic irradiance or measurement occasion (Figure 19 & Table 8). NPQ was greater at an irradiance of  $530 \mu\text{mol m}^{-2} \text{s}^{-1}$  PAR than the growth irradiance of  $230 \mu\text{mol m}^{-2} \text{s}^{-1}$  PAR on all measurement occasions.

Similarly, ETR did not differ ( $P>0.05$ ) between treatments at either actinic irradiance or measurement occasion (Figure 20 and Table 8). The electron rate was greater at an irradiance of  $530 \mu\text{mol m}^{-2} \text{s}^{-1}$  PAR than the growth irradiance of  $230 \mu\text{mol m}^{-2} \text{s}^{-1}$  PAR. As with  $\Phi_{PSII}$ , ETR declined with leaf age (d.p.i).

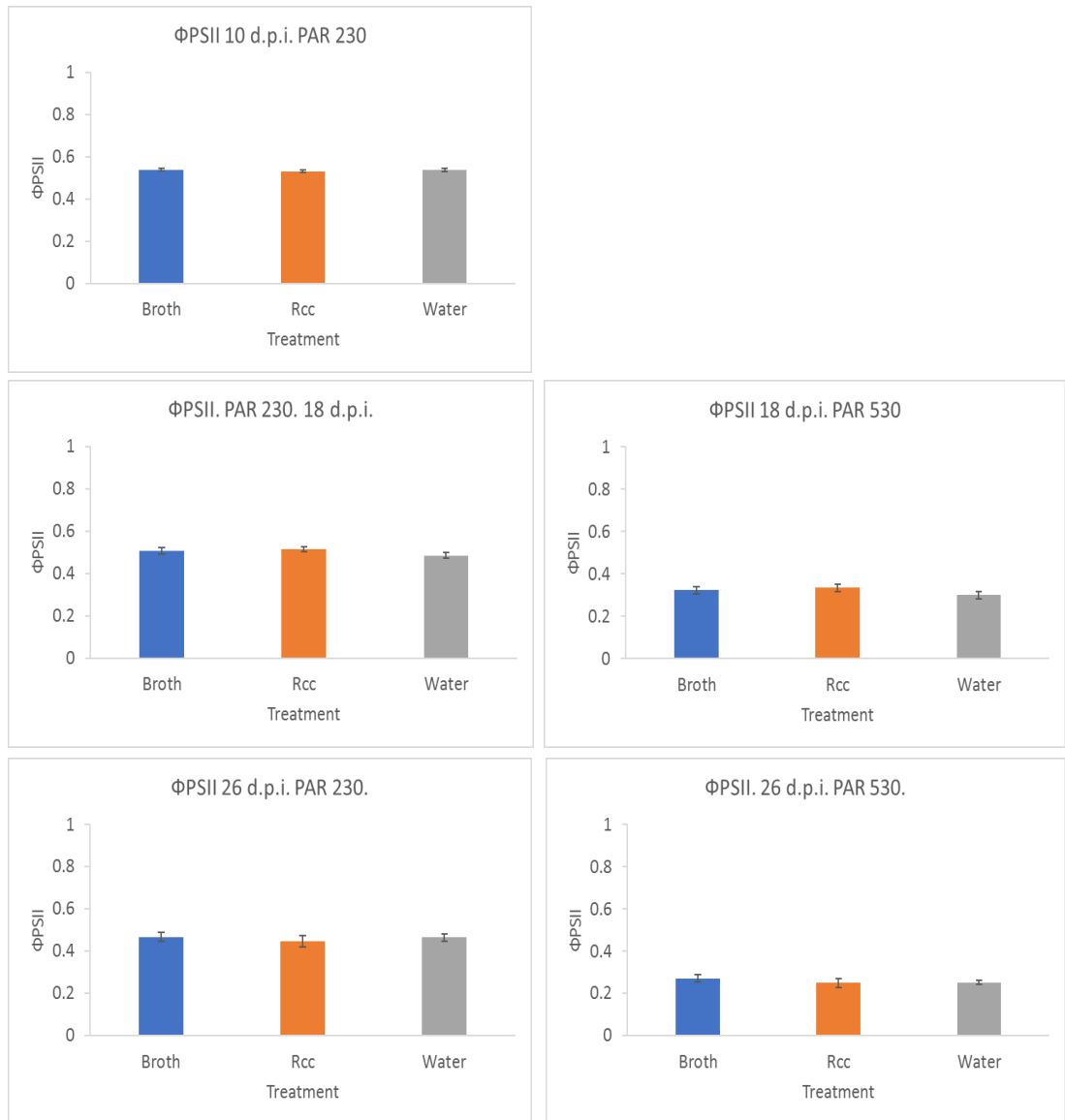


Figure 18  $\Phi_{PSII}$  at steady state photosynthesis. At 10 d.p.i.  $n =$  at least 4. At 18 d.p.i.  $n = 6$  for both light intensities. At 26 d.p.i.  $n =$  at least 5 for  $230 \mu\text{mol m}^{-2} \text{s}^{-1}$  and at least 4 for  $530 \mu\text{mol m}^{-2} \text{s}^{-1}$ .

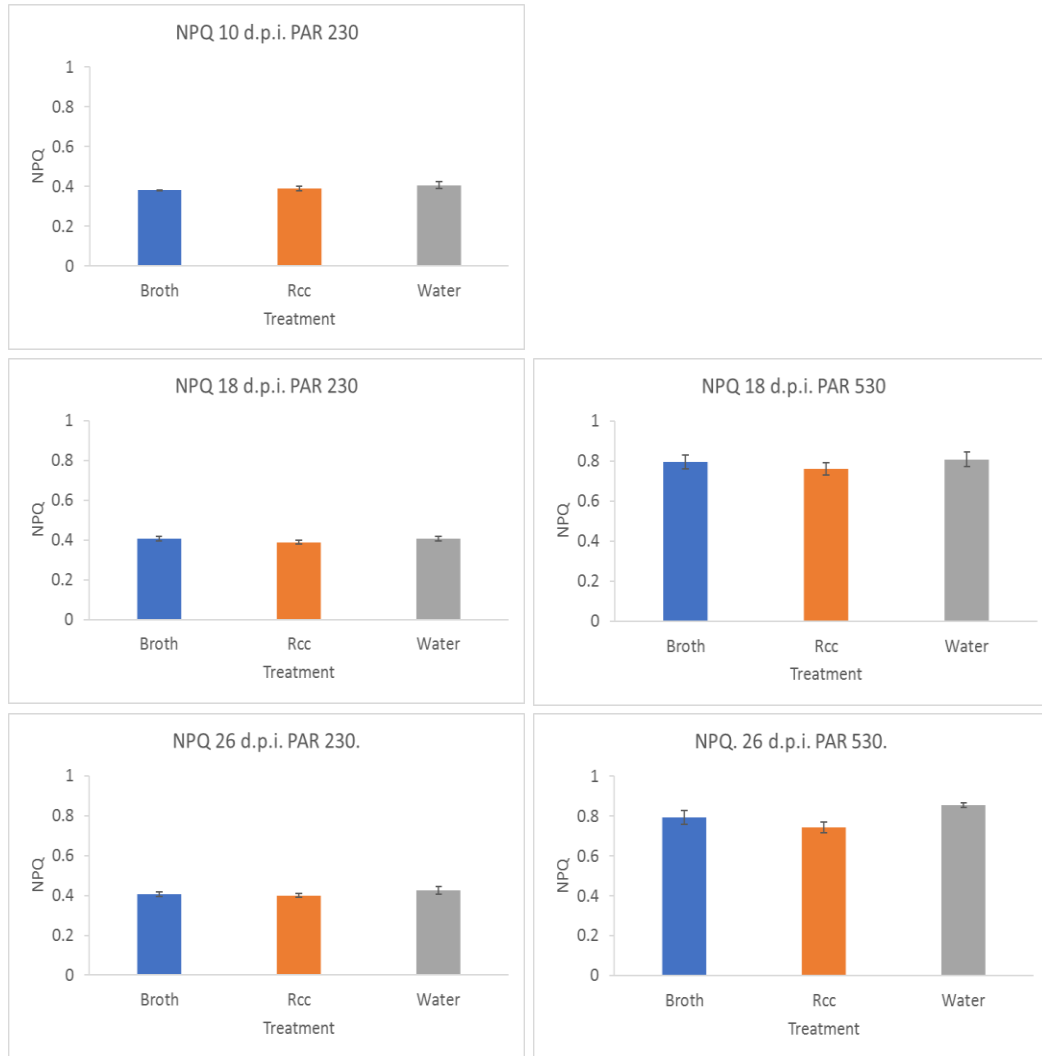


Figure 19 NPQ at steady state photosynthesis. At 10 d.p.i. n = at least 4. At 18 d.p.i. n = 6 for both light intensities. At 26 d.p.i. n = at least 5 for 230  $\mu\text{mol m}^{-2} \text{s}^{-1}$  and at least 4 for 530  $\mu\text{mol m}^{-2} \text{s}^{-1}$ .

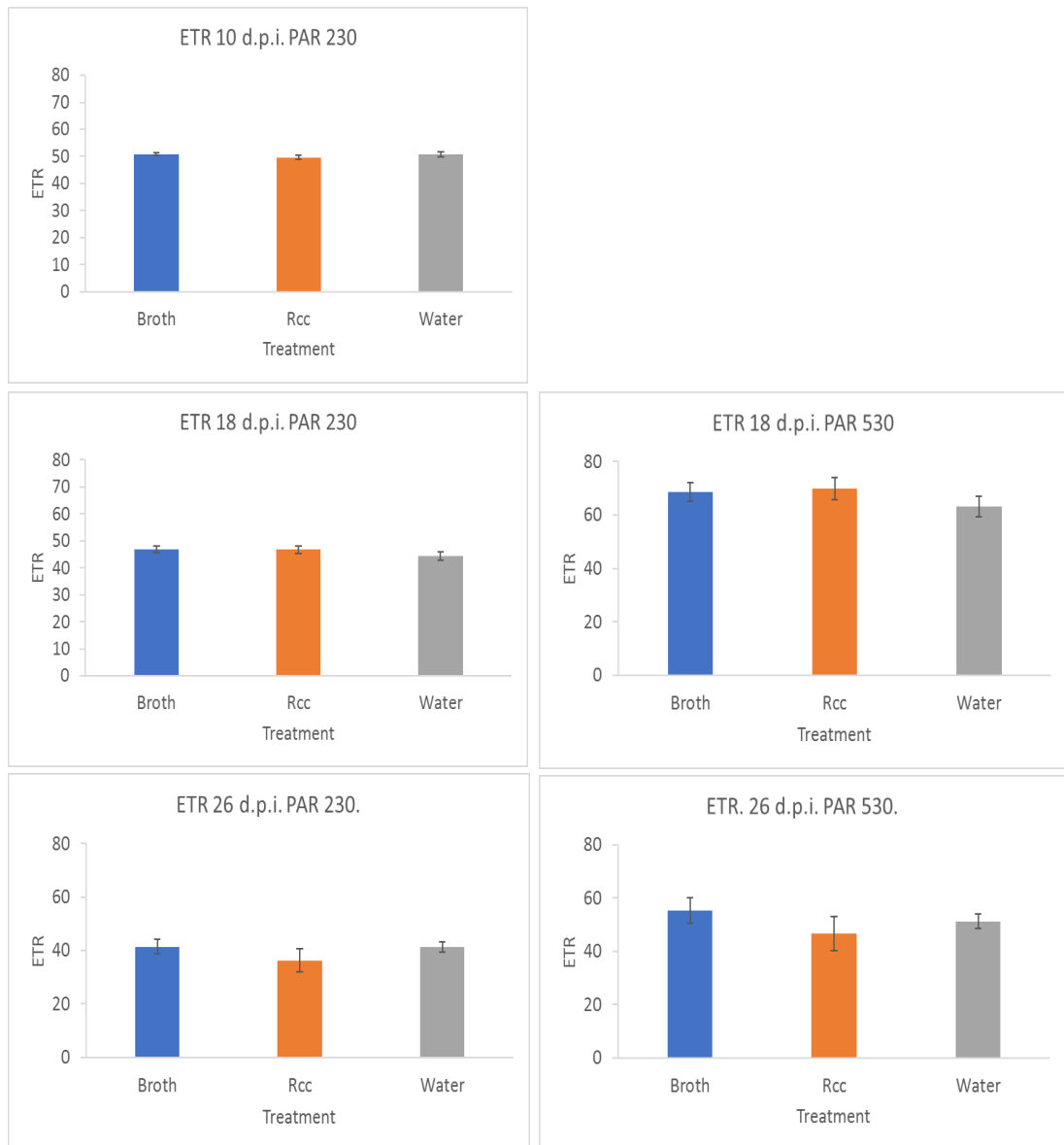


Figure 20 ETR at steady state photosynthesis. At 10 d.p.i.  $n =$  at least 4. At 18 d.p.i.  $n = 6$  for both light intensities. At 26 d.p.i.  $n =$  at least 5 for  $230 \mu\text{mol m}^{-2} \text{s}^{-1}$  and at least 4 for  $530 \mu\text{mol m}^{-2} \text{s}^{-1}$ .

## Chlorophyll fluorescence imaging – quenching analysis

An analysis of each stage of the induction curve (i.e. after the initial actinic light was switched on and again after its irradiance was increased to 530  $\mu\text{mol m}^{-2} \text{s}^{-1}$ ) was conducted by repeated measures ANOVA, where time during induction was the repeated measure. The aim was to determine whether treatments had discernible effects on the induction kinetics prior to the attainment of steady state. The analysis did not reveal any significant treatment effects or interactions between treatment and time at either light intensity for  $\phi\text{PSII}$ , NPQ or ETR at any stage of this experiment (Table 9). The full induction curves are shown in Figure 21, Figure 22 and Figure 23.

Table 9 ANOVA table repeated measures experiment 2.

Number of reps	PAR	Days after inoculation	$\phi\text{PSII}$ P values			I.s.d. values Time.Treatment
			Time	Treatment	Time.Treatment	
4	230	10	<.001	0.367	0.601	0.019
6	230	18	<.001	0.291	0.719	0.039
5	230	26	<.001	0.596	0.753	0.050
6	<b>530</b>	18	<.001	0.391	0.999	0.055
4	<b>530</b>	26	<.001	0.641	0.987	0.060
Number of reps	PAR	Days after inoculation	NPQ P values			I.s.d. values Time.Treatment
			Time	Treatment	Time.Treatment	
4	230	10	<.001	0.375	0.078	0.016
6	230	18	<.001	0.950	0.399	0.019
5	230	26	<.001	0.122	0.29	0.019
6	<b>530</b>	18	<.001	0.730	0.384	0.025
4	<b>530</b>	26	<.001	0.102	0.261	0.035
Number of reps	PAR	Days after inoculation	ETR P values			I.s.d. values Time.Treatment
			Time	Treatment	Time.Treatment	
4	230	10	<.001	0.406	0.581	2.299
6	230	18	<.001	0.364	0.696	3.800
5	230	26	<.001	0.371	0.464	4.025
6	<b>530</b>	18	<.001	0.443	0.999	11.958
4	<b>530</b>	26	<.001	0.592	0.991	18.503

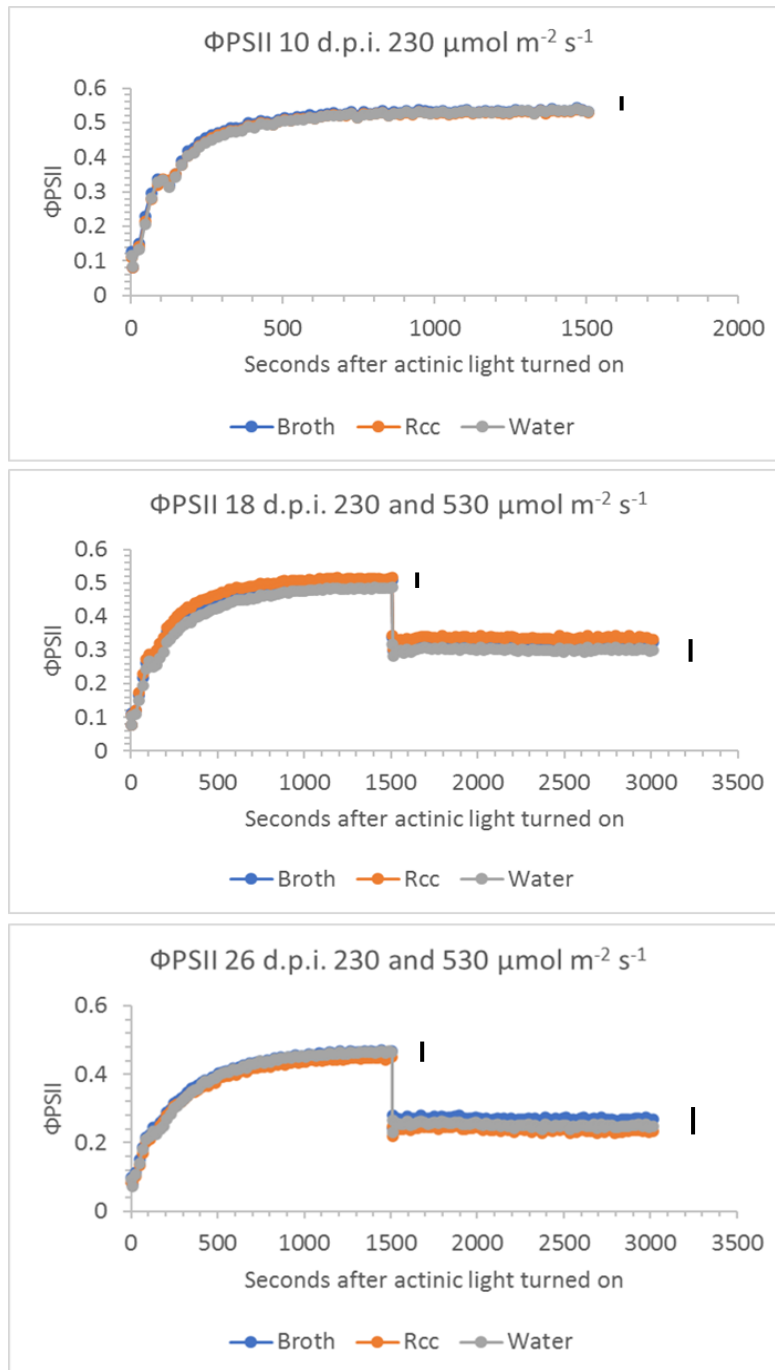


Figure 21 Operating efficiency of PSII ( $\Phi_{PSII}$ ). Actinic light applied at  $230 \mu\text{mol m}^{-2} \text{s}^{-1}$  for 1507 seconds, then increased to  $530 \mu\text{mol m}^{-2} \text{s}^{-1}$ . Black vertical lines to the right of the graphs represent the least significant difference (l.s.d.,  $P=0.05$ ) for Time.Treatment from a repeated measures ANOVA (displayed for each light intensity where applicable).

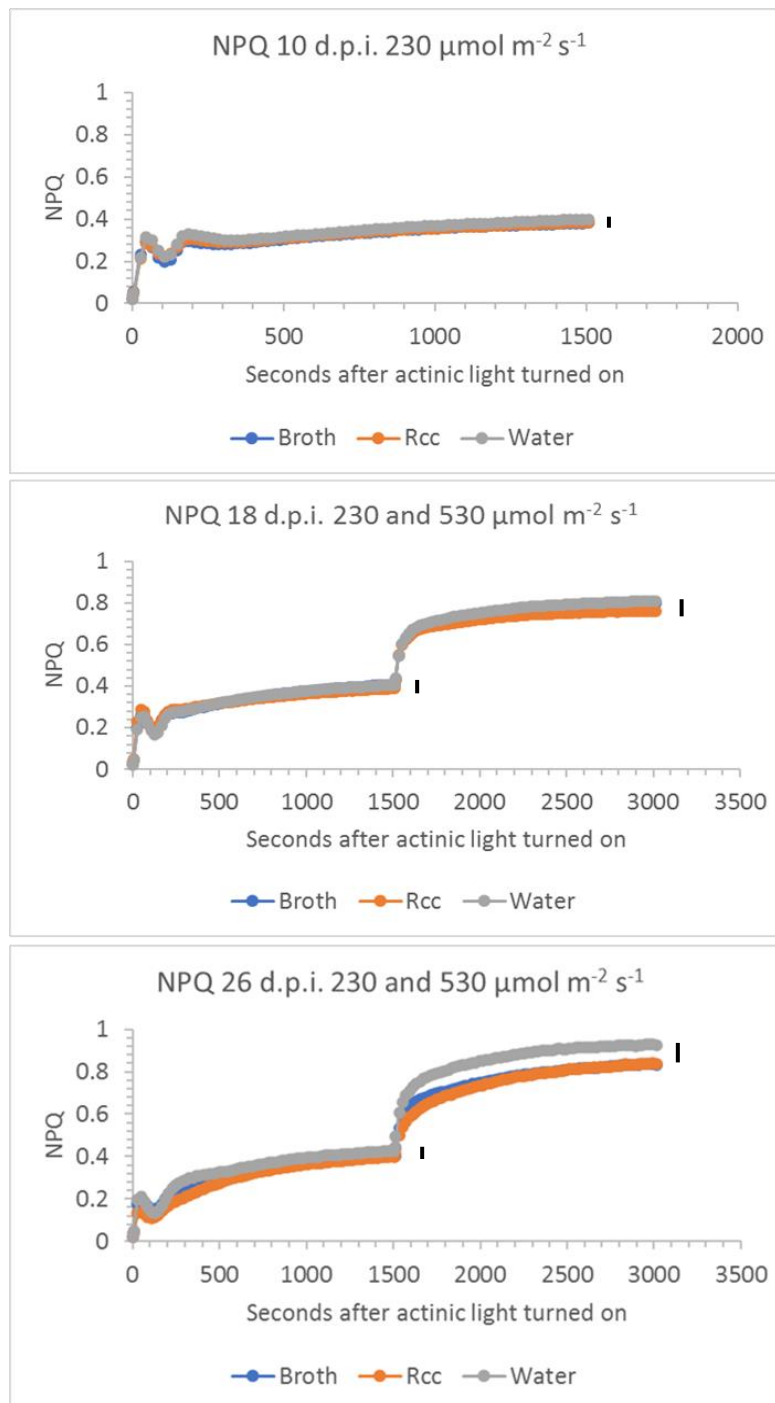


Figure 22 Experimental series 2. Quenching. NPQ. Actinic light applied at 230  $\mu\text{mol m}^{-2} \text{s}^{-1}$  for 1507 seconds, then increased to 530  $\mu\text{mol m}^{-2} \text{s}^{-1}$ . Black vertical lines to the right of the graphs represent the least significant difference (l.s.d.,  $P=0.05$ ) for Time.Treatment from a repeated measures ANOVA (displayed for each light intensity where applicable).

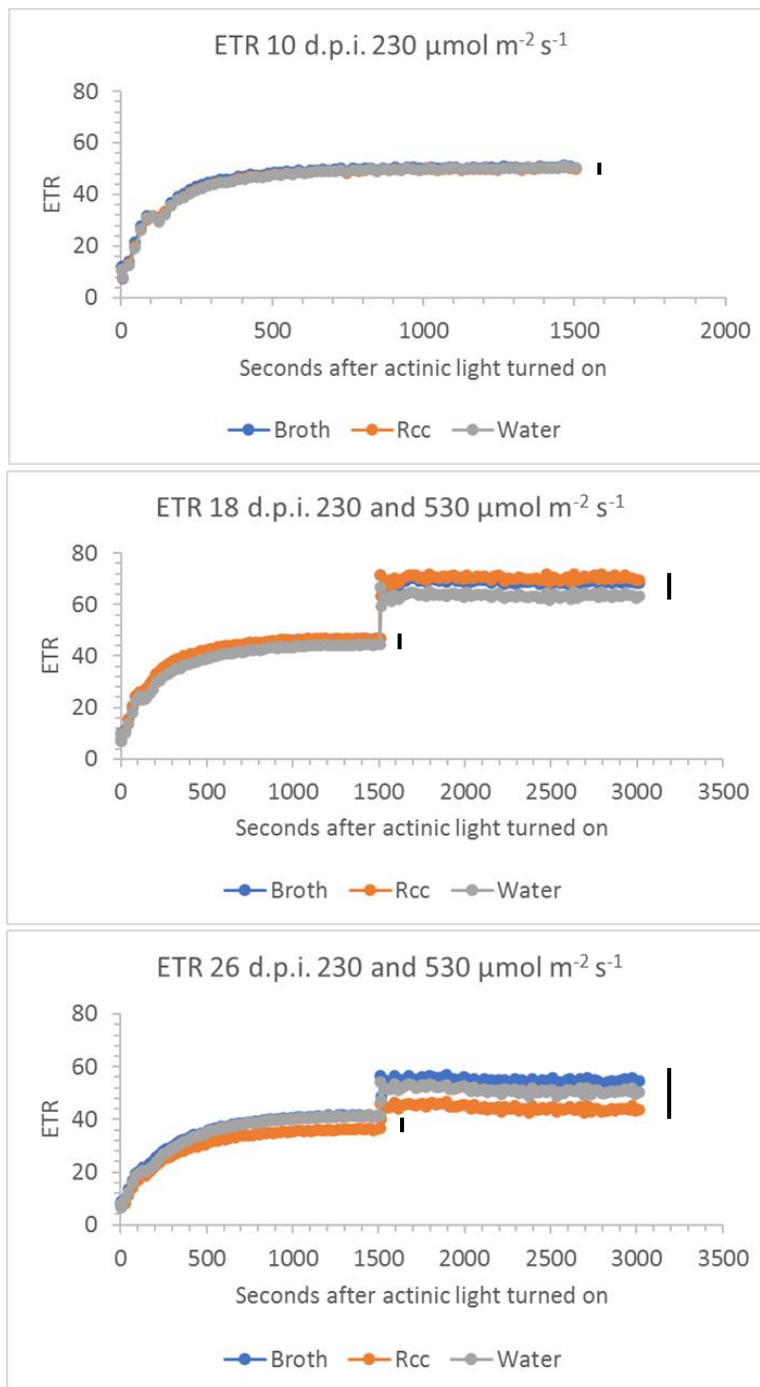


Figure 23 Experimental series 2. Quenching. ETR. Actinic light applied at  $230 \mu\text{mol m}^{-2} \text{s}^{-1}$  for 1507 seconds, then increased to  $530 \mu\text{mol m}^{-2} \text{s}^{-1}$ . Black vertical lines to the right of the graphs represent the least significant difference (l.s.d.,  $P=0.05$ ) for Time.Treatment from a repeated measures ANOVA (displayed for each light intensity where applicable).

Following dark adaptation and switching on the actinic light,  $\Phi$ PSII, NPQ and ETR demonstrated similar kinetics to those described in experiment 1. However, the changes observed with leaf age appeared to be less pronounced in experiment 2, especially for NPQ. Thus, the initial peak and transient drop in NPQ was apparent in leaves at all days after inoculation in experiment 2.

After increasing the irradiance there was an immediate decrease in  $\Phi$ PSII and increase in ETR with values remaining relatively constant thereafter. By contrast NPQ showed a rapid initial increase followed by a more gradual rise over the course of the measurement period.

### **Combined Infra-red gas analysis and chlorophyll fluorescence**

Rates of dark respiration were comparable over the course of the experiment and did not differ significantly between inoculated plants and controls (Table 10). Rates of net CO<sub>2</sub> fixation measured at both the growth irradiance and at saturating irradiance, declined with leaf age. However, before and after the appearance of visible ramularia symptoms there was no significant effect ( $P>0.05$ ) of treatment on the rate. Chlorophyll fluorescence parameters ( $\Phi$ PSII and ETR) did not differ significantly between inoculated plants and controls at any of the time points (Table 11 and Table 12), in agreement with the results obtained using the imaging fluorometer.

Table 10. CO<sub>2</sub> flux. Ramularia leaf spot symptom severity (% of measured leaf area) and net CO<sub>2</sub> flux ( $\mu\text{mol CO}_2 \text{ m}^{-2} \text{ s}^{-1}$ ) with days after inoculation and measurement irradiance ( $\mu\text{mol PAR m}^{-2} \text{ s}^{-1}$ ).

Days after inoculation	Symptom severity (%)	PAR ( $\mu\text{mol m}^{-2} \text{ s}^{-1}$ )	CO <sub>2</sub> Flux			P value
			Broth control	Ramularia	Water control	
6	0	0	-1.795	-1.445	-1.161	0.676
6		230	9.665	10.956	11.018	0.240
6		1250	15.044	16.590	16.970	0.223
16	0.8	0	-0.967	-1.718	-0.741	0.302
16		230	9.480	8.581	9.773	0.587
16		1250	13.500	12.021	13.680	0.514
27	1.4	0	-0.898	-0.788	-1.012	0.511
27		230	4.830	4.389	5.208	0.537
27		1250	6.160	5.682	6.491	0.752

Table 11 ETR. Means and P values from one-way ANOVA at each time point. Ramularia leaf spot symptom severity (% of measured leaf area) and ETR with days after inoculation and measurement irradiance ( $\mu\text{mol PAR m}^{-2} \text{ s}^{-1}$ ).

Days after inoculation	Symptom severity (%)	PAR ( $\mu\text{mol m}^{-2} \text{ s}^{-1}$ )	ETR			P value
			Broth control	Ramularia	Water control	
6	0	230	56.318	56.302	57.676	0.434
6		1250	98.361	102.347	103.402	0.789
16	0.8	230	51.943	48.219	50.750	0.301
16		1250	75.062	70.016	67.652	0.558
27	1.4	230	35.111	34.289	36.050	0.860
27		1250	37.819	35.349	38.641	0.785

Table 12  $\Phi$ PSII. Means and P values from one-way ANOVA at each time point. Ramularia leaf spot symptom severity (% of measured leaf area) and  $\Phi$ PSII with days after inoculation and measurement irradiance ( $\mu\text{mol PAR m}^{-2} \text{s}^{-1}$ ).

Days after inoculation	Symptom severity (%)	PAR ( $\mu\text{mol m}^{-2} \text{s}^{-1}$ )	$\Phi$ PSII			P value
			Broth control	Ramularia	Water control	
6	0	230	0.563	0.561	0.575	0.477
6		1250	0.181	0.187	0.189	0.828
16	0.8	230	0.516	0.497	0.503	0.788
16		1250	0.137	0.128	0.136	0.704
27	1.4	230	0.353	0.341	0.358	0.855
27		1250	0.070	0.067	0.071	0.919

## Analysis of transects across leaves

Transects were drawn across infected leaves, through one lesion in the upper leaf area (towards the leaf tip) and one lesion in the lower leaf area (towards the base), and in corresponding areas of control leaves (Figure 24). Transects were also drawn across areas of infected leaves which had no lesions, close to each transect through a lesion. Eighteen days after inoculation, three replicates had developed lesions on infected leaves (reps 1, 3 and 6). By 26 days after inoculation, an additional replicate had developed lesions on the infected leaf (rep 4). Prior to analysis of chlorophyll fluorescence outputs, each lesion was visually categorised as being either a small, developing lesion (category A) or a lesion at a more advanced stage of development (category B) (Table 13). Lesions that were selected for analysis at 18 days post inoculation were reanalysed at 26 days.

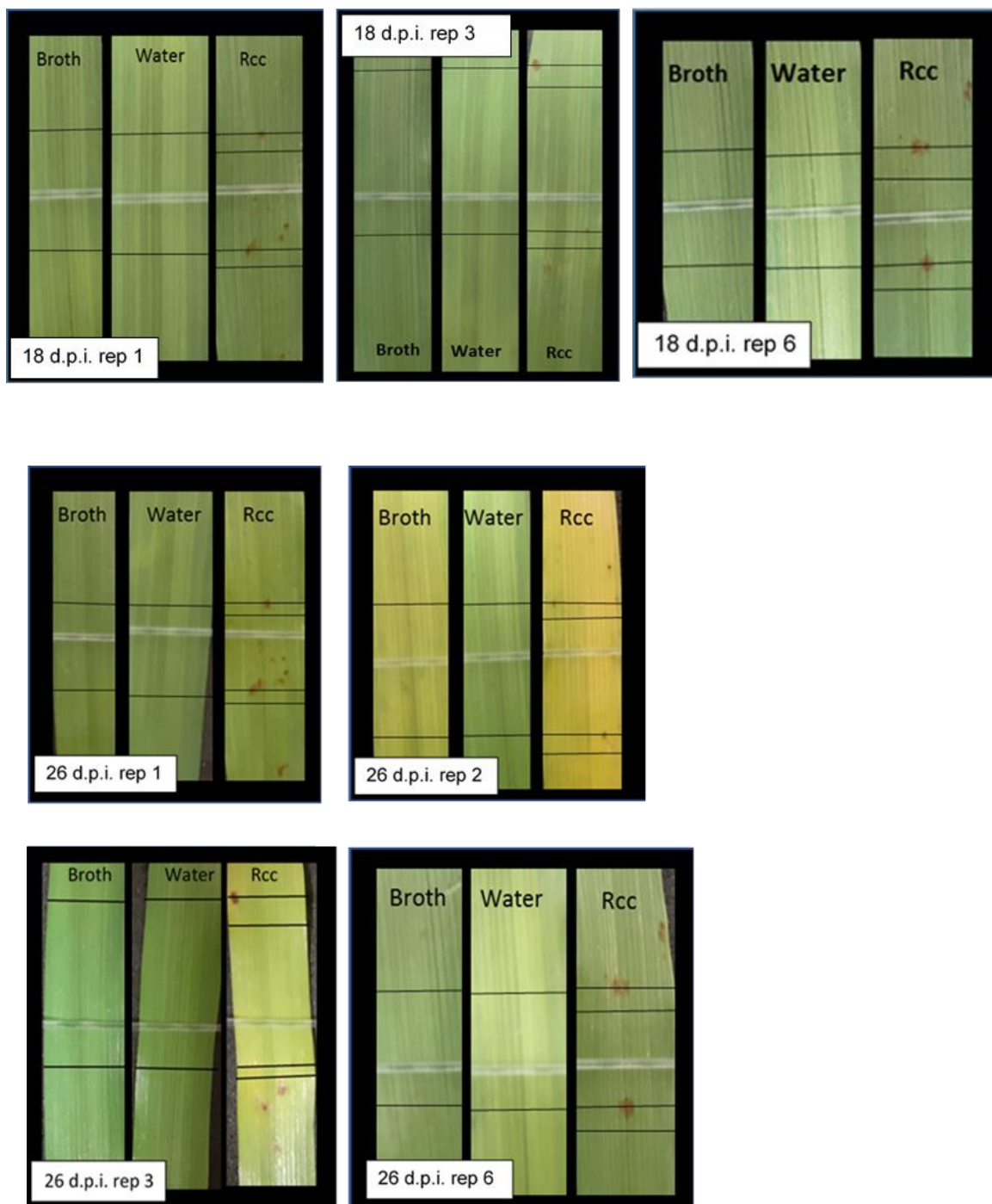


Figure 24 Leaves showing positions of upper and lower transects at 18 days and 26 days post-inoculation (d.p.i.).

Table 13 Lesion categories

D.p.i.	Rep	Lesion position	Lesion category
18	1	Upper leaf	A
18	1	Lower leaf	A
18	3	Upper leaf	B
18	3	Lower leaf	A
18	6	Upper leaf	B
18	6	Lower leaf	B
26	1	Upper leaf	B
26	1	Lower leaf	A
26	2	Upper leaf	A
26	2	Lower leaf	A
26	3	Upper leaf	B
26	3	Lower leaf	A
26	6	Upper leaf	B
26	6	Lower leaf	B

### **Chlorophyll fluorescence imaging transect analysis – steady state photosynthesis**

Values for the chlorophyll fluorescence outputs of  $F_v/F_m$ , NPQ,  $\Phi PSII$  and ETR were recorded pixel by pixel along each transect. This data is presented in full in Appendix 1. An exemplary figure is shown at Figure 25. The three black arrows on the graphs indicate the left edge, centre, and right edge of the lesions on infected leaves. The direction and relative scale of the effects observed are summarised qualitatively in Table 14.

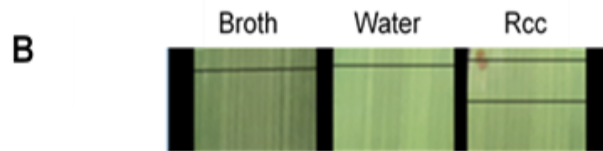


Figure 25 Chlorophyll fluorescence measured across leaf transects. Exemplary figure. Full data is presented in Appendix 1. The photographs show the location of upper and lower leaf transects. The graphs show chlorophyll fluorescence parameter values along the transects. The left-hand panels show parameters for transects across lesions and across nearby non-symptomatic areas of infected leaves. The right-hand panels show parameters for transects across lesions and across equivalent areas of control leaves. Measurements were taken at 18 and 26 days after inoculation. Replicates categorised as group A = small, developing lesion. Replicates categorised as Group B = lesion at more advanced stage of development.

Table 14 Direction and scale of change in fluorescence variables within the visible lesions on infected leaves compared to regions outside the lesion on the same leaves. Variables decreased (↓) or increased (↑) with the number of arrows indicating the relative scale from small (↓) to major (↓↓↓) change. ~ indicates a possible marginal or uncertain effect. Where no effect was observed the cell has been left empty. Lesions are identified by leaf replicate number (R1, R2 etc) and whether the lesion was on the upper (U) or lower (L) transect. Variables are: Fv/Fm, maximal photochemical efficiency; NPQ, non-photochemical quenching; ΦPSII, operating photochemical efficiency; ETR, Electron Transport Rate.

Days after inoculation	Category	Lesion	Fluorescence variable			
			Fv/Fm	NPQ	$\Phi$ PSII	ETR
18	A	R1 U	↓	↓↓		
	A	R1 L		↓↓		
	A	R3 L	↓	↓↓		~↓
18	B	R3 U	↓	↓↓	↓	↓
	B	R6 U	↓	↓↓	~↓	↓
	B	R6 L	↓↓	↓↓↓		↓
26	A	R1 L		~↑	↑	
	A	R2 U		↓		
	A	R2 L		↓	~↑	~↑
	A	R3 L		↓↓		
26	B	R1 U		↓↓		
	B	R3 U	↓↓↓	↓↓↓	↓↓↓	↓↓↓
	B	R6 U	↓↓↓	↓↓↓	↓↓↓	↓↓↓
	B	R6 L	↓↓↓	↓↓↓	↓↓↓	↓↓↓

At 18 d.p.i., in small and developing lesions (category A) the most pronounced effect observed was a reduction in NPQ within the lesion. Smaller reductions in Fv/Fm were also seen in some, but not all lesions. By contrast  $\Phi$ PSII and ETR values within lesions were similar to those in non-symptomatic areas of infected leaves or in control leaves. In the more developed category B lesions, a small reduction in  $\Phi$ PSII and ETR was also often observed. In the most developed lesions, e.g. replicate 3 upper and replicate 6 upper, a 'spike' in NPQ was visible towards the edge of the lesions, displaying higher values than those in non-symptomatic areas of infected leaves or in control leaves, while reduced NPQ was observed in the central part of these lesions.

All lesions which were in category B at 18 d.p.i. continued to develop further (replicate 3 upper lesion, and replicate 6 upper and lower lesions). In these lesions, by 26 d.p.i., values for all the measured chlorophyll fluorescence

outputs had dropped to zero or close to zero within the lesions. A spike displaying higher  $\Phi$ PSII values than those in non-symptomatic areas of infected leaves or in control leaves was observed in rep 3 upper lesion and rep 6 lower lesion, close to the edge of the lesions.

By 26 d.p.i., replicate 1 upper lesion (R1 U) appeared to have developed slightly, growing marginally darker and was re-categorised as a type B lesion. However, there was little change in its fluorescence characteristics. Thus, NPQ showed a decrease within the lesion, whilst  $\Phi$ PSII and ETR remained comparable to that in non-symptomatic regions. A spike in NPQ values, similar to those displayed by category B lesions at 18 d.p.i., was observed close to the edge of the lesion.

Other category A lesions (R1 L and R3 L) showed no further development after 18 d.p.i., although the infected leaf for rep 3 had started to display some chlorosis by 26 d.p.i (Fig xx). A new replicate (2) was added to the analysis at 26 d.p.i. as lesions had appeared on this infected leaf between 18 and 26 d.p.i. For this replicate, the infected leaf and the broth control leaf both displayed some chlorosis. This was more advanced in the infected leaf than in the broth control leaf. As with other small developing lesions, a reduction in NPQ was found, but only marginal or no effect on Fv/Fm,  $\Phi$ PSII and ETR.

## Discussion

Inoculation of barley seedlings with *R. collo-cygni* mycelial suspension achieved fewer and smaller lesions than are typical of *Ramularia* leaf spot symptoms in the field on both the spring barley varieties used in the experiments (cv Concerto and cv Fairing). Fungal biomass in infected leaves, as detected by DNA quantification, remained relatively static throughout asymptomatic growth and onset of disease symptoms when analysed in cv Concerto seedlings (this analysis was not conducted in cv Fairing). The fact

that no significant differences in fungal biomass across the time series were detected could be related to the low average severity of symptoms observed in these experiments, as increases in fungal biomass of *R. collo-cygni* in leaves of inoculated barley seedlings as foliar symptom severity increases have been described elsewhere in the literature (McGrann and Brown, 2017; Sjökvist *et al.*, 2018). In further experiments which are described in Chapter 3, significant increases in *R. collo-cygni* fungal biomass were observed in infected leaves with severe symptoms, but not during earlier stages of infection time series when limited lesions were visible on leaves. It could be valuable to further explore the distribution of fungal biomass within barley leaves infected with *R. collo-cygni*, to establish whether the fungus is distributed throughout green leaf areas beyond lesions or potentially centralised in areas where lesions develop. This could help with understanding of why lesions develop on some leaves but not others. Methylene blue staining could be a suitable method for analysis of fungal hyphae distribution relative to location of lesions on leaves, although this destructive method would not allow for repeat measurements on individual leaves as symptom severity increased. Some initial exploration of the relative location of *R. collo-cygni* fungal biomass and developing lesions within leaves of intact barley plants was conducted during this PhD project using fluorescence-microscopy imaging of plants inoculated with an isolate of *R. collo-cygni* transformed to express GFP. Although some areas of fungal biomass were observed localised to lesions, the results were not conclusive due to technical problems with accurately mapping fluorescence microscopy images against digital leaf images. Therefore, further analyses in future could help clarify these questions.

Analyses of leaf photosynthesis and dark respiration using chlorophyll fluorescence imaging and infra-red gas analysis did not detect any significant differences between infected and control leaves prior to the development of visible symptoms. As visible symptoms developed, effects on photosynthesis were localised to lesions on otherwise green leaves. After symptom development rates of net CO<sub>2</sub> fixation and photochemical efficiency were still

not found to be significantly reduced when averaged over the wider leaf measurement area. The apparent lack of a significant disease effect at this scale would seem to be a result of the low severity of disease symptoms as finer scale chlorophyll fluorescence image analyses revealed a progressive reduction in photosynthetic activity within lesions as they matured. Analysis of photosynthetic induction kinetics provided additional evidence that photochemical processes were not affected by asymptomatic infection. Induction kinetics can be altered by some factors as shown by effects of leaf age in Experimental series 1 in particular. However, *R. collo-cygni* infection was not found to affect induction kinetics.

The results indicate that *R. collo-cygni* does not impact leaf photosynthesis in asymptomatic leaves or green areas of symptomatic leaves, suggesting that asymptomatic infection or low levels of symptom expression do not necessarily have a negative impact on barley.

These results are similar in some respects to those for some previous studies of hemibiotrophic crop pathogens. Robert *et al.* (2006) reported no significant effect on net photosynthesis in wheat leaves inoculated with *Zymoseptoria tritici* prior to the appearance of visible symptoms. Thereafter net leaf photosynthesis was found to be increasingly reduced as visible symptoms developed from chlorotic to necrotic damage. Studies of bean anthracnose disease associated with *Colletotrichum lindemuthianum* (Bassanezi *et al.*, 2001; Meyer *et al.*, 2001) also found no effect on net photosynthesis prior to visible symptom appearance. In that pathosystem, once necrotic lesions appeared, greater reductions in net leaf photosynthesis were observed than could be accounted for by the extent of visible symptoms. Bassanezi *et al.* (2001) attributed this to a reduction of intercellular CO<sub>2</sub> due to stomatal resistance. However, Meyer *et al.* (2001) argued that metabolic inhibition of photosynthesis, possibly mediated through inhibition of Ribulose 1·5-bisphosphate (RuBP) regeneration, was also involved as a decrease in the photosynthetic electron transport rate was maintained under high CO<sub>2</sub> exposure.

The results presented in this chapter did not suggest any effect on photosynthesis in non-symptomatic tissue. Chlorophyll fluorescence images of developing lesions indicated a pattern whereby  $\Phi$ PSII and ETR values were initially maintained in young lesions, while NPQ and Fv/Fm values were usually reduced. Fv/Fm values were often particularly or solely reduced in a small area towards the centre of developing lesions at this early stage. As symptoms matured, all photosynthetic parameters were normally reduced, reaching near zero in the most developed lesions, presumably indicating physical damage to cells or cell death.

An analysis of the infection process of *R. collo-cygni* in barley using confocal microscopy and transgenic fungal isolates (Kaczmarek *et al.*, 2017) also found no evidence of physical damage to host cells until the appearance of visible symptoms on leaves. Host cells appeared to remain undamaged during leaf penetration via stomata, fungal growth in the substomatal cavity, and the earlier stages of intercellular growth of hyphae in the mesophyll tissue. Development and maturation of lesions was associated with localised mesophyll cell death and fungal sporulation through stomata and collapsed mesophyll cells. A loss of chlorophyll fluorescence signal was observed within necrotic lesions. Some red discolouration of the tissue immediately surrounding developing lesions was also observed, which the authors suggested could be related to the production of rubellin toxins by the fungus.

NPQ, observed in the current experiments to be lower within lesions than in green areas of infected leaves or control leaves from the early stages of lesion development onwards, has a role in preventing damage from reactive oxygen species (ROS) by dissipating excess excitation energy and down-regulating PSII. The apparent loss of, or decrease in, the ability to activate NPQ through generation of a transthylakoid gradient within lesions could increase the likelihood of damage at high light intensities or in any situations where CO<sub>2</sub> dependent electron flow is disrupted, for example due to damage to Calvin-Benson cycle enzymes. Hideg *et al.* (2008) showed that suppression of NPQ could result from inhibition of enzymes involved in the

Mehler ascorbate peroxidase (MAP) cycle, and that ROS are formed when the NPQ-generating process is thus inhibited. Possibly the reduced NPQ observed at lesion sites could indicate a direct or indirect effect of *R. collo-cygni* on processes necessary for initiation of NPQ. If this were the case, the initial maintenance of relatively high levels of  $\Phi$ PSII within developing lesions could possibly be associated with absence or reduction of NPQ-related downregulation, potentially leading to increased ROS production particularly under environmental stress such as high light intensity.

Interestingly, two recent comparative transcriptomic studies, of *Z. tritici* on wheat (Ma *et al.*, 2018) and *R. collo-cygni* on barley (Sjokvist *et al.*, 2018), have reported upregulation of host pathogenesis-related genes and down-regulation of photosynthesis-related genes during asymptomatic infection. Possibly the down-regulation of photosynthesis-related genes observed in these studies does not result in a significant effect on physiology as analysed in the experiments presented in this chapter or those presented in the reports of Robert *et al.* (2006) or Scholes and Rolfe (2009). Alternatively, differences in experimental methodology might explain the different outcomes. This reported very active transcriptome response of barley to *R. collo-cygni* contrasts with the comparatively subdued response of *Lolium arundinaceum* (tall fescue) to its fungal endophyte *Epichloë coenophiala* (Dinkins *et al.*, 2017), perhaps casting some doubt on the accuracy of describing *R. collo-cygni* as an endophyte during its asymptomatic growth period in barley.

Two other observations of interest from the study by Sjokvist *et al.* (2018) are the reported upregulation of defence-response genes associated with plant recognition of necrotic pathogens, for example associated with the production of jasmonic acid and ethylene, but no regulation of expression of genes associated with the salicylic acid pathway more commonly associated with biotrophic pathogens, and the upregulation of *R. collo-cygni* genes associated with hexose transporters. The latter suggests hexose feeding by the fungus in the apoplast once hyphae entered the mesophyll layer. Some fungal pathogens of plants are capable of utilising different nutritional sources

under different conditions (Divon and Fluhr, 2007), so understanding more about the nutritional status of *R. collo-cygni* in its different life stages could be informative in understanding shifts in host responses. Sjøkvist *et al.* (2018) reported upregulation of *R. collo-cygni* genes associated with activation of the glyoxylate cycle during asymptomatic infection, which suggests the fungus may utilise fatty acids (either fungal or host-derived) for nutrition at this stage, similar to the early stages of asymptomatic infection of wheat by *Zymoseptoria tritici* as reported by Palma-Guerrero *et al.* (2016). However, both these studies were conducted in artificially inoculated seedlings, while the period prior to symptom appearance was short (~ 10 days). As fatty acid metabolism is common in fungal pathogens of plants during leaf surface growth and leaf penetration (Divon and Fluhr, 2007), evidence pointing to fatty acid metabolism in this context does not necessarily reflect the nutritional strategy adopted during the much longer asymptomatic phase of *R. collo-cygni* observed in the field, particularly where infected seed is the source of fungal growth *in planta*, or the context of a mature plant and the onset of senescence associated with the typical timing of *Ramularia* leaf spot symptoms.

In summary, the results from Chapter 2 found no effect on host photosynthesis of *R. collo-cygni* infection prior to symptom appearance or in green areas of infected leaves, and low levels of visible disease symptoms were not found to affect net leaf photosynthesis. However, it is important to bear in mind that these experiments were conducted in seedlings using inoculation with mycelial suspension. The conditions were quite different to those of a field epidemic of *Ramularia* leaf spot. It is possible that plant developmental stage, interaction with environment, infection route (via seed or spore), or other factors could lead to a different outcome in a field situation. This is explored further in Chapter 3.

# **Chapter 3 Relative impact of different *R. collo-cygni* life phases on barley yield**

## **Introduction**

Chapter 2 assessed physiological responses of barley seedlings at leaf level to inoculation with *R. collo-cygni* in controlled environment cabinets. This approach did not detect differences in leaf photosynthesis between infected and control plants prior to symptom development, or in green areas of infected leaves during symptom development.

Several factors could impact whether these findings reflect physiological responses of a barley crop in the field to *R. collo-cygni* infection, for example plant age and growth stage, environment, microbiome population under different fungicide regimes, naturally occurring *R. collo-cygni* strain(s) and method of infection (via seed or spore).

Chapter 3 therefore focused on assessing physiological responses of field-grown barley to *R. collo-cygni* throughout the growing season.

## **Effects of fungal pathogens on crop growth and yield**

Yield formation in wheat and barley is an ongoing process throughout the growing season (Reynolds *et al.*, 2005; Bingham *et al.*, 2007a; Bingham *et al.*, 2007b; Slafer *et al.*, 2014; Distelfeld *et al.*, 2014). Canopy size and grain sink capacity, as determined by the number and survival of tillers and spikelets and the individual storage capacity of grain sites, is for the most part established prior to anthesis, while post-anthesis grain filling completes the yield formation process. Carbon assimilates from the remobilisation of

stored soluble carbohydrate reserves, as well as from post-anthesis photosynthesis, can be used for grain filling. Thus, potential impacts of pathogens on radiation interception, radiation use efficiency and biomass partitioning need to be considered throughout the growing season to understand how yield is reduced by disease. This is particularly relevant for *R. collo-cygni*, which can be present in barley from seed to harvest, and as yield formation in non-diseased spring barley in the UK is thought to be primarily sink-limited (Bingham *et al.*, 2007a; Bingham *et al.*, 2007b).

Physiological responses of plants to fungal pathogens were discussed in Chapter 2, particularly focusing on photosynthesis at individual leaf level. However, individual leaves do not tell the whole story, therefore it is necessary to scale up to consider whole-canopy effects. Effects on plants can reach beyond infected tissues, for example through increased net photosynthesis in uninfected leaves, translocation of assimilate from healthy leaves to infected leaves and/or increased retention of assimilate in infected leaves (Livne and Daly, 1966; Murray and Walters, 1992), or altered growth patterns in uninfected tissues due to changes in biomass partitioning (Walters and Ayres, 1981). In some cases healthy green tissue appears to be unaffected by infection in remote parts of plants, for example van Oijen (1990) reported that the net photosynthetic rate of uninfected leaves was not altered during partial infection of potato plants with *Phytophthora infestans* and expression of late blight symptoms, providing support to the conclusions of earlier analyses attributing tuber yield loss associated with this disease to a reduction in cumulative light interception by green tissue, rather than altered radiation use efficiency (Rotem *et al.*, 1983; Haverkort and Bicomumpaka, 1986; Waggoner and Berger, 1987).

In cases where compensatory effects are observed in symptomless parts of plants infected with foliar pathogens, the extent of infection and severity of disease symptoms may be expected to influence their expression. The growth stage of plants at the time of initial infection or during an ongoing infection could also be an important factor. Rooney and Hoad (1989)

reported a significant increase in photosynthetic rate in green, symptomless leaves of wheat plants inoculated at the three leaf stage with *Phaeosphaeria nodorum*, but this effect was not observed when plants were inoculated later at the six leaf stage, despite a greater loss of green area associated with symptomatic tissue at this stage. Bingham *et al.* (2009) hypothesised that this could possibly be due to sink limitation in younger plants allowing room for photosynthetic rates to increase in the case of a sink being created in remote leaves by an invading fungus, whereas in older plants the sink created by the developing ear could mean that photosynthesis is already operating closer to capacity, therefore leaving little room for large increases in photosynthetic rate in healthy tissue.

Effects of RLS on yield are often associated with a reduction in average grain weight, suggesting that a reduction in canopy photosynthesis and availability of assimilates during grain filling may play an important role. However, it is also plausible that the asymptomatic phase of infection may impact on grain weight by reducing the potential grain size (grain storage capacity) prior to anthesis. Sustained differences in photosynthetic activity during plant growth pre-anthesis could impact canopy size, tiller number, number of grains per ear, potential grain weight and availability of soluble carbohydrate reserves.

Effects of the symptomatic life phase of *R. collo-cygni* on barley yield could be solely due to a reduction in radiation interception associated with symptom expression during grain filling, however it is also possible that a greater or lesser impact on net photosynthesis than would be expected in relation to symptomatic area could occur. The latter scenario could be possible if, for example, compensatory effects were to occur in remote non-symptomatic parts of plants (this was not assessed in Chapter 2) or if the reduction in photosynthesis observed within necrotic lesions in Chapter 2 were to extend beyond the lesion area in the different environment of mature, field-grown barley plants.

## Chapter objectives

The work presented in this chapter aimed to determine the relative effects of asymptomatic and symptom-expressing phases of *R. collo-cygni* infection on photosynthesis and yield formation in spring barley in the field. Building on the results from Chapter 2, which did not find any evidence of effects on host photosynthesis during asymptomatic infection or in non-symptomatic areas of symptomatic leaves, the field experiment described in Chapter 3 aimed to examine whether effects of infection on host photosynthesis were also limited to symptomatic tissue in field-grown barley, and to assess the relative impact of the pre- and post-symptomatic life phases of *R. collo-cygni* on barley yield.

The specific hypotheses tested in Chapter 3 were:

- Infection of field grown barley plants with *R. collo-cygni* does not impact leaf photosynthesis prior to the appearance of visible RLS symptoms.
- Yield loss to RLS in barley is mainly due to post-anthesis reduction in PAR interception due to visible RLS symptoms.

# Materials and methods

## Site and experimental design

The experiment took place in 2017 at Boghall farm, SRUC, Edinburgh, Midlothian, EH10 7DX (latitude 55° 52' 36.35" N and longitude 003° 12' 12.59" W), in the south-east facing Anchordales field on a gentle slope at an elevation of 200 m. The soil type was sandy loam (Macmerrie Series), pH 6.0, and organic matter 6.48 % (loss on ignition). The previous crop was spring barley.

Plots (10 x 2 m) of spring barley cv. Concerto were drilled on 29<sup>th</sup> March at a seed rate of 360 seeds m<sup>-2</sup>. Concerto was the most widely grown variety of malting barley in Scotland in 2017. Disease ratings (on a scale of 1 – 9, with 1 indicating low resistance to a particular disease and 9 indicating high resistance) for Concerto in the 2017 AHDB Recommended List were Mildew 8, Yellow Rust 8, Brown Rust 5, Rhynchosporium 4, and Ramularia 6. Concerto had good resistance to Mildew and Yellow Rust. Resistance to Brown Rust and Ramularia were similar to the other varieties on the 2017 AHDB Recommended List. Resistance to Rhynchosporium was lower than average.

The experiment was laid out in a randomised block design with three treatments and four replicates. Fertiliser application was consistent with local practice for a malting barley crop (N = 120 kg/ha, and P<sub>2</sub>O<sub>5</sub> and K<sub>2</sub>O = 60 kg/ha).

The three treatments (Table 15) were:

- Treatment 1: Untreated (no inoculation or fungicide).
- Treatment 2: Full fungicide treatment (bixafen + prothioconazole [Siltra Xpro 0.4 l ha<sup>-1</sup>] at GS30 followed by prothioconazole [Proline 0.4 l ha<sup>-1</sup>] plus chlorothalonil [Bravo 1.0 l ha<sup>-1</sup>] at GS 45).

- Treatment 3: Fungicide treatment (pyraclostrobin [Comet 0.6 l ha<sup>-1</sup>]) at GS30 followed by inoculation with *R. collo-cygni* mycelial suspension at GS 32/33.

Table 15 Field experiment treatments

Treatment number	Treatment name	T1 (GS 30)	GS 32/33	TS GS 45
1	Untreated	No treatment	No treatment	No treatment
2	Fungicide	0.4 l/ha Siltra XPro	No treatment	Proline (0.4 l/ha) + Bravo (1.0 l/ha)
3	Inoculated	0.6 l/ha Comet	Inoculate with <i>R. collo-cygni</i>	No treatment

The treatments were designed with the aim of achieving plants displaying RLS symptoms only (no other diseases present), and completely disease-free plants. Disease development in untreated crops is quite unpredictable, and there was no guarantee that RLS would develop on the untreated crops, or, if it did, whether it would be the sole disease present. Therefore, one group of plants (treatment 3) were inoculated with *R. collo-cygni* in case natural infection did not occur. This group was also treated with a strobilurin fungicide (to which *R. collo-cygni* isolates are resistant) to control *Rhynchosporium commune* (barley leaf blotch/scald), *Pyrenophora teres* (net blotch) and *Puccinia hordei* (brown rust) in case these diseases took hold in the 2017 growing season. It should be noted, however, that although

strobilurin resistance has been widespread in *R. collo-cygni* isolates for around 14 years, later review of the literature regarding the isolate used for inoculation (isolate DK05 Rcc 001, isolated from susceptible spring barley cv Braemar in Denmark in 2005) suggested that this isolate is susceptible to azoxystrobin (Syngenta, Bracknell, UK) (Fountaine and Fraaije, 2009) so it is possible that it is also fully or partially susceptible to pyraclostrobin. Therefore, RLS symptoms observed in plants inoculated with *R. collo-cygni* may have been solely or largely the result of natural infection by resistant isolates. The timing of inoculation (GS32/33) was designed to achieve a period of asymptomatic fungal growth prior to the development of visible symptoms, in the case that no natural infection of *R. collo-cygni* occurred or that untreated plants developed diseases other than RLS.

Two further treatments were initially included with the aim of providing non-inoculated controls for the plants inoculated with *R. collo-cygni*. These consisted of fungicide treatment at GS 30 (pyraclostrobin [Comet 0.6 l ha<sup>-1</sup>]) and then an application of either dilute nutrient broth (to match the medium in which the fungus used for inoculations was grown) or sterile distilled water at GS 32/33. However, these treatments had to be dropped due to limited time and workload capacity.

## Measurements

Crop biomass, absolute area, and % green area (GA) were determined 85 days after sowing (GS 55 + 5 days) and then at two further time points at two-week intervals during grain filling. Plants were sampled from a 0.5 m length of rows three and four at diagonally opposite points in each plot as shown in Figure 26. For all field sampling or measurements in this experiment the outer two rows (rows one and two) and areas within 0.5 m of the ends of the plots were avoided to minimise edge effects, the roots were severed from the shoots and discarded, and plants collected in the field were

placed 'ears first' into long, clear plastic bags for transport, then stored in a walk-in chiller at -4°C in the dark prior to processing.

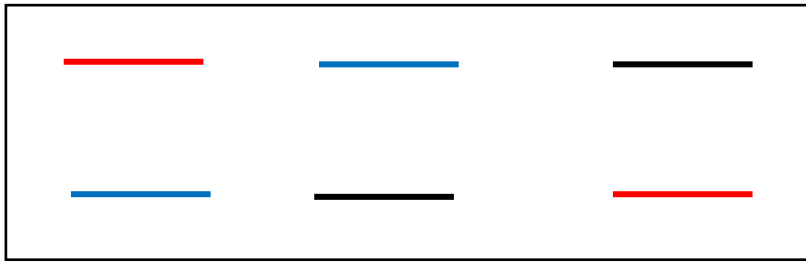


Figure 26 Diagrammatic representation of areas in each plot sampled for measurements of biomass, absolute area and % green area (GA). The three colours represent individual sampling dates. Each line represents a 0.5 m length of plants from rows 3 and 4.

The fresh samples were weighed using a precision balance (Kern PLJ, D-72336, Kern & Sohn Gontbl, Balingen, Germany). Subsamples were taken by 'dealing' shoots from each of these larger samples into ten equal piles, then selecting two of these piles at random to form the subsample. The fresh subsamples were weighed, then dried in individual paper bags in an oven (Ecocell, MMM Medcenter, Munich, Germany) for 48 hours at 80°C, and weighed again.

Ten shoots were selected randomly from the remaining original fresh samples for determination of absolute area and % GA. These were broken down into fractions of individual leaf layers, sections of stem (including leaf sheath) between leaves, peduncle and ear, as shown in Figure 27.

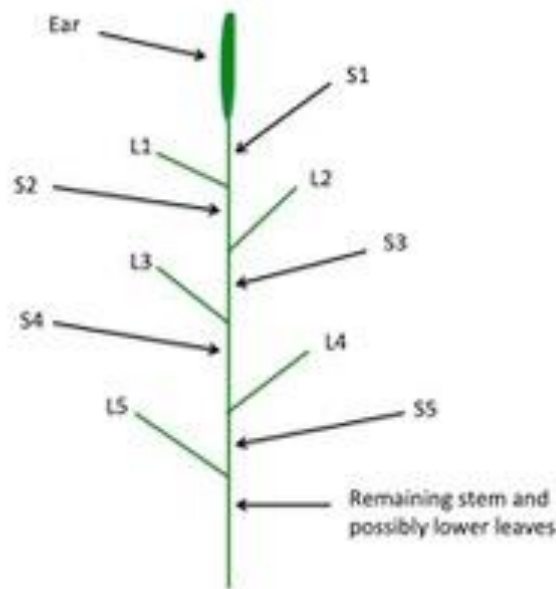


Figure 27 Diagram showing the fractions of barley shoots used for determination of absolute area and % green area (GA).

The % GA was visually estimated for each fraction (upper surfaces of fully emerged leaves, stem sections plus leaf sheaths, peduncle and ear), then the absolute projected area of each fraction was measured using a leaf area meter (Li-Cor Biosciences, Lincoln, USA). No distinction was made between GA lost specifically to disease lesions or that lost to any associated chlorosis or necrosis for these % GA visual estimates.

PAR interception by the canopy was determined on the same days on which the samples for measurement of crop biomass, absolute area and % GA were collected, using a Sunscan Canopy Analysis System (Delta T Devices Ltd, Cambridge, UK), which records simultaneous measurements of incident PAR above and transmitted PAR below the canopy. Measurements were taken at six different points in each plot. The Sunscan probe was inserted below the canopy at an angle of 45° to the crop rows for the canopy base

measurements, to capture representative samples of canopy structure throughout the plot.

Disease severity and fungal growth *in planta* were determined 65 days after sowing (approximately GS 37), then at four further time points at two-week intervals. Ten shoots were selected at random from each plot. Disease severity was visually assessed on the upper surface of each fully emerged leaf. Visual estimates were made of the % area of the leaf covered by spotting and lesions, and of the % area of the leaf that was chlorotic, necrotic or still green. Leaves were then snap-frozen in liquid nitrogen and stored at –20°C. Due to time constraints, only the leaf below the flag leaf (F-1) was later processed for DNA quantification. The DNA extraction and quantification methodology was as described in Chapter 2.

Photosynthetic efficiency was assessed 73 days after sowing (one week before GS 55), then at four further time points at intervals of 8 to 9 days on average. Maximal efficiency of PSII (Fv/Fm) was determined for five randomly selected F-1 leaves per plot using an OS-30p+ Chlorophyll Fluorometer (Opti-Sciences, Hudson, New Hampshire, USA). Leaves were dark-adapted for 30 minutes prior to measurement. Dark-adaption clips consisted of a light-weight, padded clamp with a sliding shutter to exclude light positioned at the bottom of a hollow tube. The tube was designed to fit the measuring probe of the fluorometer without allowing incident light to reach the area of the leaf which was to be measured. Dark-adaption clips were placed onto the leaves, and after 30 minutes the fluorometer measuring probe was positioned in the tube, then the shutter was opened for the measurement to be taken. The fluorometer measured minimum fluorescence using a weak, red, modulated light source, then maximal fluorescence using a saturating actinic light (3500 µmol). Measurements were taken in the medial area of the leaf, avoiding the midrib, on green areas initially, until lesions and/or chlorotic/necrotic tissue spread across this area.

The date of canopy senescence was recorded when less than 5% of peduncles remained green. Meteorological data were monitored continuously

at the site. Plots were harvested by small plot combine for determination of grain yield. Samples were taken for measurement of mean grain weight (MGW) and grain moisture content was determined gravimetrically after oven drying. Yields and MGW were adjusted and expressed at 15% moisture content. Grain number  $\text{m}^{-2}$  was determined by dividing yield values by MGW values.

## Calculations and statistical analysis

The fresh and dry weights recorded for crop biomass samples were used to calculate an average dry weight value ( $\text{kg m}^{-2}$ ) for each plot. The total quadrat area from which plants were collected for each sample was, in this case,  $0.23 \text{ m}^{-2}$  (a total row length of 2 m of plants collected from rows planted with 11.5 cm spacing). Whole sample fresh weight was divided by subsample fresh weight, and the resulting values were then multiplied by subsample dry weight to obtain the dry weight per quadrat. Dry weight  $\text{m}^{-2}$  was obtained by multiplying the dry weight per quadrat by the quadrat area.

PAR interception by healthy (green) tissue was estimated using methods adapted from Bingham *et al.* (2019) and (Bingham *et al.*, 2021). The measurements of incident and transmitted PAR were used to calculate a canopy area index (*CAI*) representing the total projected area per ground unit area, as shown in Equation 1, using Beer's law analogy and an assumed light extinction coefficient (*k*) of 0.5.

### Equation 1

$$CAI = [\ln(I_t/I_o)]/k$$

where  $I_t$  is the incident PAR above the canopy and  $I_o$  is the transmitted PAR at the canopy base.

The proportional distribution of projected area was calculated using the measurements of absolute area for the sections shown in Figure 27. The projected area was taken as the sum of the absolute areas within five 'layers', then expressed as a fraction of the sum of all the layers. The ear was counted as a separate layer, then leaf layer 1 consisted of the peduncle and the flag leaf lamina, leaf layer 2 consisted of the leaf below the flag leaf and the section of stem plus leaf sheath between that leaf and the flag leaf, and so on down to leaf 5. The stem below leaf 5 was included in leaf layer 5, along with any remaining senesced leaves found there. The fractional distribution of projected area from the measured samples was then used to estimate the CAI in each layer as shown in Equation 2.

#### Equation 2

$$CAI_h = CAI \times fLA_h$$

where  $CAI_h$  is the CAI of layer  $h$  and  $fLA_h$  is the projected area of layer  $h$  given as a fraction of the total projected area of all layers.

PAR intercepted by each layer was then calculated as shown in Equation 3.

#### Equation 3

$$I_h = I_{oh} \times [1 - \exp(-k \times CAI_h)]$$

where  $I_h$  is the PAR intercepted by layer  $h$ , and  $I_{oh}$  is the PAR incident on leaf  $h$  (calculated as the difference between the daily incident PAR at the top of the canopy and the sum of that daily incident PAR intercepted by all the layers above layer  $h$ ).  $k$  is the assumed light extinction coefficient of 0.5.

PAR intercepted by healthy (green) tissue in each layer was then calculated as shown in Equation 4.

#### Equation 4

$$HA_{inth} = I_h \times [HAI_h/CAI_h]$$

where  $HA_{inth}$  is the healthy area PAR interception by layer  $h$  and  $HA_{Ih}/CAI_h$  is the healthy (green) fraction of the CAI in layer  $h$  (calculated from a weighted average of the measured % GA of the leaf lamina and stem plus leaf sheath for the leaf layers, or from the measured % GA for the ear).

$HA_{int}$  for the canopy as a whole was calculated as the sum of all the individual layers, then expressed as a fraction ( $F_{PAR}$ ) of the incident PAR for a given day ( $I_o \text{ day}$ ) as shown in Equation 5.

#### Equation 5

$$F_{PAR} = HA_{int}/I_o \text{ day}$$

To estimate  $HA_{int}$  over a selected interval between growth stages, the value of  $F_{PAR}$  for each of the bordering growth stages was averaged and multiplied by the sum of the daily incident PAR for the selected interval.

To test whether reductions in light interception resulting from symptom development could account for the yield differences between the fungicide-treated and the inoculated and untreated plots, a predicted yield loss was calculated. The reduction in post anthesis  $HA_{int}$  was calculated for each replicate block by subtracting the  $HA_{int}$  for inoculated and untreated plots from that of the fungicide-treated plot. This was multiplied by the average post-anthesis RUE for the experiment and the resulting dry matter estimated, adjusted to 15% moisture content. This represents the difference in grain yield at 15% moisture content assuming that all post-anthesis net dry matter produced is allocated to grain and there are no differences between treatments in the contribution from remobilised stem carbohydrate reserves. Statistical significance of differences between predicted and observed yield losses were tested using a paired t-test for each treatment. All other data were analysed using analysis of variance using GenStat software (19th Edition, VSN International, Hemel Hempstead, UK). Residuals were checked for normality of distribution and homogeneity of variance before analysis.

# Results

## Disease severity and % green area

RLS was the only disease identified on the crop during the experiments, as assessed by visual inspections. Graphs showing the progress over time of the % area of leaves covered by spotting, lesions, and chlorotic, necrotic or green tissue (averaged over the top three leaves of plants; flag leaf, F-1 and F-2) are presented in Figure 28. (These data are from the detailed disease progress assessments of plants sampled at 65 days after sowing and at four further two-week intervals thereafter).

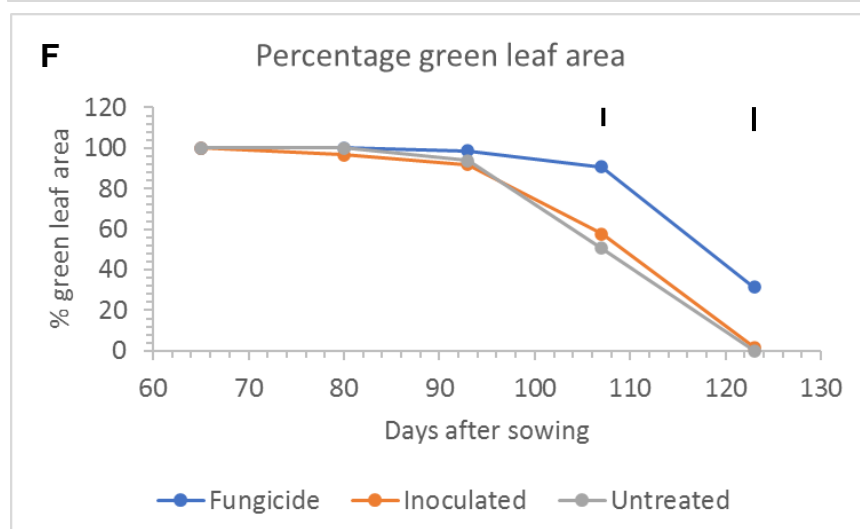
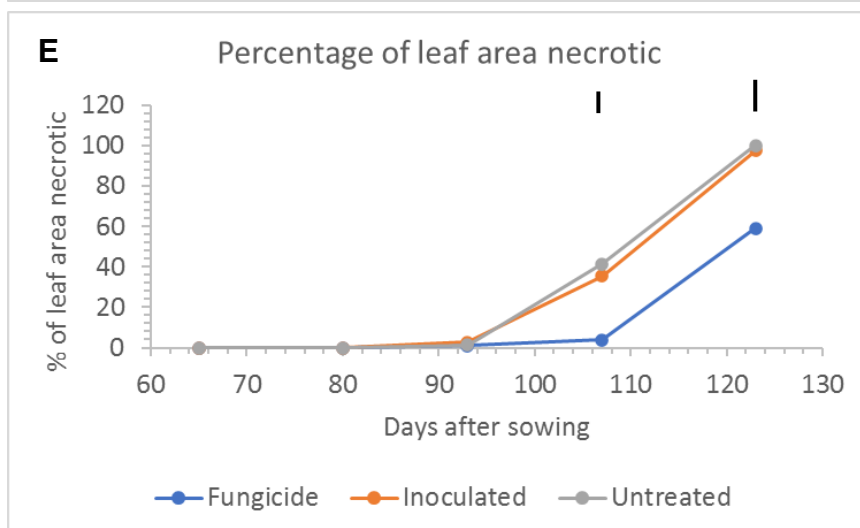
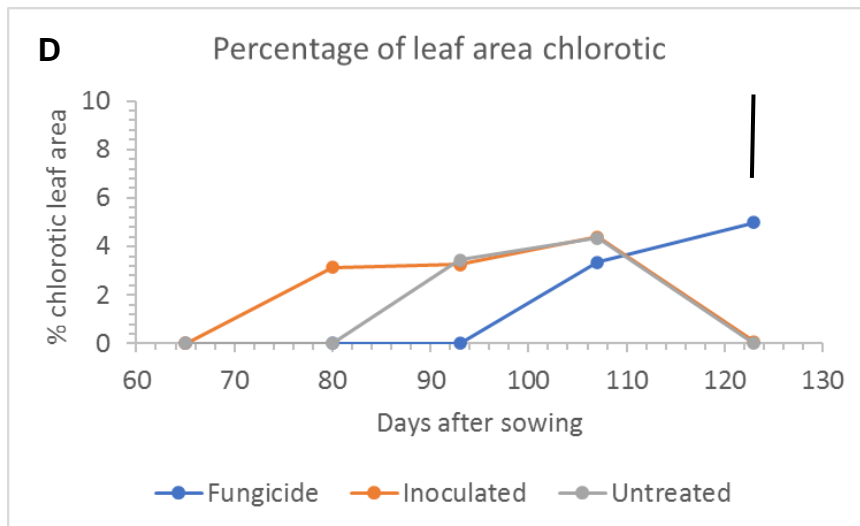


Figure 28 RLS symptom development and green leaf area in field grown barley cv Concerto.

Each point at 65, 80, 107 and 123 days after sowing represents the mean of 4 replicates for fungicide treated and inoculated plots, and 3 replicates for untreated plots (10 plants per replicate). Each point at 93 days after sowing represents the mean of 2 replicates (10 plants per replicate). The mean value of the top 3 leaves (Flag leaf, F-1 and F-2) is presented, with the exception of points at 107 days after sowing for the symptom graphs (A, B and C), for which the mean of the top 2 leaves only (Flag and F-1) is presented. Black vertical lines above the graphs represent the l.s.d. for treatment effect from an analysis of variance at that time point. L.s.d. bars are only shown where significant ( $P < 0.050$ ) differences were found between any of the three treatment groups.

Table 16 Analysis of variance results for disease severity and % green area.  
P values and l.s.d. values from analysis of variance at each time point.

Days after sowing	P value	l.s.d.
Spotting		
65	NA	NA
80	0.230	0.094
93	0.396	1.629
107	<0.001	0.854
123	NA	NA
Lesions		
65	NA	NA
80	0.204	0.157
93	0.290	3.426
107	<0.001	0.642
123	NA	NA
Spotting plus lesions		
65	NA	NA
80	0.213	0.251
93	0.309	4.739
107	<0.001	1.185
123	NA	NA
Leaf chlorosis		
65	NA	NA
80	0.073	3.082
93	0.447	8.430
107	0.845	4.646
123	0.010	3.194
Leaf necrosis		
65	NA	NA
80	NA	NA
93	0.731	6.843
107	<0.001	8.130
123	<0.001	14.320
Leaf Green area (GA)		
65	NA	NA
80	0.075	3.284
93	0.483	16.280
107	<0.001	7.430
123	<0.001	12.160

By 107 days after sowing (GS 73), the percentage of leaf area covered by symptoms (spotting plus lesions) varied significantly ( $P < 0.001$ ) between treatments. At this point untreated plants had a higher level of symptoms overall than either of the other treatment groups, however the composition of the symptom type observed differed, as inoculated leaves displayed on average more lesions relative to spotting, and untreated leaves displayed on average more spotting relative to lesions. By 107 days after sowing, mean necrotic leaf area was significantly greater ( $P < 0.001$ ) in both inoculated and untreated plants, and mean green leaf area was significantly higher ( $P < 0.001$ ) in fungicide treated plants than in either of the other treatment groups.

By 123 days after sowing (GS 83), the mean area of chlorotic leaf tissue had increased slightly on fungicide treated plants, while both inoculated and untreated plants were, on average, almost completely necrotic and had lost all, or almost all, remaining chlorotic or green leaf area. At this point fungicide treated leaves retained a significantly higher ( $P < 0.001$ ) percentage of green leaf area (~30%) compared to both inoculated and untreated plants, which retained 1.7% and 0%, respectively.

## **Fungal growth *in planta***

*R. collo-cygni* DNA was extracted from leaves directly below the flag leaf (known as leaf 2 or sometimes the F-1 leaf). A low level of *R. collo-cygni* DNA (0.4 ng on average across the first four sampling dates) was found to be present in fungicide-treated plants (Figure 29). *R. collo-cygni* remained low on average for all treatment groups up to and including 107 days after sowing, although by 93 days after sowing the average *R. collo-cygni* DNA quantity in both inoculated and untreated plants was more than double that in fungicide-treated plants, and by 107 days after sowing the average quantity of *R. collo-cygni* DNA in fungicide-treated plants was just 3 % and 0.2 % of

that in inoculated and untreated plants, respectively. By 123 days after sowing, the quantity of *R. collo-cygni* DNA in all treatment groups had increased, and was significantly higher ( $P < 0.05$  as shown by the l.s.d. for the time x treatment interaction) in both inoculated and untreated plants than in fungicide-treated plants (Table 17), as analysed by ANOVA with time as a factor, however there was no significant difference between treatment groups prior to this point, meaning that the overall treatment effect was not found to be significant ( $P = 0.067$ ).

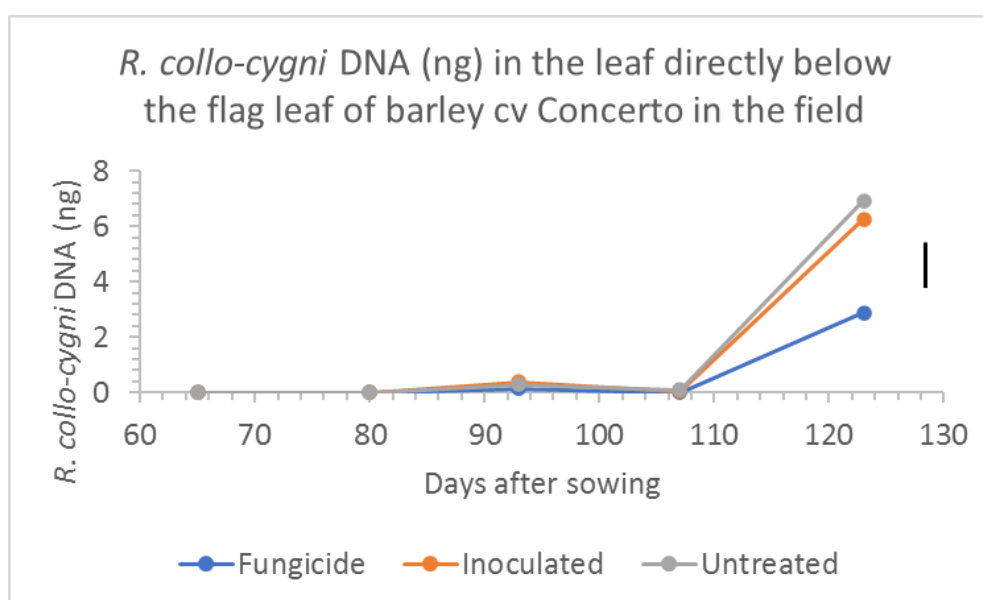


Figure 29 *R. collo-cygni* DNA (ng) in F-1 leaves of field-grown barley cv Concerto. Each point represents the mean of 4 replicates for fungicide treated and inoculated plots and 3 replicates for untreated plots (10 plants per replicate). The black bar to the right of the graph represents the l.s.d. for Treatment. Days after sowing from an analysis of variance.

Table 17 Analysis of Variance results for an analysis of the quantity of *R. collo-cygni* DNA in F-1 leaves of field-grown barley cv Concerto. L.s.d at 5% level.

	P value	l.s.d.
Treatment	0.067	0.781
Days after sowing	<0.001	1.008
Treatment.Days after sowing	0.028	1.746

## Crop biomass

*R. collo-cygni* infection was not found to affect above-ground biomass (dry weight m<sup>-2</sup>) in this experiment (Figure 30 and Table 18). An analysis of variance including time as a factor showed no significant treatment effect ( $P = 0.632$ ) and no significant interaction between treatment and time ( $P = 0.882$ ). Crop biomass was measured at 85, 99 and 113 days after sowing, incorporating the period from anthesis to late grain fill, but not end of grain fill and the period of major canopy senescence.

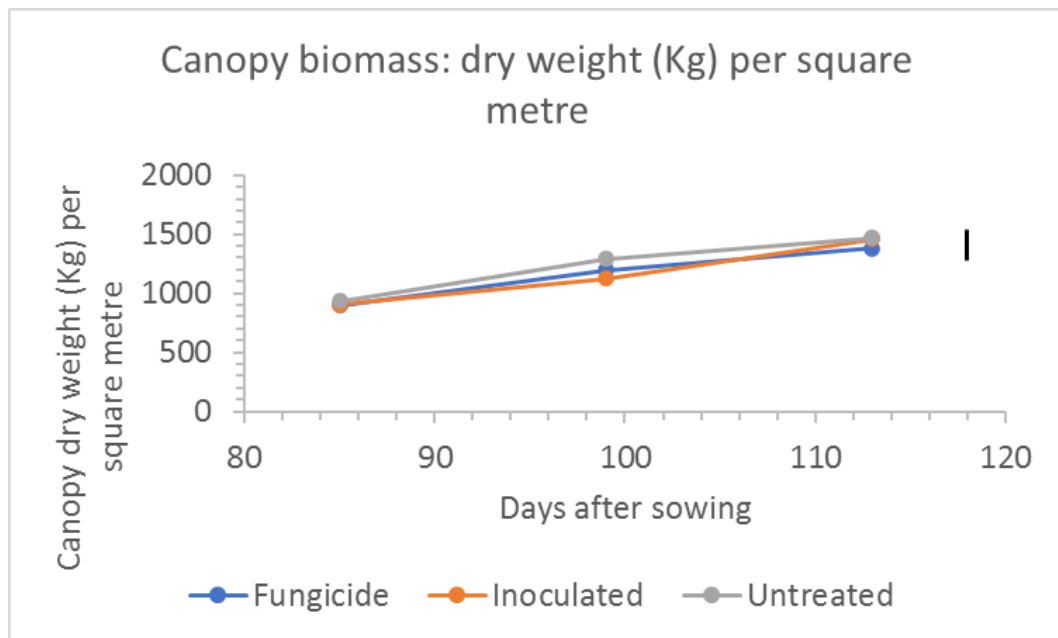


Figure 30 Canopy biomass of field-grown barley cv Concerto. Each point represents the mean of 4 replicates for fungicide treated and inoculated plots and 3 replicates for untreated plots. The black line to the right of the graph represents the l.s.d. (5% level) for the Treatment.Days after sowing interaction from an analysis of variance.

Table 18 Analysis of variance results for above-ground biomass of field-grown barley cv Concerto.

	P value	l.s.d.
Treatment	0.632	142.7
Days after sowing	<0.001	142.7
Treatment.Days after sowing	0.882	247.1

## Chlorophyll fluorescence

An analysis of variance with time as a factor detected no significant differences in maximal chlorophyll fluorescence ( $F_v/F_m$ ) between treatments until 111 days after sowing, by which point symptoms and associated green leaf area loss on inoculated and untreated leaves were well-developed. At this point  $F_v/F_m$  was significantly ( $P = 0.007$ ) reduced in both inoculated and untreated plots, relative to fungicide treated plots (Figure 31).

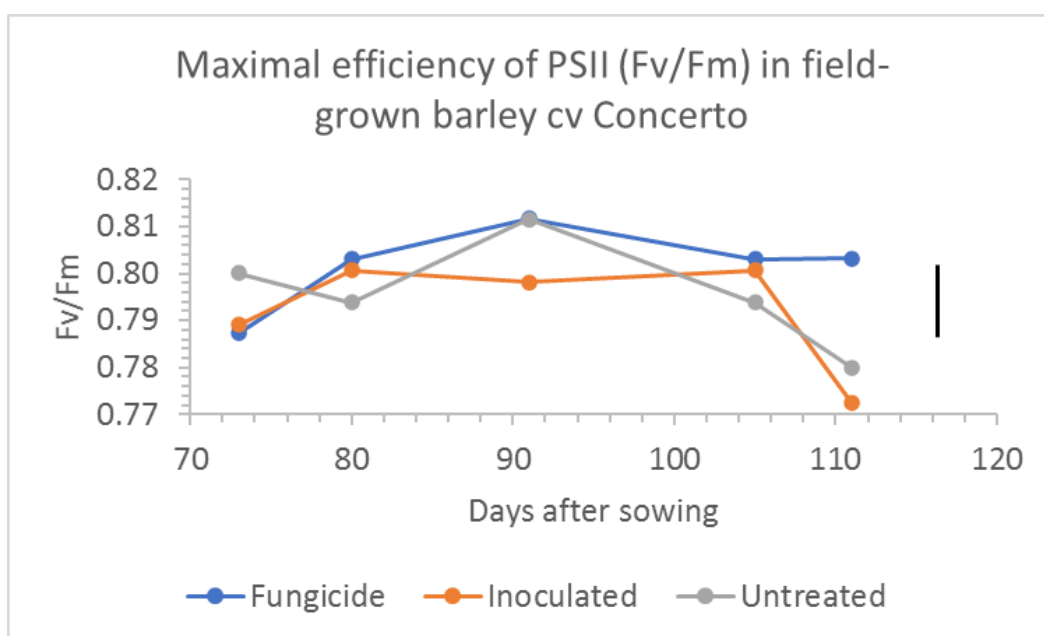


Figure 31 Maximal efficiency of PSII ( $F_v/F_m$ ) measured on F-1 leaves of field-grown barley. Each point represents the mean of 4 replicates for fungicide treated and inoculated plots and 3 replicates for untreated plots (5 plants per replicate).

Table 19 Analysis of variance results for maximal efficiency of PSII (Fv/Fm) measured on F-1 leaves of field-grown barley.

	P value	I.s.d.
Treatment	0.013	0.006
Days after sowing	<0.001	0.008
Treatment.Days after sowing	0.007	0.014

## Healthy area light interception

The fraction of the incident PAR intercepted by plants that was intercepted by healthy (green) tissue was calculated from measurements taken at three time points during grain filling at 85, 99 and 113 days after sowing. The data were analysed using analysis of variance for each time point (Table 20). At 85 days after sowing no significant differences were found between treatment groups.

At 99 days after sowing, inoculated and untreated plots were found to be significantly different ( $P = 0.005$ ) to fungicide treated plots. At this point the fraction of PAR intercepted by healthy tissue for fungicide treated plots remained the same as it had been at 85 days after sowing (0.97), however that for both inoculated and untreated plots had fallen to 0.94.

At 113 days after sowing, the fraction of PAR intercepted by healthy tissue had fallen again for inoculated and untreated plots (to 0.83 and 0.81, respectively), significantly lower ( $P < 0.001$ ) than that for fungicide treated plots (0.93).

The total PAR ( $\text{MJ m}^{-2}$ ) intercepted by healthy (green) tissue during grain filling was also analysed using analysis of variance (Table 21). Significant differences were found between all treatment groups ( $P < 0.001$ ). PAR

intercepted by healthy tissue was reduced relative to fungicide treated plots for both inoculated and untreated plots (~18% and ~23% reduction, respectively). The difference between inoculated and untreated plots was also found to be significant ( $P < 0.001$ ). PAR intercepted by healthy tissue was reduced by ~ 5% for untreated plots relative to inoculated plots.

Table 20 Treatment means and analysis of variance results for the fraction of incident PAR that was intercepted by healthy (green) tissue of field grown barley plants cv Concerto at 3 time points during grain filling.

Days after sowing	Treatment means for the fraction of total light intercepted by plants that was intercepted by healthy (green) tissue			P value	l.s.d.
	Fungicide	Inoculated	Untreated		
85	0.97	0.96	0.96	0.805	0.018
99	0.97	0.94	0.94	0.005	0.018
113	0.93	0.82	0.81	<0.001	0.040

Table 21 Treatment means and analysis of variance results for total PAR ( $\text{MJ m}^{-2}$ ) intercepted by healthy (green) tissue of field grown barley plants cv Concerto during grain filling.

Treatment means for total PAR ( $\text{MJ m}^{-2}$ ) intercepted by healthy (green) tissue during grain filling			P value	l.s.d.
Fungicide	Inoculated	Untreated		
289.80	236.70	223.90	<0.001	5.810

## Crop yield

### Yield components

An analysis of variance (Table 22) detected significant differences between the three treatment groups for grain number  $\text{m}^{-2}$  and yield ( $\text{t ha}^{-1}$  at 15% moisture content); ( $P < 0.001$  and  $P = 0.001$  respectively). Yield and grain number  $\text{m}^{-2}$  for both inoculated and untreated plots were reduced relative to fungicide treated plots, however, inoculated plots had a higher grain number relative to untreated plots (a difference of  $\sim 1000$  grains  $\text{m}^{-2}$ ) and a higher yield (a difference of  $\sim 1 \text{ t ha}^{-1}$ ).

Table 22 Yield components. I.s.d. values are for 5% level.

	Mean treatment value			P value	I.s.d.
	Fungicide	Inoculated	Untreated		
Grain number $\text{m}^{-2}$	15571	13899	12689	<0.001	978.400
Mean grain weight (mg)	46.90	45.63	43.17	0.115	3.651
Yield ( $\text{t ha}^{-1}$ at 15% Moisture Content)	7.30	6.34	5.49	0.001	0.715

### Radiation use efficiency

Radiation use efficiency (RUE) was estimated by plotting the biomass gain during the first half of grain filling against the cumulative healthy PAR interception over the same period. Simple linear regression with groups was used to compare the slopes and the intercepts for the different treatments. The slopes were not significantly different. The slope for fungicide was 2.30, for inoculated it was 2.83 and for untreated it was 2.05  $\text{g DM MJ}^{-1}$  PAR. The

slope of the initial single regression applied to all data, assuming slopes and constants to be equal, was 2.41 g DM MJ<sup>-1</sup>. This was used in the yield loss prediction equation as the constant value for RUE (g biomass per MJ of light intercepted).

### **Predicted and observed yield loss**

The reduction in yield relative to fungicide-treated plots predicted from the loss of green leaf area and healthy area PAR interception (Figure 32) was 1.51 t ha<sup>-1</sup> for inoculated plots and 1.87 t ha<sup>-1</sup> for untreated plots. These were found not to be significantly different from the observed yield losses at harvest when analysed by paired t-test ( $P = 0.126$  and  $P = 0.881$ , respectively).

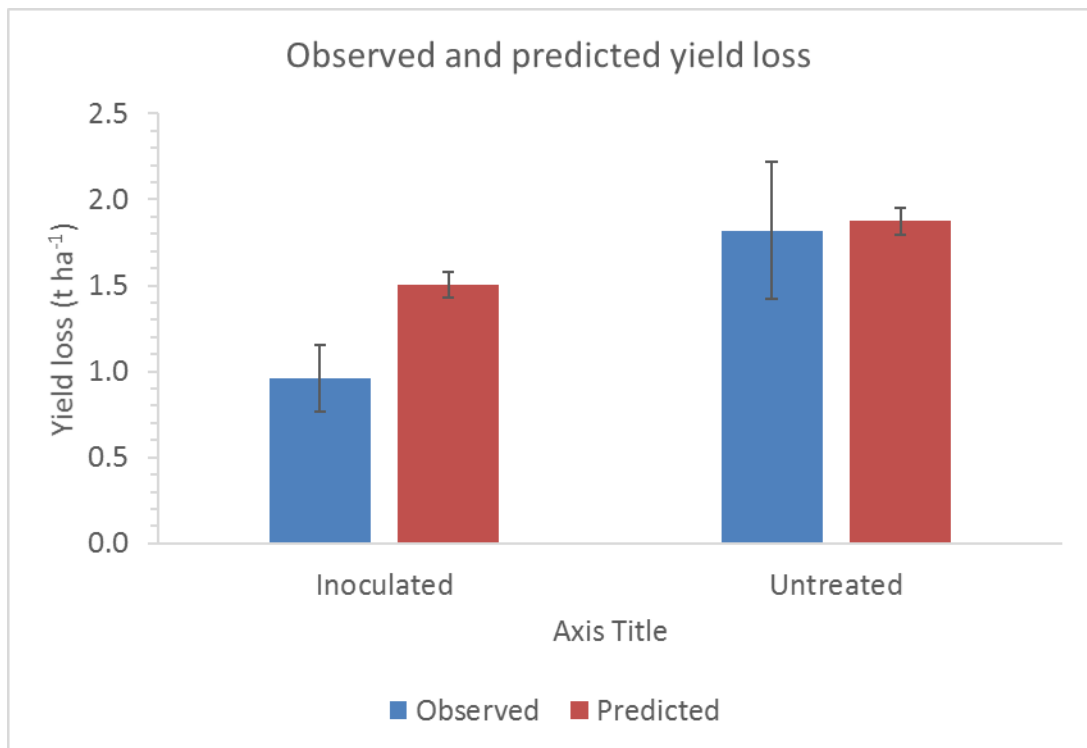


Figure 32 Reduction in yield of inoculated and untreated plots relative to fungicide treated plots. Blue columns = observed reduction. Red columns = reduction predicted from the loss of green leaf area and healthy area PAR interception. Each column represents the average of 4 replicates (inoculated) and 3 replicates (untreated). Error bars are  $\pm$ SEM.

## Discussion

The timing of symptom appearance and disease development observed during the experiment were consistent with those previously described as typical for RLS (see Chapter 1). Symptoms had begun to develop on the upper three leaves of inoculated and untreated plants by 93 days after sowing (around a week after flowering), increasing significantly relative to fungicide treated plots by 107 days after sowing (GS 73), at which point symptom severity, assessed as the percentage of leaf area covered by symptoms including both spotting and lesions, was greater in untreated plots than in inoculated.

*R. collo-cygni* growth *in planta*, as measured by quantification of fungal DNA in leaf 2 (the leaf directly below the flag leaf) was not found to be significantly higher in untreated and inoculated plots relative to fungicide treated plots before 123 days after sowing, when untreated and inoculated plots were nearing total senescence. Average disease severity in leaf 2, as measured by % leaf area covered by symptoms (lesions and spotting), was already significantly higher ( $P < 0.001$ ) in inoculated and untreated plots than in fungicide treated plots by 107 days after sowing (average *R. collo-cygni* DNA in leaf 2 at 107 days after sowing was 0.7 ng, 8.2 ng and 10.1 ng in fungicide treated, inoculated, and untreated plots, respectively). This pattern was similar to that observed for average values of symptom severity across the top three leaves, as presented in the Results section. Thus, although symptom severity increased with increasing fungal DNA, a steep increase in fungal DNA was observed at the stage of leaf senescence when most of the green area of leaves had been lost.

At GS 73, fungicide treated plants retained >90% of green leaf area on average across the upper three leaves, while inoculated and untreated plants had lost ~50% and ~60% of green leaf area, respectively. Fungicide treated plants retained ~30% green leaf area on average across the upper three

leaves at 123 days after sowing (GS 83), when inoculated and untreated plants were nearing total senescence. Total canopy senescence occurred at approximately 123, 127 and 135 days after sowing for untreated, inoculated and fungicide treated plots, respectively. These effects of treatments on post-anthesis green leaf area duration resulted in associated changes in PAR interception by healthy tissue during grain filling.

Maximal chlorophyll fluorescence ( $F_v/F_m$ ) was not found to be affected by *R. collo-cygni* infection in asymptomatic leaves or green areas of symptomatic leaves. It was significantly reduced in symptomatic tissue after lesions developed indicating damage to photosystem II reaction centres. These results reflect those found in barley seedlings inoculated with *R. collo-cygni*, described in Chapter 2. The lack of any significant effect on photosynthetic activity prior to symptom development is consistent with whole canopy measurements of RUE. In the current work RUE was estimated from the relationship between light interception by green (healthy) tissue and above ground biomass gain. There was no significant difference in RUE between fungicide treated, untreated or inoculated plants implying that RUE was not affected by *R. collo-cygni* infection when necrotic lesions are excluded from estimates of light interception and the analysis confined to non-symptom expressing tissue. When RUE is estimated this way it measures the efficiency of conversion of light energy intercepted by healthy tissue into biomass and is thus the net outcome of effects of environment and experimental treatments on photosynthesis, respiration and partitioning of biomass between shoots and roots. These data, therefore, support the conclusion that there is no discernible effect of asymptomatic *R. collo-cygni* infection on RUE.

Average yield ( $\text{t ha}^{-1}$  at 15% moisture content) was significantly reduced in both inoculated and untreated plots relative to that of fungicide treated plots in this experiment. However, the yield of inoculated plots was significantly higher than that of untreated plots. If the effects of ramularia leaf spot on yield are the simply the result of reductions in green leaf area because of

symptom development and tissue necrosis, it should be possible to estimate the difference in yield between diseased and non-diseased plants from the difference in light interception without needing to invoke effects of disease on RUE or remobilisation of soluble carbohydrate reserves for grain filling. The results for the analysis of healthy area light interception and comparison of predicted and observed yield loss indicated that the difference in post-anthesis PAR interception by healthy tissue between fungicide-treated and the inoculated and untreated plots was sufficient to account for the observed yield losses.

The reduction in post-anthesis PAR interception by healthy tissue in inoculated and untreated plots was associated with RLS symptom development; the production of lesions and associated chlorosis and necrosis, and reduced duration of the period between anthesis and complete canopy senescence relative to fungicide treated plots. However, whilst the maintenance of green leaf area following fungicide treatment may be sufficient to account for the yield differences between treatments, the actual mechanisms responsible for increasing yield appear to be more complex. The greater yield of fungicide-treated plots was the result of a larger grain number  $\text{m}^{-2}$  and not a greater mean grain weight as might be expected were fungicide solely protecting post-anthesis photosynthetic activity.

It is conceivable that loss of post-anthesis assimilation due to disease-associated reduction in healthy area light interception could lead to loss of ears or abortion of grains. However, experiments using shading to reduce light interception in spring barley as a proxy for the effects of foliar disease symptoms (Kennedy *et al.*, 2018) found no evidence of grain abortion, nor a significant reduction in ear number, when shading was imposed 14 days after GS55 to reduce net photosynthesis activity during grain filling.

It is also possible that fungicide treatment increased grain numbers directly and that the increase in grain sink capacity operated in tandem with protection of canopy PAR interception and photosynthesis to provide sufficient assimilate for grain filling and to maintain mean grain weight.

Yield effects associated with some fungicide groups extending beyond visible disease control have been a topic of research for some time. SDHI, triazole and strobilurin fungicides have been found to delay leaf senescence in wheat, correlating with increased yields (Wu and Von Tiedemann, 2001; Cromey *et al.*, 2004; Berdugo *et al.*, 2012). Suggested mechanisms for strobilurin-associated delayed leaf senescence in wheat include reduced production of ethylene linked to reduced rates of cytokinin degradation (Grossmann and Retzlaff, 1997; Grossmann *et al.*, 1999) or increased production of antioxidants leading to reduced oxidative stress (Wu and Von Tiedemann, 2001).

Bingham *et al.* (2021) reported increased grain numbers  $\text{m}^{-2}$  in spring barley with applications of triazole and strobilurin fungicides during booting (prothioconazole and pyraclostrobin) in the absence of any visible disease. In the same study chlorothalonil application provided equivalent disease control, including a reduction in *R. collo-cygni* DNA during asymptotic infection prior to flowering, but did not lead to increased grain number  $\text{m}^{-2}$ . This suggests that the increased grain number  $\text{m}^{-2}$  associated with triazole and strobilurin fungicides was a direct physiological effect, and not due, for example, to asymptomatic pathogen control. The authors suggested that increased grain numbers per ear and decreased spikelet mortality could be responsible for the observed effects of triazole and strobilurin fungicides on grain number.

The experiment described in this chapter used prothioconazole as part of the full fungicide treatment to achieve disease-free plants and pyraclostrobin to control diseases other than *R. collo-cygni* in the inoculated treatment group (Table 15). Both of these fungicides have been linked to direct effects on grain number  $\text{m}^{-2}$  as described above, therefore it is possible that this was a contributing factor to the yield differences observed between treatment groups.

In summary, *R. collo-cygni* was not found to impact photosynthesis in field grown barley cv. Concerto prior to the appearance of visible RLS disease symptoms, reflecting the situation observed in inoculated seedlings described

in Chapter 2, suggesting that the long asymptomatic life stage of *R. collo-cygni* in field grown barley may not have a negative impact. Analysis of healthy area light interception and comparison of predicted and observed yield loss indicated that the difference in post-anthesis PAR interception by healthy tissue between fungicide-treated and the inoculated and untreated plots was sufficient to account for the observed yield losses. This indicates that the symptomatic life stage of *R. collo-cygni* in barley is of primary importance for yield loss to RLS.

The results raise some questions about disease control strategies, for example whether it is necessary to control asymptomatic growth of *R. collo-cygni* in barley prior to flowering, as is current practice, and whether it is necessary to keep barley free of RLS until the crop has naturally senesced or whether it is the case that certain levels of RLS may not sufficiently impact yield to justify this. Results from Chapters 2 and 3 indicate that the asymptomatic life stage of *R. collo-cygni* in barley is not an important contributor to eventual yield loss. Therefore, early season applications of fungicide, designed to prevent growth of *R. collo-cygni* fungus in barley prior to the appearance of visible disease symptoms, may be unnecessary for control of RLS. However, this conclusion relates only to the impact of the fungus on barley physiology during the asymptomatic growth period, and does not consider possible secondary effects of fungicides during this period or whether the cumulative effects of a two-spray program may provide greater efficacy of control during the post-flowering period when RLS symptoms typically develop in the field.

The results indicated that the difference in post-anthesis PAR interception by healthy tissue between fungicide-treated and the inoculated and untreated plots was sufficient to account for the observed yield losses, suggesting that protection of green canopy during grain filling is a key factor for control of RLS. However, this does not necessarily mean that protecting light interception by green canopy for the entire duration of grain filling is necessary to avoid or minimise yield losses to RLS. Experiments using

shading as a proxy for the effects of reduced healthy area light interception by spring barley due to foliar disease (Bingham *et al.*, 2019) found that yield was not affected by large reductions in PAR caused by shading once 72–90% of eventual grain dry matter had been deposited. It is possible that protection of green canopy during the early to mid-stages of grain filling could be sufficient to avoid yield loss. Disease incidence and severity are highly variable year on year for RLS. Clearly the severity of symptoms and timing of symptom development during grain filling will impact the extent of reduction in healthy area light interception during this period. Potentially, disease control strategies targeted at reducing symptom severity and/or delaying onset of symptom development, rather than keeping plants completely free of RLS symptoms until natural senescence of the crop, could be a useful avenue for further investigation.

# Chapter 4 Effects of varying rates of leaf senescence on RLS disease development

## Introduction

Chapters 2 and 3 found no evidence to suggest that *R. collo-cygni* impacts barley photosynthesis during asymptomatic growth. Changes in the photosynthetic responses of infected plants were only detected in areas of leaves visually affected by lesions or associated chlorosis and necrosis. Some initial maintenance of photosynthetic capacity was observed within developing lesions, and within chlorotic, but not necrotic, leaf areas, and symptom expression at low severity levels was not found to significantly affect whole-leaf photosynthesis. Chapter 3 concluded that the post-anthesis reduction in PAR interception by healthy tissue associated with RLS symptoms and wider loss of green area in infected plants was sufficient to explain the yield reduction in infected plants relative to fungicide treated plants. Taken together, these results suggest that inhibiting or delaying the onset and proliferation of visible symptoms could prevent or reduce negative effects of *R. collo-cygni* on barley.

The appearance of RLS symptoms on barley in the field typically occurs after the plant has shifted to the reproductive phase, and RLS has been linked to premature leaf senescence in susceptible barley varieties (Oxley *et al.*, 2008), but the relationship between the onset of leaf senescence and the onset and development of RLS symptoms is not yet fully clear. Senescence has been suggested as a promoter of RLS development, resulting from the age-related breakdown of antioxidative protection systems in leaves (Schützendübel *et al.*, 2008). However, Sjøkvist *et al.* (2018) reported that genes associated with senescence processes were up-regulated during *R. collo-cygni* symptom formation in inoculated seedlings, which could indicate a

role for *R. collo-cygni* in triggering foliar senescence. McGrann *et al.*, (2015) found that transgenic barley seedlings displaying a delayed senescence phenotype, linked to overexpression of a *Stress-responsive NAC1* transcription factor, also displayed reduced RLS symptom expression. Both symptom severity and fungal growth were reduced in transgenic plants. However, this did not appear to be a direct result of increased resistance to damage induced by reactive oxygen species (ROS) as the over-expression lines did not differ significantly from the non-transgenic plants in either their constitutive levels of antioxidant transcripts or sensitivity to ROS-induced cell death. Later work (McGrann and Brown, 2018; McGrann *et al.*, 2020) indicated that differences in rates of senescence between barley varieties are not directly correlated with disease severity, and elevated ROS levels do not always increase symptom expression. The authors (McGrann and Brown, 2018) proposed that senescence itself may not be a direct cause of the switch to necrotrophic growth and RLS symptom development in inoculated barley seedlings, but that factors that result in changes to host ROS levels, which can mediate senescence processes, may be involved. Results from Chapter 3 showed earlier and more rapid green leaf area loss in plants infected with *R. collo-cygni* compared to control plants that received a full fungicide treatment regime. This could be due to disease effects, fungicide effects, or a combination.

One of the markers of senescence is a decrease in leaf cytokinin levels. These hormones are involved in multiple regulatory processes during plant growth and development, such as cell division, seed development, shoot and root growth, and senescence (Jameson, 2016). Increasing plant cytokinin levels can be used to delay senescence, either by application of exogenous cytokinin or by manipulation of endogenous cytokinin levels (Richmond and Lang, 1957; Gan and Amasino, 1996; Zubo *et al.*, 2008; Zwack and Rashotte, 2013). Cytokinins can also play a more direct role in plant-pathogen interactions (Häffner *et al.*, 2015). Walters and McRoberts (2006) discussed the role of cytokinins in the creation of nutrient sinks at infection sites and green island development associated with some biotrophic fungal

pathogens, suggesting fungal production of cytokinins or manipulation of host cytokinin levels as a strategy for fungal establishment and nutrient acquisition. Several biotrophic and hemi-biotrophic fungal pathogens are known to be capable of producing cytokinins, for example *Cladosporium fulvum* (Tomato leaf mould) (Murphy *et al.*, 1997), *Leptosphaeria maculans* (Stem canker of oilseed rape) (Trdá *et al.*, 2017), *Ustilago maydis* (Maize smut) (Morrison *et al.*, 2017), and *Magnaporthe oryzae* (Rice blast) (Chanclud *et al.*, 2016). Großkinsky *et al.*, (2011) also reported a role for cytokinins in the mediation of defence against *Pseudomonas syringae* in tobacco, demonstrating increased production of antimicrobial phytoalexins in response to both exogenous cytokinin application and increased endogenous cytokinin production.

Delayed senescence might benefit biotrophic plant pathogens by preserving living cells as a source of nutrition. It is conceivable that maintaining green leaf area by delaying senescence could lead to *R. collo-cygni* remaining in the asymptomatic life stage for longer. If the onset of leaf senescence, or changes in ROS status that can lead to senescence, are factors involved in triggering the *R. collo-cygni* switch to necrotrophic growth and RLS symptom development, then it may be possible to delay the appearance of symptoms using treatments that delay leaf senescence.

## Chapter objectives

The objective of this chapter was to delay foliar senescence in barley seedlings, using different treatment regimes of exogenous cytokinin or fertiliser applications, to investigate the effect of delaying foliar senescence on *R. collo-cygni* growth *in planta* and RLS symptom development.

The following hypotheses were tested in Chapter 4:

- Delaying foliar senescence in barley seedlings infected with *R. collo-cygni* reduces visible RLS symptom severity.
- Delaying foliar senescence in barley seedlings infected with *R. collo-cygni* reduces fungal growth *in planta*.

## Materials and methods

### Overview

All seedlings (cv Fairing) were inoculated with *R. collo-cygni* 14 days after sowing, when the third leaf was partially emerged. The inoculation method and plant and fungal growth conditions were as described in Chapter 2.

The experiments were designed with the aim of assessing the impact of treatments to delay leaf senescence relative to untreated plants on RLS symptom development, both independently and in combination. No un-inoculated plants were included, as the aim was to compare impacts on RLS symptom development, and cabinet-space and time constraints made inclusion of any extra control groups impractical. However, it is accepted that inclusion of un-inoculated control plants would be beneficial where possible and serve to strengthen the robustness of the conclusions.

Seven days after inoculation with *R. collo-cygni*, a foliar cytokinin spray (0.1 mM 6-Benzylaminopurine (6-BAP) solution) was applied to half of the plants (see methodology for preparation and application below), and a control foliar spray application of sterile distilled water (SDW) was applied to the remaining plants.

After a further seven days (28 days after sowing) half the plants which had previously been treated with cytokinin, and half the plants which had been sprayed with SDW, were given additional nutrients. 0.06 ml of Liquid Growmore fertiliser solution (Doff Portland Ltd., Nottingham, UK) was added to 10 ml of water, then this solution was pipetted directly onto the surface of the soil at the base of the plants (10 ml of solution applied to each plant). The undiluted fertiliser solution contained 7 % Nitrogen (N), 7 % Phosphorus Pentoxide ( $P_2O_5$ ), and 7 % Potassium Oxide ( $K_2O$ ). This process was repeated at 35 and 42 days after sowing.

Disease progress and leaf senescence were tracked over the course of the experiment by visual assessment, use of a Soil Plant Analysis Development (SPAD) chlorophyll meter, and quantification of *R. collo-cygni* DNA extracted from leaves. The methodology for extraction and quantification of DNA was as described in Chapter 2.

Materials and methods not described in previous chapters are detailed below.

### **Preparation and foliar application of pH 6.5 cytokinin (6-Benzylaminopurine) solution**

To make 100 ml of 0.1 mM 6-Benzylaminopurine (6-BAP) solution, 2.5 mg of 6-BAP powder (Sigma-Aldrich, Dorset, UK) was dissolved in 10 ml of 1 M HCl (Sigma-Aldrich, Dorset, UK). This solution was then added to 90 ml of SDW. NaOH tablets (Sigma-Aldrich, Dorset, UK) were added gradually to bring the solution up to pH 6.5.

Polyoxyethylene-sorbitan monolaurate (Tween 20) (Sigma-Aldrich, Dorset, UK) was added at approximately 1 drop per 50 ml to either 6-BAP solution or SDW for the controls to give a final concentration of 0.01% v/v.

Foliar applications were conducted using an air brush (Clarke Wiz Air®, Clarke International, Essex, UK) at an application rate of 0.5 ml per plant. The plants were sprayed evenly from different directions to ensure uniform coverage. Care was taken to carry out the application of 6-BAP and SDW in different rooms, using a large plastic bag around the plants as an additional screen, to minimise the chance of aerial drift of cytokinin to control plants. Plants that were treated with cytokinin were kept separate from those that were not until the leaves were completely dry.

## **Measurement of relative leaf-chlorophyll content**

Two measurements were made on the adaxial surface of second leaves of intact plants using a SPAD 502 Plus Chlorophyll Meter (Konica Minolta, Warrington, UK). One measurement was made in the distal region of the leaf, approximately mid-way between the tip and centre point of the leaf length. The other was made in the basal section of the leaf, approximately mid-way between the ligule and the centre point of the leaf length. The two measurements from the leaf were averaged.

## **Data and statistical analysis**

264 plants were divided into five randomised blocks of 52 plants each, with 13 replicates in each block. Each replicate consisted of one plant from each of four treatment groups: 1) no cytokinin and no fertiliser; 2) with cytokinin and no fertiliser; 3) no cytokinin and with fertiliser; 4) with cytokinin and with fertiliser. A full description of the treatment regime for these four groups is presented in Table 23.

Table 23 Senescence experiment treatments

Treatment number	Treatment description	Treatment abbreviation	Treatment colour code
1	Rcc inoculum at 0.5 ml per plant applied 14 days after seeds sown. SDW at 0.5 ml per plant applied 21 days after seeds sown.	no cyt no fert	
2	Rcc inoculum at 0.5 ml per plant applied 14 days after seeds sown. 0.1 mM cytokinin at 0.5 ml per plant applied 21 days after seeds sown.	with cyt no fert	
3	Rcc inoculum at 0.5 ml per plant applied 14 days after seeds sown. SDW at 0.5 ml per plant applied 21 days after seeds sown. 0.06 ml Growmore fertiliser in 10 ml water added to each pot 28, 35 and 42 days after seeds sown.	no cyt with fert	
4	Rcc inoculum at 0.5 ml per plant applied 14 days after seeds sown. 0.1 mM cytokinin at 0.5 ml per plant applied 21 days after seeds sown. 0.06 ml Growmore fertiliser in 10 ml water added to each pot 28, 35 and 42 days after seeds sown.	with cyt with fert	

A subset of plants consisting of five replicates was repeatedly assessed for visual disease development and relative chlorophyll content throughout the experiment; 1, 2, 3, 4, 5, 8, 11, 15, 18, 20, 22 and 27 days after cytokinin application (d.a.c.). These five replicates were destructively sampled for DNA extraction and quantification of *R. collo-cygni* DNA at the end of the experiment (27 d.a.c.). Four unique sets of plants (5 replicates on each occasion) were also destructively sampled for DNA extraction and quantification at 1, 5, 11 and 15 days after cytokinin application. Data was analysed using either repeated measures or standard analysis of variance as appropriate using GenStat software (19<sup>th</sup> Edition, VSN International, Hemel

Hempstead, UK). Residuals were checked for normality of distribution and homogeneity of variance before analysis.

## **Results**

### **Senescence and visible symptom progression**

#### **Relative chlorophyll content**

Relative leaf chlorophyll content reduced over time in all treatment groups (Figure 33). The rate and extent of decline was greater in plants that were not treated with cytokinin. A repeated measures analysis of variance (Table 24) revealed a significant ( $P < 0.001$ ) main effect of cytokinin treatment on relative chlorophyll content, and a significant interaction ( $P < 0.001$ ) between cytokinin treatment and time (days after inoculation). The analysis did not reveal a statistically significant main effect of fertiliser treatment ( $P = 0.181$ ), and there was no significant interaction between fertiliser treatment and time ( $P = 0.122$ ), between fertiliser treatment and cytokinin treatment ( $P = 0.332$ ), or between fertiliser treatment, cytokinin treatment and time ( $P = 0.403$ ). Leaving fertiliser treatment out of consideration, therefore, plants in the treatment groups that did not receive cytokinin had, on average, significantly lower ( $P < 0.001$ ) relative chlorophyll content than those that did from 24 days after inoculation onwards.

## Green Leaf Area

A repeated measures analysis of variance revealed a significant ( $P = 0.003$ ) main effect of cytokinin treatment on % Green Leaf Area, and a significant interaction ( $P < 0.001$ ) between cytokinin treatment and time (days after inoculation) (Figure 33 and Table 24). The analysis did not reveal a statistically significant main effect of fertiliser treatment ( $P = 0.064$ ), and there was no significant interaction between fertiliser treatment and time ( $P = 0.081$ ) or between fertiliser treatment and cytokinin treatment ( $P = 0.086$ ). There was a borderline significant ( $P = 0.052$ ) interaction between fertiliser treatment, cytokinin treatment and time. By 24 days after inoculation, plants that received neither fertiliser nor cytokinin (treatment group 1) had lower % GLA ( $P = 0.052$ ) than plants in all the other treatment groups (Figure 33). There were no significant differences between plants in any of the other treatment groups at this stage. This pattern remained stable up to and including 28 days after inoculation. By 33 days after inoculation, plants in both the treatment groups that did not receive cytokinin (groups 1 and 3) displayed lower ( $P = 0.052$ ) % GLA than those that did (treatment groups 2 and 4). By this stage there was no longer a statistically significant difference between plants that received fertiliser but no cytokinin and plants that received neither fertiliser nor cytokinin (groups 1 and 3). There were no significant differences between plants in either of the treatment groups that received cytokinin (groups 2 and 4) at any point throughout the experiment, regardless of fertiliser status. Thus, fertiliser application delayed decline in % GLA temporarily compared to plants that were not treated with either cytokinin or additional fertiliser (controls – treatment group 1). Plants treated with cytokinin maintained a greater percentage of green leaf area over a longer period than those that did not, irrespective of the fertiliser treatment (Figure 33).

## **RLS symptoms**

In inoculated plants that were not treated with either cytokinin or additional fertiliser (controls – treatment group 1), the first symptoms of RLS appeared 9 days after inoculation. Symptom severity steadily increased reaching around 9% by the end of the experiment. Application of additional fertiliser significantly reduced the severity of symptoms compared to controls from around day 17 onwards such that symptom severity at the end of the experiment was ~5%. Treatment of plants with cytokinin either on its own or in combination with additional fertiliser had a greater effect on symptom development than fertiliser alone. The final disease severity was <3% in plants treated with cytokinin alone.

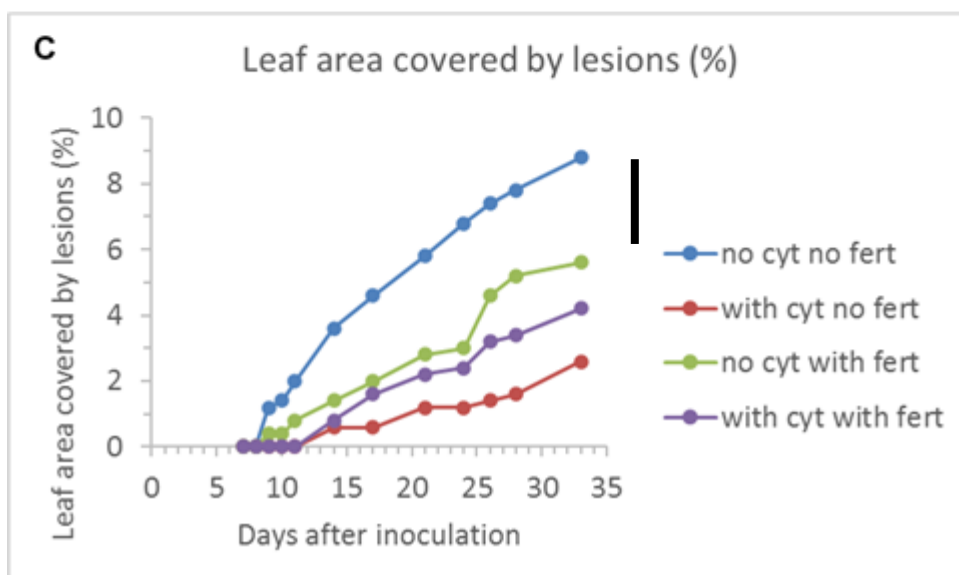
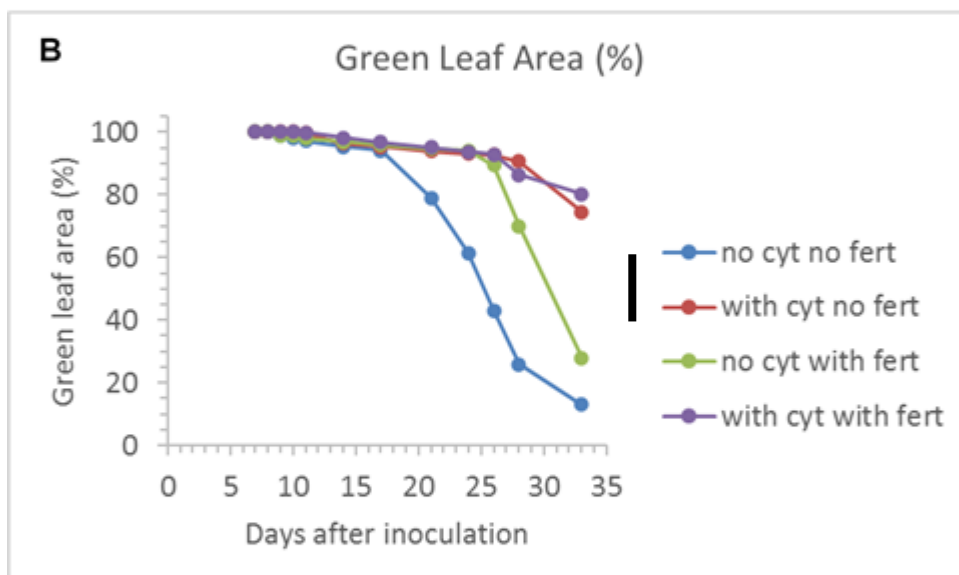
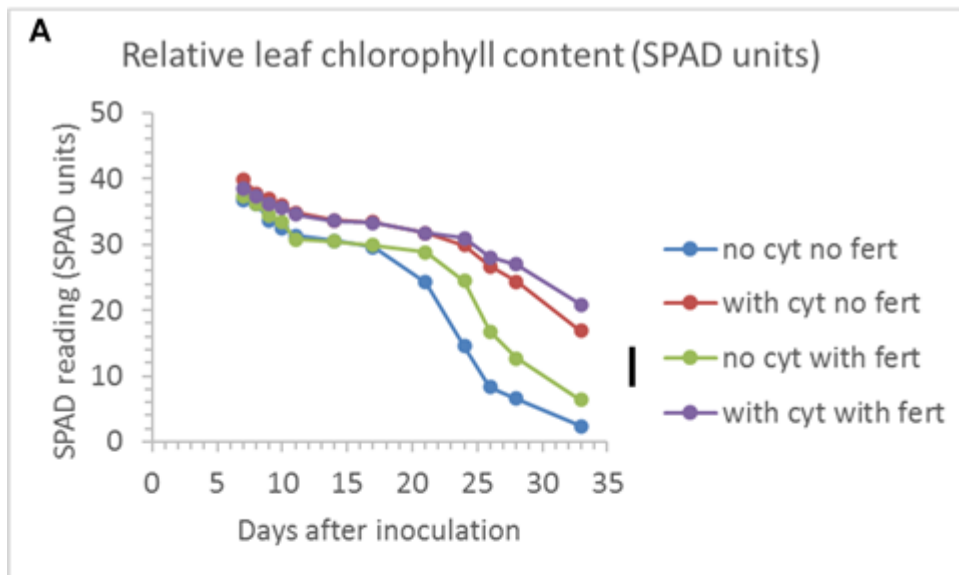


Figure 33 Effects of cytokinin and additional fertiliser treatments on leaf senescence and RLS symptom development on barley cv Fairing seedlings over time (days after inoculation). **A)** Relative leaf chlorophyll content (SPAD units): average value of measurements taken in distal and basal leaf sections. **B)** Green Leaf Area (%) **C)** Leaf area covered by RLS lesions (%). Points are means of 5 replicates. All data is from second leaves of barley seedlings. Vertical black lines to the right of the graphs represent the least significant difference (l.s.d. 5%) value for the interaction between cytokinin, fertiliser treatment, and time (days after inoculation) from a repeated measures ANOVA.

Table 24 P values from repeated measures ANOVA of effects of cytokinin treatment (yes or no), fertiliser treatment (yes or no) and time (days after inoculation) on the relative chlorophyll content (SPAD readings), % Green Leaf Area, and % area of leaf covered by RLS lesions of second leaves of barley seedlings N = 5.

	SPAD reading leaf average	Green area of leaf (%)	Area of leaf covered by lesions (%)
Cyt	<0.001	0.003	0.004
Fert	0.181	0.064	0.310
Cyt.Fert	0.332	0.086	0.039
Time	<0.001	<0.001	<0.001
Time.Cyt	<0.001	<0.001	0.003
Time.Fert	0.122	0.081	0.523
Time.Cyt.Fert	0.403	0.052	0.045

## **Fungal growth *in planta***

### ***R. collo-cygni* DNA levels in leaves during the experiment**

*R. collo-cygni* DNA was quantified from unique sets of plants destructively sampled at 7, 11, 17 and 21 days after inoculation (1, 5, 11 and 15 days after cytokinin application). An analysis of variance using cytokinin treatment (yes or no), fertiliser treatment (yes or no) and time (days after inoculation) as factors detected significant main effects of cytokinin treatment ( $P < 0.001$ ), fertiliser treatment ( $P = 0.023$ ) and time ( $P < 0.001$ ). All interactions tested were also found to be significant (Figure 34 and Table 25). By 21 days after inoculation, *R. collo-cygni* DNA levels were significantly higher ( $P = 0.023$ ) in plants that received neither cytokinin nor fertiliser treatment than in all other treatment groups.

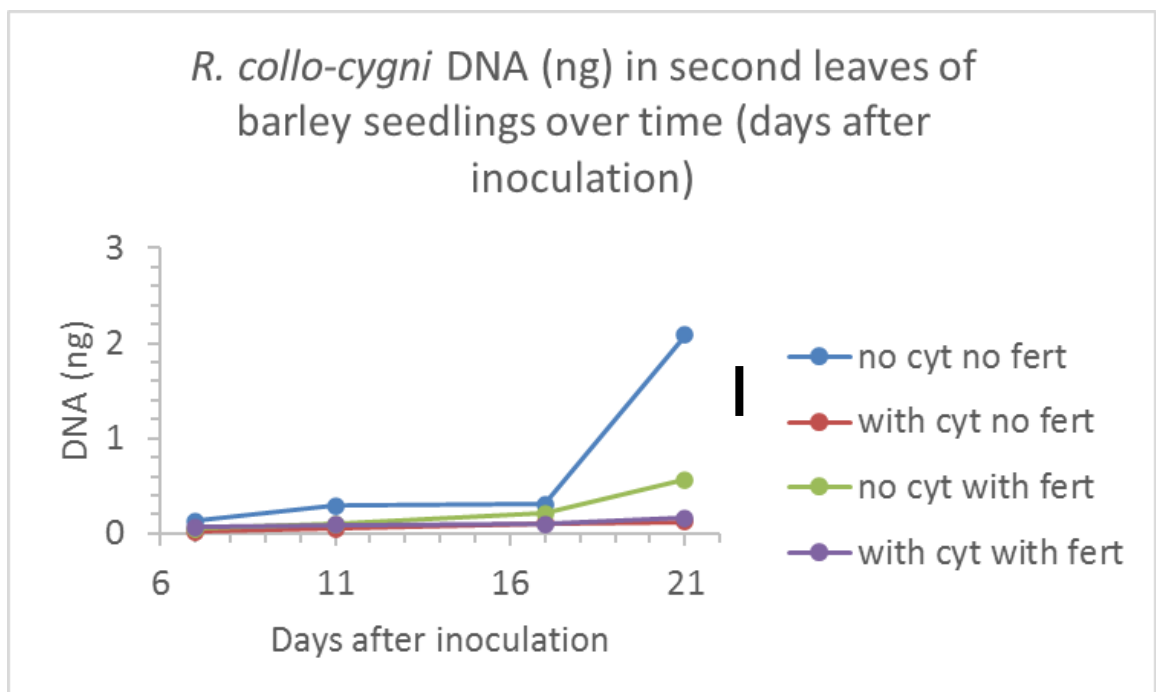


Figure 34 *R. collo-cygni* DNA (ng) in second leaves of barley seedlings cv Fairing over time. From an experiment to compare the effects of cytokinin and fertiliser treatments on green leaf area retention and RLS disease development. Each point shows the average of 5 replicates. The black, vertical bar to the right of the graph represents the least significant difference (l.s.d. 5%) for the interaction between cytokinin treatment, fertiliser treatment and time from an analysis of variance.

Table 25 ANOVA results for fungal growth *in planta*. P values and l.s.d. values from ANOVA with cytokinin treatment (yes or no, fertiliser treatment (yes or no) and time (days after inoculation) as factors. N = 5. From an experiment to compare the effects of cytokinin and fertiliser treatments on green leaf area retention and RLS disease development.

	P value	l.s.d.
Cytokinin	<0.001	0.185
Fertiliser	0.023	0.185
Days after inoculation	<0.001	0.262
Cytokinin.Fertiliser	0.010	0.262
Cytokinin.Days after inoculation	<0.001	0.371
Fertiliser.Days after inoculation	0.027	0.371
Cytokinin.Fertiliser.Days after inoculation	0.023	0.524

### ***R. collo-cygni* DNA levels in leaves at the end of the experiment**

The same set of plants which had been measured repeatedly and non-destructively throughout the experiment to monitor leaf senescence and RLS symptom development were destructively sampled at 33 days after inoculation, and the *R. collo-cygni* DNA level in second leaves was quantified.

A one-way ANOVA comparing the four treatment groups showed that *R. collo-cygni* DNA levels were significantly higher ( $P = 0.025$ ) in the plants that received no cytokinin and no fertiliser treatment than in any of the other groups (Figure 35). No significant differences were found between any of the other treatment groups ( $P > 0.05$ ).

A two-way ANOVA including the interaction between fertiliser treatment and cytokinin treatment (Table 26) found no significant effect of fertiliser treatment ( $P = 0.093$ ) and a weak interaction between fertiliser and cytokinin treatment ( $P = 0.059$ ). This method of analysis showed a significant main effect of cytokinin treatment ( $P = 0.032$ ).

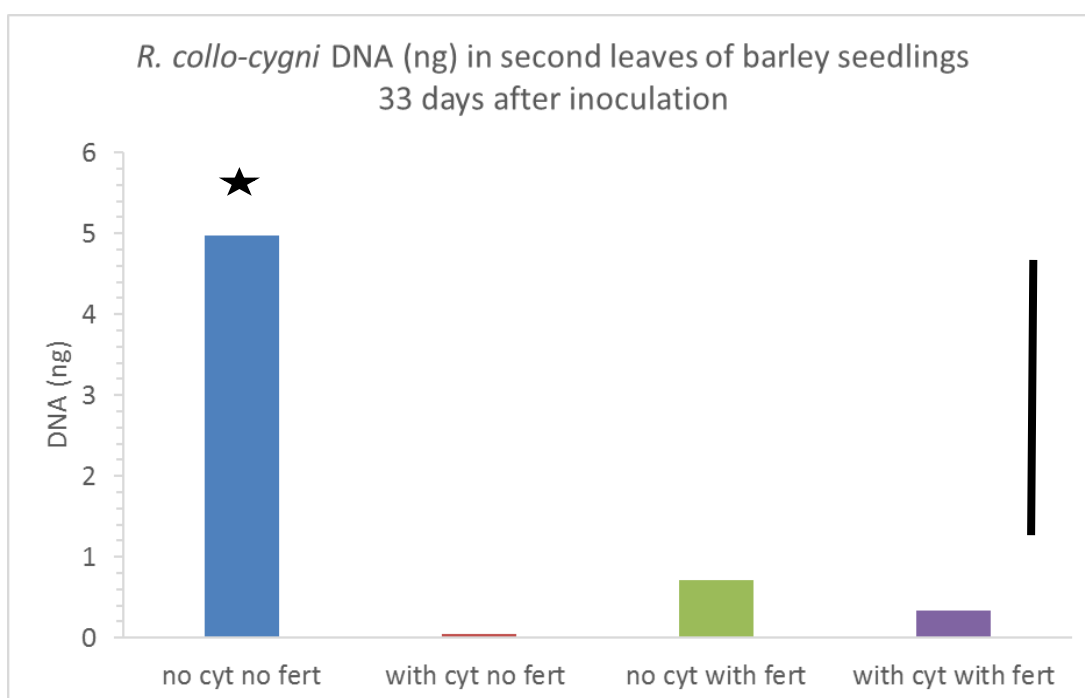


Figure 35 *R. collo-cygni* DNA (ng) in second leaves of barley seedlings Cv Fairing at 33 days after inoculation. Bars show average of 5 replicates. The black, vertical line to the right of the graph represents the l.s.d. (3.39) for Cytokinin.Fertiliser from a two-way ANOVA. The star above treatment group 1 (no cytokinin or fertiliser treatment) indicates that the plants in this treatment group had significantly higher *R. collo-cygni* DNA levels than those in any of the other treatment groups ( $P = 0.025$ ), when analysed using one-way ANOVA.

Table 26 ANOVA results for fungal DNA in plants at the end of the experiment. P values from a two-way ANOVA including interaction between fertiliser and cytokinin treatment. N = 5.

	P value
Cytokinin	0.032
Fertiliser	0.093
Cytokinin.Fertiliser	0.059

## Discussion

RLS symptom severity and fungal growth *in planta* was reduced in plants that received treatments designed to delay leaf senescence relative to control plants that did not. Exogenous application of cytokinin was more effective than fertiliser application at maintaining green leaf area and relative leaf chlorophyll content.

Symptom expression and fungal DNA levels were highest in plants that received neither of the senescence-delaying treatments. RLS lesions first appeared, and symptom severity differed significantly between treatments, before differences in relative chlorophyll content or % GLA became apparent. *R. collo-cygni* DNA was significantly reduced in all plants relative to controls (treatment group 1), including those treated with fertiliser alone. Symptom severity between treatments differed significantly before significant differences in fungal DNA level were apparent between treatments, so the quantity of fungus within leaves did not appear to be a basis for initial symptom expression or severity. The association between increased symptom severity and higher levels of *R. collo-cygni* DNA observed towards the end of the experiment was similar to that reported by Taylor *et al.* (2010).

In the field experiment described in Chapter 3, *R. collo-cygni* DNA levels increased significantly in infected plants at the later stages of symptom development once leaves were senescing. It may be that this rise coincides with fungal sporulation.

The statistical analysis of the results included four time points prior to the first application of fertiliser in repeated measurements ANOVA analyses of % leaf area covered by symptoms, % green leaf area and relative leaf chlorophyll content measurements. Two time points prior to the first application of fertiliser were included in ANOVA analysis including time as a factor of *R. collo-cygni* DNA quantity (ng) in leaves. As fertiliser was included as a treatment in these analyses, it was worth considering how analysis of the results excluding these initial time points prior to the first application of fertiliser might impact interpretation of the results, although this of course meant excluding time points at which all plants were symptom-free and retained full green leaf area. When analysed in this way, the outcomes were broadly unaltered. However, this method found no significant interaction between cytokinin, fertiliser and days after inoculation for % green leaf area and % leaf area covered by symptoms, and no significant interaction between fertiliser and days after inoculation or between, cytokinin, fertiliser and days after inoculation for *R. collo-cygni* DNA level in leaves. Therefore, the limited scope of this method of analysis restricted the conclusions that could be drawn about interactions between fertiliser and cytokinin. The effect of cytokinin treatment and the interaction between cytokinin treatment and days after inoculation was found to be significant for all analyses (as was the case for the method of analysis presented in the results section). Using this method of analysis it was found that plants in the treatment groups that did not receive cytokinin had, on average, significantly higher ( $P < 0.001$ ) % leaf area covered by symptoms and significantly lower ( $P = 0.014$ ) % green leaf area than those that did from 21 and 28 days after inoculation, respectively. Significant main effects of treatment on the quantity of *R. collo-cygni* DNA in leaves were found for both fertiliser ( $P = 0.039$ ) and cytokinin (0.001), as was the case for the method of analysis presented in the results section.

The early lesion development observed in control plants, before differences in relative chlorophyll content or % GLA became apparent, could indicate that senescence itself may not act as a trigger for RLS symptom expression, similar to the conclusions of McGrann and Brown (2018). It could be that symptom expression is triggered by pre-senescence signals or signals associated with the onset of senescence in barley at a very early stage, including potentially changes in ROS status. However, the results also do not rule out the possibility of the fungal switch to necrotrophy instead acting as a trigger for senescence, as suggested by the results reported in Sjökvist *et al.*, (2018), in which the authors reported upregulation of cytokinin oxidases and abscisic acid response genes in barley seedlings during infection with *R. collo-cygni*, in the period just before visible symptom appearance, and during early symptom development. In this scenario the treatments used to delay senescence in the current experiments may have interfered with this process.

The results show a negative relationship between % green leaf area and symptom severity. The mechanisms underlying the reduced level of symptoms observed in 'greener' leaves over the course of the experiment cannot be deduced from the results. However, although plants that received fertiliser only (no cytokinin) developed fewer symptoms on average over the course of the experiment and maintained a greater average percentage of green leaf area than control plants that received neither fertiliser nor cytokinin, these observed effects were stronger in plants that received cytokinin (both alone or in combination with fertiliser treatment). This suggests different mechanisms behind the activity of the two methods used to delay leaf senescence, and/or different effects on the fungus. It is possible, for example, that the treatments used to delay senescence had differing effects on phytotoxin production by *R. collo-cygni*. This could potentially have an impact on leaf necrosis, perhaps accelerating loss of green leaf area.

Interestingly, fungal growth as measured by average *R. collo-cygni* DNA levels in leaves was reduced in all plants that received fertiliser, cytokinin or a combination of both treatments, relative to control plants that received neither

treatment. This was the case from 21 days after inoculation. Analysis of a different set of plants 33 days after inoculation found the average level of *R. collo-cygni* DNA in control plants to be almost four times that for any of the other treatment groups, between which no significant differences in DNA level were found despite the differences in green leaf area apparent by this point in the experiment. This suggests that the significantly higher *R. collo-cygni* DNA level in control leaves might not have been solely due to reduced green leaf area, and again highlights that a linear relationship between disease severity and fungal biomass in leaves cannot be assumed with this disease. It is possible that stress, for example nutrient deficiency, in the control plants influenced fungal growth, perhaps leading to increased hyphal growth or increased or earlier sporulation.

Protection of green canopy light interception against foliar diseases using fungicides is currently an integral part of management strategies for spring barley, however Bingham *et al.*, (2019) demonstrated that maintenance of green canopy for the entire duration of grain filling is not always necessary to protect against yield loss to foliar disease in sink-limited spring barley crops. Results from previous chapters indicated that the life stage of *R. collo-cygni* that is most damaging to spring barley yield is the period of foliar symptom proliferation after the switch to necrotrophic growth, during which substantial reductions in green canopy area can occur. This normally coincides with grain filling in field epidemics of RLS. As fungicide treatments for RLS are becoming more limited due to both resistance and withdrawal of effective products there could be merit in further investigation of whether prolonging green canopy area using methods such as exogenous cytokinin application for a portion of the duration of grain filling would result in reduced RLS symptom expression in the field. However, any such strategy would need to take account of overlapping functions of plant hormones and consider possible effects on factors such as remobilisation of nitrogen to the ear for grain filling.

Nitrogen remobilisation from senescing tissues contributes to grain protein content in cereals, and earlier leaf senescence and proteolysis in barley has been associated with high grain protein content (Jukanti and Fischer, 2008). Kichey *et al.* (2007) found that nitrogen remobilised from leaves accounts for 90% of total grain nitrogen content in wheat. However, Zhao *et al.* (2015) found that delayed leaf senescence in wheat associated with overexpression of a NAC transcription factor increased grain nitrogen content, which the authors ascribed to post-anthesis nitrogen assimilation rather than amino acids remobilised from vegetative tissue. Relatively low grain nitrogen is a preferred trait for malting barley.

## Chapter 5 General discussion

RLS epidemics can cause significant yield loss in barley, yet our understanding of the relative impact of different stages of the *R. collo-cygni* lifecycle is limited. This fungus can undergo a long period of asymptomatic growth in barley prior to the appearance of visible foliar disease symptoms, typically late in the growing season after flowering has occurred. It was not previously known with any certainty whether yield loss to RLS is mainly associated with reduced radiation interception after the appearance of visible disease symptoms, or whether the long asymptomatic phase contributes significantly to yield loss, for example through effects on host radiation use efficiency during plant development and establishment of grain sink capacity.

Physiological responses to infection were examined in barley seedlings inoculated with *R. collo-cygni* during asymptomatic growth and as visible foliar disease symptoms developed. Steady state photosynthesis, photosynthetic induction kinetics of dark-adapted plants, and dark respiration were assessed using chlorophyll fluorescence and infra-red gas analysis techniques.

No evidence was found to indicate an effect of *R. collo-cygni* infection on barley leaf photosynthesis prior to the appearance of visible symptoms. Furthermore, limited lesion development on otherwise green leaves was not found to impact net leaf photosynthesis. Within RLS lesions, as lesions developed and matured photosynthesis was eventually reduced to near zero, indicating cell damage or death.

Experiments were then scaled-up to field level to determine whether the results shown in inoculated seedlings in controlled environment experiments translated to mature plants in the field environment, and further experiments were undertaken to probe the relative impact on yield loss associated with RLS of the asymptomatic and symptomatic life stages of *R. collo-cygni* in

barley. Chlorophyll fluorescence analysis was used to examine photosynthesis in barley leaves during asymptomatic growth and throughout the development of visible foliar disease symptoms, and an analysis of healthy tissue light interception and comparison of predicted and observed yield loss was used to assess whether differences in post-anthesis PAR interception by healthy tissue between infected and fungicide-treated plots could account for the observed yield loss.

In agreement with the results shown in inoculated seedlings in controlled environment experiments, no evidence was found to indicate an effect of *R. collo-cygni* infection on barley leaf photosynthesis prior to the appearance of visible symptoms in the field. The results for the analysis of healthy area light interception and comparison of predicted and observed yield loss indicated that the difference in post-anthesis PAR interception by healthy tissue between fungicide-treated and the inoculated and untreated plots was sufficient to account for the observed yield losses, without needing to invoke effects of disease on RUE or remobilisation of soluble carbohydrate reserves for grain filling. This suggests that the effects of RLS on yield are largely the result of reductions in green leaf area associated with symptom development and tissue necrosis in diseased plants relative to fungicide-treated plants.

Building on these outcomes, further experiments were designed to investigate whether it was possible to reduce or delay the appearance of RLS symptoms in barley plants inoculated with *R. collo-cygni*. RLS can be associated with rapid and premature senescence (Oxley *et al.*, 2008), although some uncertainty remains around the mechanisms which link senescence and RLS symptom expression. If the onset of leaf senescence, or other factors such as changes in ROS status that can lead to senescence, are involved in triggering the *R. collo-cygni* switch to necrotrophic growth and RLS symptom development, then it could be possible to delay the appearance of symptoms using treatments that delay leaf senescence. Exogenous cytokinin application and applications of fertiliser were used to

treat barley seedlings inoculated with *R. collo-cygni*, in order to delay foliar senescence.

Cytokinin application was the most successful treatment in this regard. *R. collo-cygni* growth *in planta* and RLS symptom severity was reduced in barley seedlings displaying delayed foliar senescence. Symptom expression and fungal DNA levels were highest in plants that received neither of the senescence-delaying treatments. RLS lesions first appeared, and symptom severity differed significantly between treatments, before differences in relative chlorophyll content or % GLA became apparent, suggesting that either the fungal switch to necrotrophy may be involved in triggering senescence, or that the fungus is capable of detecting pre-senescence signals or signals associated with the onset of senescence in barley at a very early stage.

The potential implications of this research have relevance for both practitioners and researchers. The results indicate that the asymptomatic life stage of *R. collo-cygni* in barley may not negatively affect plants and is therefore not in itself an important target for RLS disease control strategies. They suggest that the necrotrophic life stage of *R. collo-cygni* is primarily responsible for yield loss to RLS, therefore the switch to necrotrophy and development of visible symptoms are the most important targets for RLS disease control strategies. As RLS symptoms typically develop on barley after flowering this suggests that earlier season sprays to limit fungal growth in plants before flowering may not play an important role in avoiding yield loss to this disease. The results also showed that whole-leaf photosynthesis was not significantly affected when mild RLS symptoms were present on barley leaves. This suggests that keeping leaves completely free of RLS symptoms is less important than minimising symptom severity. A greater focus on the integrated management principal of disease suppression, rather than prevention, may therefore be warranted when considering disease control strategies for RLS. This research focused on spring barley varieties. Although previously primarily associated with spring barley crops, incidences

of RLS in winter barley crops have increased over recent years (Havis and Brown, 2018). As both winter and spring barley crops are considered to be primarily sink-limited in the UK (Bingham *et al.*, 2007a; Kennedy *et al.*, 2017), it is likely that the conclusions of the research are also applicable to winter barley crops. However, future experiments in winter barley would be beneficial to confirm this, particularly as the effect of environmental conditions on RLS disease development is not yet fully understood. A recent report from Hoheneder *et al.*, (2021) identified some barley varieties that showed durable quantitative resistance to RLS under different field conditions over three consecutive years. Frequently, however, environment appears to have a strong effect on disease severity year-on-year or across different locations, and there are currently no commercially available barley varieties that exhibit durable resistance to RLS.

The complementary approaches of measuring photosynthesis in leaves throughout the lifecycle of *R. collo-cygni* in barley and assessing the relationship between visible symptom severity and yield loss captured a more comprehensive and robust picture of the impact of different fungal life stages on barley yield than using either method in isolation would have. This approach could potentially be usefully applied in studies of other crop-pathogen interactions. It is also an interesting point that this research, using physiological analysis techniques to assess photosynthetic activity, did not find evidence of reduced photosynthesis in asymptomatic leaves of barley infected with *R. collo-cygni*. However, down-regulation of photosynthesis-associated genes during asymptomatic infection of barley by *R. collo-cygni* has been reported in studies using comparative transcriptomic techniques (Sjokvist *et al.*, 2018). This highlights the value of conducting studies at both molecular and physiological levels to gain a broader understanding of interactions between barley and *R. collo-cygni*, and indeed between plants and pathogens more generally.

The results highlight the importance of further research to understand the mechanism of the *R. collo-cygni* lifestyle switch to necrotrophy and identify

factors that may act as triggers for this switch. If it were possible to identify and/or control such triggers this could potentially reduce the need for fungicidal control of *R. collo-cygni* in barley, or otherwise inform a more targeted approach based on understanding of risk factors for transition of the fungus from asymptomatic to symptomatic growth. The results showed that appearance of RLS symptoms was delayed, and RLS symptom severity reduced, relative to control plants in barley seedlings treated with exogenous cytokinin. Further research to understand the way in which the internal environment of the leaf is changed by cytokinin application and how this could affect the activity of *R. collo-cygni* could therefore be informative. A useful next step would be to establish whether RLS symptom expression is also reduced in mature barley plants treated with cytokinin. Thereafter, effects on yield and interaction with environment would be important factors to consider. Exposure of barley plants to abiotic stress has been linked to RLS symptom expression and increased disease severity. Genotype-environment interaction is therefore a primary consideration in studies of barley resistance to RLS, and further investigation of the relationship between abiotic stress tolerance in barley, whether genetic or provided by treatments, and RLS disease severity is warranted.

This research identified that the reduction in radiation interception due to loss of healthy, green leaf tissue during the symptomatic life stage of *R. collo-cygni* is likely to play a key role in barley yield loss to RLS. Loss of green leaf area during field epidemics of RLS occurs due to lesions and also due to wider leaf chlorosis and necrosis that typically develops on leaves alongside lesions as they proliferate. Further research to understand the role of secondary metabolites produced by *R. collo-cygni* in lesion development and/or wider leaf necrosis is needed as these could well impact the extent and/or rate of green leaf area loss to RLS. The development of *R. collo-cygni* knock-out mutants for gene clusters associated with secondary metabolite production could provide a useful tool for use in experiments to assess the impact of phytotoxins or other secondary metabolites.

In conclusion, this research suggests that should methods to stop the lifestyle switch of *R. collo-cygni* to necrotrophy or to minimise visible symptom development be identified in future, the presence of this fungus in barley crops could potentially no longer be a cause for concern, and that a mind-set of disease suppression rather than prevention may be a useful lens through which to view disease control strategy for RLS.

## References

- Baker, N. R. (2008) 'Chlorophyll fluorescence: a probe of photosynthesis in vivo.', *Annual review of plant biology*, 59, pp. 89–113. doi: 10.1146/annurev.arplant.59.032607.092759.
- Bassanezi, R. B. *et al.* (2001) 'Accounting for photosynthetic efficiency of bean leaves with rust, angular leaf spot and anthracnose to assess crop damage', *Plant Pathology*, 50(4), pp. 443–452. doi: 10.1046/j.1365-3059.2001.00584.x.
- Bastiaans, L. (1991) 'Ratio Between Virtual and Visual Lesion Size as a Measure to Describe Reduction in Leaf Photosynthesis of Rice Due to Leaf Blast', *Phytopathology*, 81(6), pp. 611–615.
- BEHR, M. *et al.* (2010) 'The Hemibiotroph *Colletotrichum graminicola* Locally Induces Photosynthetically Active Green Islands but Globally Accelerates Senescence on Aging Maize Leaves', *Molecular plant-microbe interactions*. St. Paul, MN: APS Press, 23(7), pp. 879–892. doi: 10.1094/MPMI-23-7-0879.
- Berdugo, C. A. *et al.* (2012) 'Effect of bixafen on senescence and yield formation of wheat', *Pesticide Biochemistry and Physiology*. Elsevier Inc., 104(3), pp. 171–177. doi: 10.1016/j.pestbp.2012.07.010.
- Berger, S. *et al.* (2004) 'Complex regulation of gene expression, photosynthesis and sugar levels by pathogen infection in tomato', *Physiologia Plantarum*, 122(4), pp. 419–428. doi: 10.1111/j.1399-3054.2004.00433.x.
- Biemelt, S. and Sonnewald, U. (2006) 'Plant-microbe interactions to probe regulation of plant carbon metabolism', *Journal of Plant Physiology*, 163(3), pp. 307–318. doi: 10.1016/j.jplph.2005.10.011.
- Bilgin, D. D. *et al.* (2010) 'Biotic stress globally downregulates photosynthesis

genes', *Plant, Cell and Environment*, 33(10), pp. 1597–1613. doi: 10.1111/j.1365-3040.2010.02167.x.

Bingham, I. J. *et al.* (2007a) 'Is barley yield in the UK sink limited?. I. Post-anthesis radiation interception, radiation-use efficiency and source-sink balance', *Field Crops Research*, 101(2), pp. 198–211. doi: 10.1016/j.fcr.2006.11.005.

Bingham, I. J. *et al.* (2007b) 'Is barley yield in the UK sink limited?. II. Factors affecting potential grain size', *Field Crops Research*, 101(2), pp. 212–220. doi: 10.1016/j.fcr.2006.11.004.

Bingham, I. J. *et al.* (2009) 'Crop traits and the tolerance of wheat and barley to foliar disease', *Annals of Applied Biology*, 154(2), pp. 159–173. doi: 10.1111/j.1744-7348.2008.00291.x.

Bingham, I. J. *et al.* (2019) 'In sink-limited spring barley crops, light interception by green canopy does not need protection against foliar disease for the entire duration of grain filling', *Field Crops Research*. doi: 10.1016/j.fcr.2019.04.020.

Bingham, I. J. *et al.* (2021) 'Mechanisms by which fungicides increase grain sink capacity and yield of spring barley when visible disease severity is low or absent', *Field Crops Research*. Elsevier B.V., 261(November 2020), p. 108011. doi: 10.1016/j.fcr.2020.108011.

Boote, K. *et al.* (1983) 'Coupling Pests to Crop Growth Simulators to Predict Yield Reductions.', *Phytopathology*, 73(11), pp. 1581–1587.

Von Bothmer, R. and Komatsuda, T. (2011) 'Barley Origin and Related Species', in *Barley: Production, Improvement, and Uses*, pp. 14–62. doi: 10.1002/9780470958636.ch2.

Bottalico, A. and Perrone, G. (2002) 'Toxigenic *Fusarium* species and mycotoxins associated with head blight in small-grain cereals in Europe', *European Journal of Plant Pathology*, 108(7), pp. 611–624. doi:

10.1023/A:1020635214971.

Cavara, F. (1893) 'Über einige parasitische Pilze auf dem Getreide', *Zeitschrift für Pflanzenkrankheiten*, 3, pp. 16–26.

Chanclud, E. *et al.* (2016) 'Cytokinin Production by the Rice Blast Fungus Is a Pivotal Requirement for Full Virulence', *PLoS Pathogens*, 12(2), pp. 1–25. doi: 10.1371/journal.ppat.1005457.

Chou, H. M. *et al.* (2000) 'Infection of *Arabidopsis thaliana* leaves with *Albugo candida* (white blister rust) causes a reprogramming of host metabolism.', *Molecular plant pathology*, 1(2), pp. 99–113. doi: 10.1046/j.1364-3703.2000.00013.x.

Coghlan, S. E. and Walters, D. R. (1992) 'Photosynthesis in green-islands on powdery mildew infected barley leaves', *Physiological and Molecular Plant Pathology*, 40(1), pp. 31–38. doi: 10.1016/0885-5765(92)90069-8.

Cromey, M. G. *et al.* (2004) 'Effects of the fungicides azoxystrobin and tebuconazole on *Didymella exitialis*, leaf senescence and grain yield in wheat', *Crop Protection*, 23(11), pp. 1019–1030. doi: 10.1016/j.cropro.2004.03.002.

Crous, P. *et al.* (2000) 'The genus *Mycosphaerella* and its anamorphs', *STUDIES IN MYCOLOGY. CENTRAALBUREAU SCHIMMELCULTURE, UPPSALALAAN 8, 3584 CT UTRECHT, NETHERLANDS*, (45), pp. 107–121.

Crous, P. W. *et al.* (2009) 'Unravelling *Mycosphaerella*: do you believe in genera?', *Persoonia. RIJKSHERBARIUM, PO BOX 9514, 2300 RA LEIDEN, NETHERLANDS*, 23, pp. 99–118. doi: 10.3767/003158509X479487.

Crous, P. W., Kang, J.-C. and Braun, U. (2001) *A Phylogenetic Redefinition of Anamorph Genera in Mycosphaerella Based on ITS rDNA Sequence and Morphology*, *Mycologia*.

Daub, M. E. and Ehrenshaft, M. (2000) 'THE PHOTOACTIVATED

CERCOSPORA TOXIN CERCOSPORIN : Contributions to Plant Disease and Fundamental Biology', *Annual review of phytopathology*, 38, pp. 461–490.

Denmig, B. and Bjorkman, O. (1987) 'Comparison of the effect of excessive light on chlorophyll fluorescence (77 K) and photon yield of O<sub>2</sub> evolution in leaves of higher plants', *Planta*, 171(2), pp. 171–184.

Dinkins, R. D. *et al.* (2017) 'Transcriptome response of *Lolium arundinaceum* to its fungal endophyte *Epichloë coenophiala*', *New Phytologist*, 213(1), pp. 324–337. doi: 10.1111/nph.14103.

Distelfeld, A., Avni, R. and Fischer, A. M. (2014) 'Senescence, nutrient remobilization, and yield in wheat and barley.', *Journal of experimental botany*, 65(14), pp. 3783–3798. doi: 10.1093/jxb/ert477.

Divon, H. H. and Fluhr, R. (2007) 'Nutrition acquisition strategies during fungal infection of plants', *FEMS Microbiology Letters*, 266(1), pp. 65–74. doi: 10.1111/j.1574-6968.2006.00504.x.

Dussart, F. *et al.* (2018) 'Genome-based discovery of polyketide-derived secondary metabolism pathways in the barley pathogen *Ramularia collo-cygni*', *Molecular Plant Microbe Interactions*, p. doi:10.1094/MPMI-12-17-0299-R. doi: 10.1094/MPMI-12-17-0299-R.

Dussart, F., Hoebe, P. N. and Spoel, S. H. (2018) 'Determining the role of the phytotoxic secondary metabolite rubellin D in the pathology of *Ramularia collo-cygni*, the fungus responsible for *Ramularia* leaf spot disease of barley', in *Proceedings Crop Production in Northern Britain*, pp. 97–102.

Ehness, R. *et al.* (1997) 'Glucose and stress independently regulate source and sink metabolism and defense mechanisms via signal transduction pathways involving protein phosphorylation', *Plant Cell*, 9(10), pp. 1825–1841. doi: 10.1105/tpc.9.10.1825.

FAOSTAT (2020) *Food and Agricultural Organization of the United Nations*.

Available at: <http://faostat3.fao.org/home/E> (Accessed: 30 August 2020).

Formayer, H., Huss, H. and Kromp-Kolb, H. (2004) 'Influence of Climatic Factors on the Formation of Symptoms of *Ramularia collo-cygni*', in Yahyaoui, A. et al. (eds) *Proceedings of the Second International Workshop on Barley Leaf Blights. Aleppo, Syria.*, pp. 329–330.

Fotopoulos, V. et al. (2003) 'The Monosaccharide Transporter Gene, AtSTP4, and the Cell-Wall Invertase, at $\beta$ fruct1, Are Induced in Arabidopsis during Infection with the Fungal Biotroph *Erysiphe cichoracearum*', 132(2), pp. 821–829. doi: 10.1104/pp.103.021428.ferred.

Fountaine, J. M. and Fraaije, B. A. (2009) 'Development of Qol resistant alleles in populations of *Ramularia collo-cygni*', in *Proceedings of the second European Ramularia Workshop, Edinburgh, United Kingdom*, pp. 123–126.

Frei, P. et al. (2007) 'Direct-PCR detection and epidemiology of *Ramularia collo-cygni* associated with barley necrotic leaf spots', *Journal of Phytopathology*, 155(5), pp. 281–288. doi: 10.1111/j.1439-0434.2007.01228.x.

Frei, P. and Gindro, K. (2015) 'Ramularia collo-cygni - un nouveau champignon pathogene de l'orge', *Recherche Agronomique Suisse*, 6, pp. 210–217.

Gan, S. and Amasino, R. M. (1996) 'Cytokinins in plant senescence: from spray and pray to clone and play', *BioEssays*, 18(7), pp. 557–565.

Gaunt, R. E. (1995) 'The relationship between plant disease severity and yield.', *Annual review of phytopathology*, 33, pp. 119–144. doi: 10.1146/annurev.py.33.090195.001003.

Granum, E. et al. (2015) 'Metabolic responses of avocado plants to stress induced by *Rosellinia necatrix* analysed by fluorescence and thermal imaging', *European Journal of Plant Pathology*, 142(3), pp. 625–632. doi: 10.1007/s10658-015-0640-9.

- Großkinsky, D. K. *et al.* (2011) 'Cytokinins mediate resistance against *Pseudomonas syringae* in tobacco through increased antimicrobial phytoalexin synthesis independent of salicylic acid signaling', *Plant Physiology*, 157(2), pp. 815–830. doi: 10.1104/pp.111.182931.
- Grossmann, K., Kwiatkowski, J. and Caspar, Gü. (1999) 'Regulation of phytohormone levels, leaf senescence and transpiration by the strobilurin kresoxim-methyl in wheat (*Triticum aestivum*)', *Journal of Plant Physiology*, 154(5–6), pp. 805–808. doi: 10.1016/S0176-1617(99)80262-4.
- Grossmann, K. and Retzlaff, G. (1997) 'Bioregulatory effects of the fungicidal strobilurin kresoxim-methyl in wheat (*Triticum aestivum*)', *Pesticide Science*, 50(1), pp. 11–20. doi: 10.1002/(SICI)1096-9063(199705)50:1<11::AID-PS556>3.0.CO;2-8.
- Habeshaw, D. (1984) *Effects of pathogens on photosynthesis. In Plant diseases: infection, damage and loss*. Edited by R. K. S. Wood and G. J. Jellis. Oxford: Blackwell Scientific Publications.
- Häffner, E., Konietzki, S. and Diederichsen, E. (2015) *Keeping Control: The Role of Senescence and Development in Plant Pathogenesis and Defense, Plants*. doi: 10.3390/plants4030449.
- Hahn, M. *et al.* (1997) 'A putative amino acid transporter is specifically expressed in haustoria of the rust fungus *Uromyces fabae*', *Molecular Plant-Microbe Interactions*, 10(4), pp. 438–445. doi: 10.1094/MPMI.1997.10.4.438.
- Haverkort, A. J. and Bicamumpaka, M. (1986) 'Correlation between intercepted radiation and yield of potato crops infested by *Phytophthora infestans* in central Africa', *Netherlands Journal of Plant Pathology*, 92(5), pp. 239–247. doi: 10.1007/BF01977690.
- Havis, N. and Brown, J. (2018) 'AHDB Ramularia leaf spot in barley factsheet'.
- Havis, N. D. *et al.* (2006) 'Rapid nested PCR-based detection of *Ramularia*

*collo-cygni* direct from barley', *FEMS Microbiology Letters*, 256(2), pp. 217–223. doi: 10.1111/j.1574-6968.2006.00121.x.

Havis, N. D. *et al.* (2015) 'Ramularia collo-cygni - an emerging pathogen of barley crops', *Phytopathology*, 105(7), pp. 895–904. doi: 10.1094/PHYTO-11-14-0337-FI.

Havis, N. D., Nyman, M. and Oxley, S. J. P. (2014) 'Evidence for seed transmission and symptomless growth of *Ramularia collo-cygni* in barley (*Hordeum vulgare*)', *Plant Pathology*, 63(4), pp. 929–936. doi: 10.1111/ppa.12162.

Havis, N., Evans, N. and Hughes, G. (2018) *Development of UK wide risk forecast for Ramularia leaf spot in barley. AHDB Report PR600.*

Hecker, K. D. *et al.* (1998) 'Barley  $\beta$ -glucan is effective as a hypocholesterolaemic ingredient in foods', *Journal of the Science of Food and Agriculture*, 77(2), pp. 179–183. doi: 10.1002/(sici)1097-0010(199806)77:2<179::aid-jsfa23>3.0.co;2-0.

Heiser, I. *et al.* (2004) 'Fatty acid peroxidation by rubellin B, C and D, phytotoxins produced by *Ramularia collo-cygni* (Sutton et Waller)', *Physiological and Molecular Plant Pathology*, 64(3), pp. 135–143. doi: 10.1016/j.pmpp.2004.08.002.

Heiser, I., Sachs, E. and Liebermann, B. (2003) 'Photodynamic oxygen activation by rubellin D, a phytotoxin produced by *Ramularia collo-cygni* (Sutton et Waller)', *Physiological and Molecular Plant Pathology*, 62(1), pp. 29–36. doi: 10.1016/S0885-5765(03)00007-9.

Heisterüber, D., Schulte, P. and Moerschbacher, B. . (1994) 'Soluble carbohydrates and invertase activity in stem rust-infected, resistant and susceptible near-isogenic wheat leaves', *Physiological and molecular plant pathology*. London: Elsevier India Pvt Ltd, 45(2), pp. 111–123. doi: 10.1016/S0885-5765(05)80070-0.

Hideg, É., Kós, P. B. and Schreiber, U. (2008) 'Imaging of NPQ and ROS formation in tobacco leaves: Heat inactivation of the water-water cycle prevents down-regulation of PSII', *Plant and Cell Physiology*, 49(12), pp. 1879–1886. doi: 10.1093/pcp/pcn170.

Hjortshøj, R. L. *et al.* (2012) 'High levels of genetic and genotypic diversity in field populations of the barley pathogen *Ramularia collo-cygni*', *European Journal of Plant Pathology*, 136(1), pp. 51–60. doi: 10.1007/s10658-012-0137-8.

Hofer, K. *et al.* (2014) '*MILDEW LOCUS O* mutation does not affect resistance to grain infections with *Fusarium* spp. and *Ramularia collo-cygni*', *Igarss 2014*, (1), pp. 1–5. doi: 10.1007/s13398-014-0173-7.2.

Hoheneder, F. *et al.* (2021) 'Ramularia leaf spot disease of barley is highly host genotype-dependent and suppressed by continuous drought stress in the field', *Journal of Plant Diseases and Protection*. Springer Berlin Heidelberg, (0123456789). doi: 10.1007/s41348-020-00420-z.

Huss, H. (2004) 'The biology of *Ramularia collo-cygni*. Meeting the challenges of barley blights', in Yahyaoui, A. *et al.* (eds) *Proceedings of the second international workshop on barley leaf blights. Aleppo, Syria.*, pp. 321–328.

Jameson, P. (2016) 'Cytokinins', *Encyclopedia of Applied Plant Sciences*, 1, pp. 391–402. doi: 10.1016/B978-0-12-394807-6.00102-7.

Jebbouj, R. and El Yousfi, B. (2009) 'Barley yield losses due to defoliation of upper three leaves either healthy or infected at boot stage by *Pyrenophora teres* f. *teres*', *European Journal of Plant Pathology*, 125(2), pp. 303–315. doi: 10.1007/s10658-009-9483-6.

Johnson, K. (1987) 'Defoliation, Disease, and Growth: A Reply', *Phytopathology*, 77(11), pp. 7–9.

Jordan, V. W. L., Best, G. R. and Allen, E. C. (1985) 'Effects of *Pyrenophora*

teres on dry matter production and yield components of winter barley', *Plant Pathology*, 34(2), pp. 200–206. doi: <https://doi.org/10.1111/j.1365-3059.1985.tb01350.x>.

Jukanti, A. K. and Fischer, A. M. (2008) 'A high-grain protein content locus on barley (*Hordeum vulgare*) chromosome 6 is associated with increased flag leaf proteolysis and nitrogen remobilization', *Physiologia Plantarum*, 132(4), pp. 426–439.

Kaczmarek, M. *et al.* (2017) 'Infection strategy of *Ramularia collo-cygni* and development of ramularia leaf spot on barley and alternative graminaceous hosts', *Plant Pathology*, 66(1), pp. 45–55. doi: [10.1111/ppa.12552](https://doi.org/10.1111/ppa.12552).

Kennedy, S. P. *et al.* (2018) 'Grain number and grain filling of two-row malting barley in response to variation in post-anthesis radiation: Analysis by grain position on the ear and its implications for yield improvement and quality', *Field Crops Research*. Elsevier, 225(June), pp. 74–82. doi: [10.1016/j.fcr.2018.06.004](https://doi.org/10.1016/j.fcr.2018.06.004).

Kennedy, S. P., Bingham, I. J. and Spink, J. H. (2017) 'Determinants of spring barley yield in a high-yield potential environment', *Journal of Agricultural Science*, 155(1), pp. 60–80. doi: [10.1017/S0021859616000289](https://doi.org/10.1017/S0021859616000289).

Kichey, T. *et al.* (2007) 'In winter wheat (*Triticum aestivum* L.), post-anthesis nitrogen uptake and remobilisation to the grain correlates with agronomic traits and nitrogen physiological markers', *Field Crops Research*, 102(1), pp. 22–32. doi: [10.1016/j.fcr.2007.01.002](https://doi.org/10.1016/j.fcr.2007.01.002).

Koch, K. E. (1996) 'Carbohydrate-modulated gene expression in plants', *Annual Review of Plant Physiology and Plant Molecular Biology*, 47(1), pp. 509–540. doi: [10.1146/annurev.arplant.47.1.509](https://doi.org/10.1146/annurev.arplant.47.1.509).

Last, F. T. (1963) 'Metabolism of barley leaves inoculated with *Erysiphe graminis mérat*', *Annals of Botany*, 27(4), pp. 685–690. doi: [10.1093/oxfordjournals.aob.a083880](https://doi.org/10.1093/oxfordjournals.aob.a083880).

- Livne, A. and Daly, J. (1966) 'Translocation in healthy and rust-affected beans', *Phytopathology*, 56, pp. 170–175.
- Ma, X. *et al.* (2018) 'Comparative transcriptomics reveals how wheat responds to infection by *Zymoseptoria tritici*', *Molecular Plant-Microbe Interactions*, 31(4), pp. 420–431. doi: 10.1094/MPMI-10-17-0245-R.
- Mäe, A., Põllumaa, L. and Sooväli, P. (2018) 'Ramularia collo-cygni: A new pathogen spreading in barley fields in Estonia', *Agricultural and Food Science*, 27(2), pp. 138–145. doi: 10.23986/afsci.69116.
- Makepeace, J. C. (2006) *The effect of the mlo mildew resistance gene on spotting diseases of barley*.
- Makepeace, J. C. *et al.* (2008) 'A method of inoculating barley seedlings with *Ramularia collo-cygni*', *Plant Pathology*, 57(6), pp. 991–999. doi: 10.1111/j.1365-3059.2008.01892.x.
- Mařík, P., Šnejdar, Z. and Matušinsky, P. (2011) 'Expression of Resistance to Ramularia Leaf Spot in Winter Barley Cultivars Grown in Conditions of the Czech Republic', *Czech Journal of Genetics and Plant Breeding*, 47(1), pp. 37–40.
- Martin, P. J. (1986) 'Gaseous exchange studies of barley leaves infected with *Rhynchosporium secalis* (Oudem) J. J. Davis', *Physiological and Molecular Plant Pathology*. Academic Press Inc. (London) Limited, 28(1), pp. 3–14. doi: 10.1016/S0048-4059(86)80003-0.
- McGrann, G. *et al.* (2015) 'Contribution of the drought tolerance-related *Stress-responsive NAC 1* transcription factor to resistance of barley to Ramularia leaf spot.', *Molecular plant pathology*, 16(201–209). doi: 10.1111/mpp.12173.
- McGrann, G. R. D. *et al.* (2014) 'A trade off between *mlo* resistance to powdery mildew and increased susceptibility of barley to a newly important disease, Ramularia leaf spot.', *Journal of experimental botany*, 65(4), pp.

1025–37. doi: 10.1093/jxb/ert452.

McGrann, G. R. D. *et al.* (2016) 'The genome of the emerging barley pathogen *Ramularia collo-cygni*', *BMC Genomics*. BMC Genomics, 17(1), p. 584. doi: 10.1186/s12864-016-2928-3.

McGrann, G. R. D. and Brown, J. K. M. (2017) 'The role of reactive oxygen in the development of *Ramularia* leaf spot disease in barley seedlings', *Annals of Botany*, pp. 415–430. doi: 10.1093/aob/mcx170.

McGrann, G. R. D. and Brown, J. K. M. (2018) 'The role of reactive oxygen in the development of *Ramularia* leaf spot disease in barley seedlings', *Annals of Botany*, 121, pp. 415–430. doi: 10.1093/aob/mcx170.

McGrann, G. R. D. and Havis, N. D. (2017) 'Ramularia Leaf Spot: A Newly Important Threat to Barley Production', *Outlooks on Pest Management*. doi: 10.1564/v28\_apr\_05.

McGrann, G. R. D., Miller, S. and Havis, N. D. (2020) 'The ENHANCED MAGNAPORTHE RESISTANCE 1 locus affects *Ramularia* leaf spot development in barley', *European Journal of Plant Pathology*. European Journal of Plant Pathology, 156(1), pp. 123–132. doi: 10.1007/s10658-019-01869-x.

Meyer, S. *et al.* (2001) 'Inhibition of photosynthesis by *Colletotrichum lindemuthianum* in bean leaves determined by chlorophyll fluorescence imaging', *Plant, Cell and Environment*, 24(9), pp. 947–955. doi: 10.1046/j.0016-8025.2001.00737.x.

Miethbauer, S. *et al.* (2006) 'Biosynthesis of photodynamically active rubellins and structure elucidation of new anthraquinone derivatives produced by *Ramularia collo-cygni*', *Phytochemistry*, 67(12), pp. 1206–1213. doi: 10.1016/j.phytochem.2006.05.003.

Miethbauer, S., Heiser, I. and Liebermann, B. (2003) 'The phytopathogenic fungus *Ramularia collo-cygni* produces biologically active rubellins on

infected barley leaves', *Journal of Phytopathology*, 151, pp. 665–668. doi: 10.1046/j.1439-0434.2003.00783.x.

Morrison, E. N., Emery, R. J. N. and Saville, B. J. (2017) 'Fungal derived cytokinins are necessary for normal *Ustilago maydis* infection of maize', *Plant Pathology*, 66(5), pp. 726–742. doi: 10.1111/ppa.12629.

Murchie, E. H. and Lawson, T. (2013) 'Chlorophyll fluorescence analysis: A guide to good practice and understanding some new applications', *Journal of Experimental Botany*, 64(13), pp. 3983–3998. doi: 10.1093/jxb/ert208.

Murphy, A. M. *et al.* (1997) 'Comparison of cytokinin production in vitro by *Pyrenopeziza brassicae* with other plant pathogens', *Physiological and Molecular Plant Pathology*, 50(1), pp. 53–65. doi: 10.1006/pmpp.1996.0070.

Murray, D. C. and Walters, D. R. (1992) 'Increased photosynthesis and resistance to rust infection in upper, uninfected leaves of rusted broad bean (*Vicia faba* L.)', *New Phytologist*, 120(2), pp. 235–242. doi: 10.1111/j.1469-8137.1992.tb05659.x.

Newton, A. C. *et al.* (2011) 'Crops that feed the world 4. Barley: a resilient crop? Strengths and weaknesses in the context of food security', *Food Security*, 3(2), pp. 141–178. doi: 10.1007/s12571-011-0126-3.

van Oijen, M. (1990) 'Photosynthesis is not impaired in healthy tissue of blighted potato plants', *Netherlands Journal of Plant Pathology*, 96(2), pp. 55–63. doi: 10.1007/BF02005129.

Owera, S., Farrar, J. and Whitbred, R. (1983) 'Translocation from Leaves of Barley Infected with Brown Rust', *New Phytologist*, 94(1), pp. 111–123.

Oxley, S. *et al.* (2008) *Impact and interactions of Ramularia collo-cygni and oxidative stress in barley. HGCA Project Report No. 431.*

Palma-Guerrero, J. *et al.* (2016) 'Comparative transcriptomic analyses of *Zymoseptoria tritici* strains show complex lifestyle transitions and intraspecific

variability in transcription profiles', *Molecular plant pathology*, 17(6), pp. 845–859. doi: 10.1111/mpp.12333.

Peraldi, a. *et al.* (2014) 'Brachypodium distachyon exhibits compatible interactions with Oculimacula spp. and Ramularia collo-cygni, providing the first pathosystem model to study eyespot and ramularia leaf spot diseases', *Plant Pathology*, 63(3), pp. 554–562. doi: 10.1111/ppa.12114.

Pérez-Bueno, M. L. *et al.* (2006) 'Imaging viral infection: Studies on Nicotiana benthamiana plants infected with the pepper mild mottle tobamovirus', *Photosynthesis Research*, 90(2), pp. 111–123. doi: 10.1007/s11120-006-9098-0.

Piffanelli, P. *et al.* (2002) 'The barley MLO modulator of defense and cell death is responsive to biotic and abiotic stress stimuli', *Plant Physiology*, 129(3), pp. 1076–1085. doi: 10.1104/pp.010954.

Pineda, M. *et al.* (2008) 'Conventional and combinatorial chlorophyll fluorescence imaging of tobamovirus-infected plants', *Photosynthetica*, 46(3), pp. 441–451. doi: 10.1007/s11099-008-0076-y.

Pinnschmidt, H. O., Sindberg, S. A. and Willas, J. (2006) 'Resistant barley varieties may facilitate control of Ramularia leaf spot', *Danish Research Centre for Organic Farming*, (November 2006), pp. 2006–2008.

Pinnschmidt, H. and Sindberg, S. A. (2009) 'Assessing Ramularia leaf spot resistance of spring barley cultivars in the presence of other diseases', *Aspects of Applied Biology*, 92, pp. 71–80.

Piotrowska, M. J. *et al.* (2016) 'Development and use of microsatellite markers to study diversity, reproduction and population genetic structure of the cereal pathogen Ramularia collo-cygni.', *Fungal genetics and biology : FG & B*. doi: 10.1016/j.fgb.2016.01.007.

Piotrowska, M. J. *et al.* (2017) 'Characterisation of Ramularia collo-cygni laboratory mutants resistant to succinate dehydrogenase inhibitors', *Pest*

*Management Science*, 73(6), pp. 1187–1196. doi: 10.1002/ps.4442.

Reynolds, M. P., Pellegrineschi, A. and Skovmand, B. (2005) 'Sink-limitation to yield and biomass: A summary of some investigations in spring wheat', *Annals of Applied Biology*, 146(1), pp. 39–49. doi: 10.1111/j.1744-7348.2005.03100.x.

Richmond, A. E. and Lang, A. (1957) 'Effect of kinetin on protein content and survival of detached Xanthium leaves', *Science*, 125, pp. 650–651.

Robert, C. *et al.* (2004) 'Analysis and modelling of effects of leaf rust and Septoria tritici blotch on wheat growth.', *Journal of experimental botany*, 55(399), pp. 1079–1094. doi: 10.1093/jxb/erh108.

Robert, C. *et al.* (2005) 'Wheat leaf photosynthesis loss due to leaf rust, with respect to lesion development and leaf nitrogen status', *New Phytologist*, 165(1), pp. 227–241. doi: 10.1111/j.1469-8137.2004.01237.x.

Robert, C. *et al.* (2006) 'Quantification of the effects of Septoria tritici blotch on wheat leaf gas exchange with respect to lesion age, leaf number, and leaf nitrogen status', *Journal of Experimental Botany*, 57(1), pp. 225–234. doi: 10.1093/jxb/eri153.

Roitsch, T. *et al.* (2003) 'Extracellular invertase: Key metabolic enzyme and PR protein', *Journal of Experimental Botany*, 54(382), pp. 513–524. doi: 10.1093/jxb/erg050.

Rooney, J. M. and Hoad, G. V. (1989) 'Compensation in growth and photosynthesis of wheat (*Triticum aestivum* L.) following early inoculations with *Septoria nodorum* (Berk.) Berk.', *New Phytologist*, 113(4), pp. 513–521. doi: 10.1111/j.1469-8137.1989.tb00363.x.

Rotem, J., Bashi, E. and Kranz, J. (1983) 'Studies of crop loss in potato blight caused by *Phytophthora infestans*', *Plant Pathology*, 32, pp. 117–122.

Salamati, S. and Reitan, L. (2006) *Ramularia collo-cygni* on spring barley, an

overview of its biology and epidemiology, *Ramularia collo-cygni*: a new disease and challenge in Barley production; Proceedings of the First European Ramularia Workshop, Georg-August University, Göttingen, Germany. Edited by A. von Tiedemann, A. Schützendübel, and B. Koopman.

Scholes, J. D. *et al.* (1994) 'Invertase: understanding changes in the photosynthetic and carbohydrate metabolism of barley leaves infected with powdery mildew', *New Phytologist*, 126(2), pp. 213–222. doi: 10.1111/j.1469-8137.1994.tb03939.x.

Scholes, J. D. and Farrar, J. F. (1986) 'Increased Rates of Photosynthesis in Localized Regions of a Barley Leaf Infected With Brown Rust', *New Phytologist*, 104, pp. 601–612.

Scholes, J. D. and Rolfe, S. A. (1996) 'Photosynthesis in localised regions of oat leaves infected with crown rust (*Puccinia coronata*): quantitative imaging of chlorophyll fluorescence', *Planta*, 199(4), pp. 573–582. doi: 10.1007/BF00195189.

Scholes, J. D. and Rolfe, S. A. (2009) 'Chlorophyll fluorescence imaging as tool for understanding the impact of fungal diseases on plant performance: A phenomics perspective', *Functional Plant Biology*, 36(11), pp. 880–892. doi: 10.1071/FP09145.

Schützendübel, a. *et al.* (2008) 'A hypothesis on physiological alterations during plant ontogenesis governing susceptibility of winter barley to ramularia leaf spot', *Plant Pathology*, 57(3), pp. 518–526. doi: 10.1111/j.1365-3059.2007.01820.x.

Scott, S. W. and Griffiths, E. (1980) 'Effects of controlled epidemics of powdery mildew on grain yield of spring barley', *Annals of Applied Biology*, 94(1), pp. 19–31. doi: 10.1111/j.1744-7348.1980.tb03892.x.

Sjokvist, E. *et al.* (2018) 'Dissection of Ramularia Leaf Spot Disease by Integrated Analysis of Barley and Ramularia collo-cygni Transcriptome

Responses ', *Molecular Plant-Microbe Interactions*, 32(2), pp. 176–193. doi: 10.1094/mpmi-05-18-0113-r.

Slafer, G. A., Savin, R. and Sadras, V. O. (2014) 'Coarse and fine regulation of wheat yield components in response to genotype and environment', *Field Crops Research*. Elsevier B.V., 157, pp. 71–83. doi: 10.1016/j.fcr.2013.12.004.

Smedegaard-Petersen, V. and Stolen, O. (1981) 'Effect of Energy-Requiring Defense Reactions on Yield and Grain Quality in a Powdery Mildew-Resistant Barley Cultivar', *Phytopathology*, 71(4), pp. 396–399. doi: 10.1094/phyto-71-396.

Stabentheiner, E., Minihofer, T. and Huss, H. (2009) 'Infection of barley by *Ramularia collo-cygni*: scanning electron microscopic investigations.', *Mycopathologia*, 168(3), pp. 135–43. doi: 10.1007/s11046-009-9206-8.

Stam, R. *et al.* (2019) 'The Current Epidemic of the Barley Pathogen *Ramularia collo-cygni* Derives from a Population Expansion and Shows Global Admixture', *Phytopathology*. American Phytopathological Society, 109(12), pp. 2161–2168. doi: 10.1094/PHYTO-04-19-0117-R.

Struck, C., Ernst, M. and Hahn, M. (2002) 'Characterization of a developmentally regulated amino acid transporter (AAT1p) of the rust fungus *Uromyces fabae*', *Molecular Plant Pathology*, 3(1), pp. 23–30. doi: 10.1046/j.1464-6722.2001.00091.x.

Sutton, B. C. and Waller, J. M. (1988) 'Taxonomy of *Ophiocladium hordei*, causing lead lesion on triticale and other Gramineae', *Transactions of the British Mycological Society*, pp. 55–61. doi: 10.1016/S0007-1536(88)80180-3.

Taylor, J. M. G., Paterson, L. J. and Havis, N. D. (2010) 'A quantitative real-time PCR assay for the detection of *Ramularia collo-cygni* from barley (*Hordeum vulgare*).', *Letters in applied microbiology*, 50(5), pp. 493–9. doi:

10.1111/j.1472-765X.2010.02826.x.

The Scottish Government (2020) 'Cereal and Oilseed Rape Harvest 2020'.

Thirugnanasambandam, a. *et al.* (2011) 'Agrobacterium-mediated transformation of the barley pathogen *Ramularia collo-cygni* with fluorescent marker tags and live tissue imaging of infection development', *Plant Pathology*, 60(5), pp. 929–937. doi: 10.1111/j.1365-3059.2011.02440.x.

Tottman, D. R., Makepeace, R. J. and Broad, H. (1979) 'An explanation of the decimal code for the growth stages of cereals, with illustrations', *Annals of Applied Biology*, 93(2), pp. 221–234. doi: 10.1111/j.1744-7348.1979.tb06534.x.

Trdá, L. *et al.* (2017) 'Cytokinin metabolism of pathogenic fungus *Leptosphaeria maculans* involves isopentenyltransferase, adenosine kinase and cytokinin oxidase/dehydrogenase', *Frontiers in Microbiology*, 8(JUL), pp. 1–20. doi: 10.3389/fmicb.2017.01374.

Voegelé, R. T. *et al.* (2001) 'The role of haustoria in sugar supply during infection of broad bean by the rust fungus *Uromyces fabae*', *Proceedings of the National Academy of Sciences of the United States of America*, 98(14), pp. 8133–8138. doi: 10.1073/pnas.131186798.

Waggoner, P. E. and Berger, R. D. (1987) 'Defoliation, disease, and growth', *Phytopathology*. St. Paul, MN: American Phytopathological Society, 77(3), pp. 393–398.

Walters, D. R. and Ayres, P. G. (1981) 'Growth and Branching Pattern of Roots of Barley Infected with Powdery Mildew', 47(1), pp. 159–162.

Walters, D. R., Havis, N. D. and Oxley, S. J. P. (2008) '*Ramularia collo-cygni*: The biology of an emerging pathogen of barley', *FEMS Microbiology Letters*, 279(1), pp. 1–7. doi: 10.1111/j.1574-6968.2007.00986.x.

Walters, D. R. and McRoberts, N. (2006) 'Plants and biotrophs: a pivotal role

for cytokinins?', *Trends in Plant Science*, 11(12), pp. 581–586. doi: 10.1016/j.tplants.2006.10.003.

Wu, Y. X. and Von Tiedemann, A. (2001) 'Physiological effects of azoxystrobin and epoxiconazole on senescence and the oxidative status of wheat', *Pesticide Biochemistry and Physiology*, 71(1), pp. 1–10. doi: 10.1006/pest.2001.2561.

Wu, Y. X. and Von Tiedemann, A. (2002) 'Evidence for oxidative stress involved in physiological leaf spot formation in winter and spring barley', *Phytopathology*, 92(2), pp. 145–155. doi: 10.1094/PHYTO.2002.92.2.145.

Zhao, D. *et al.* (2015) 'Overexpression of a NAC transcription factor delays leaf senescence and increases grain nitrogen concentration in wheat', *Plant Biology*, 17(4), pp. 904–913. doi: 10.1111/plb.12296.

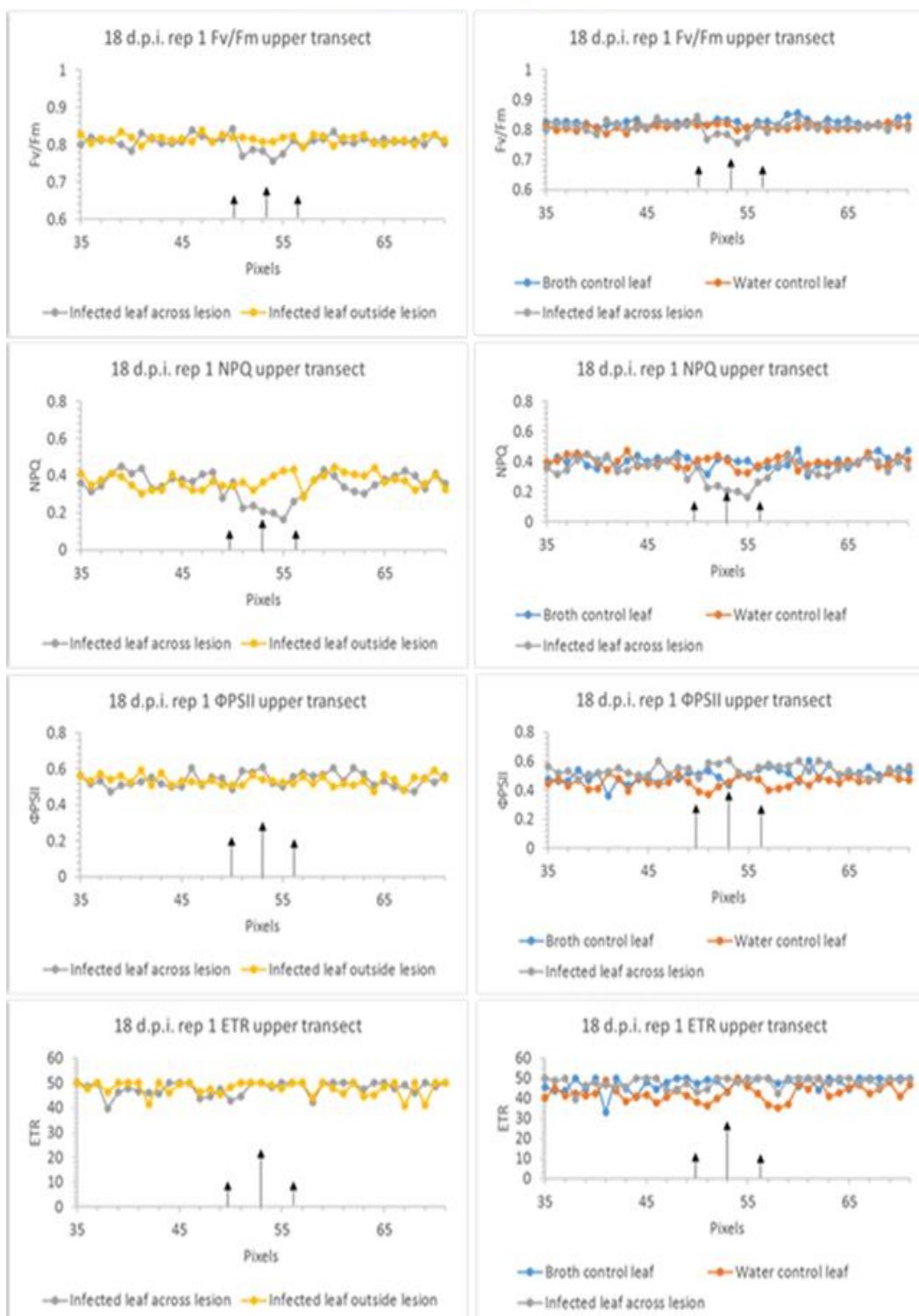
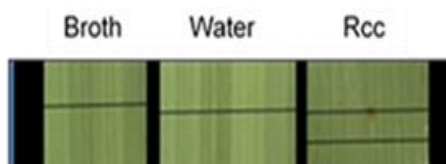
Zubo, Y. O. *et al.* (2008) 'Cytokinin Stimulates Chloroplast Transcription in Detached Barley Leaves', *Plant Physiology*, 148(2), pp. 1082–1093. doi: 10.1104/pp.108.122275.

Zwack, P. J. and Rashotte, A. M. (2013) 'Cytokinin inhibition of leaf senescence', *Plant Signalling and Behaviour*, 8(7). doi: 10.4161/psb.24737.

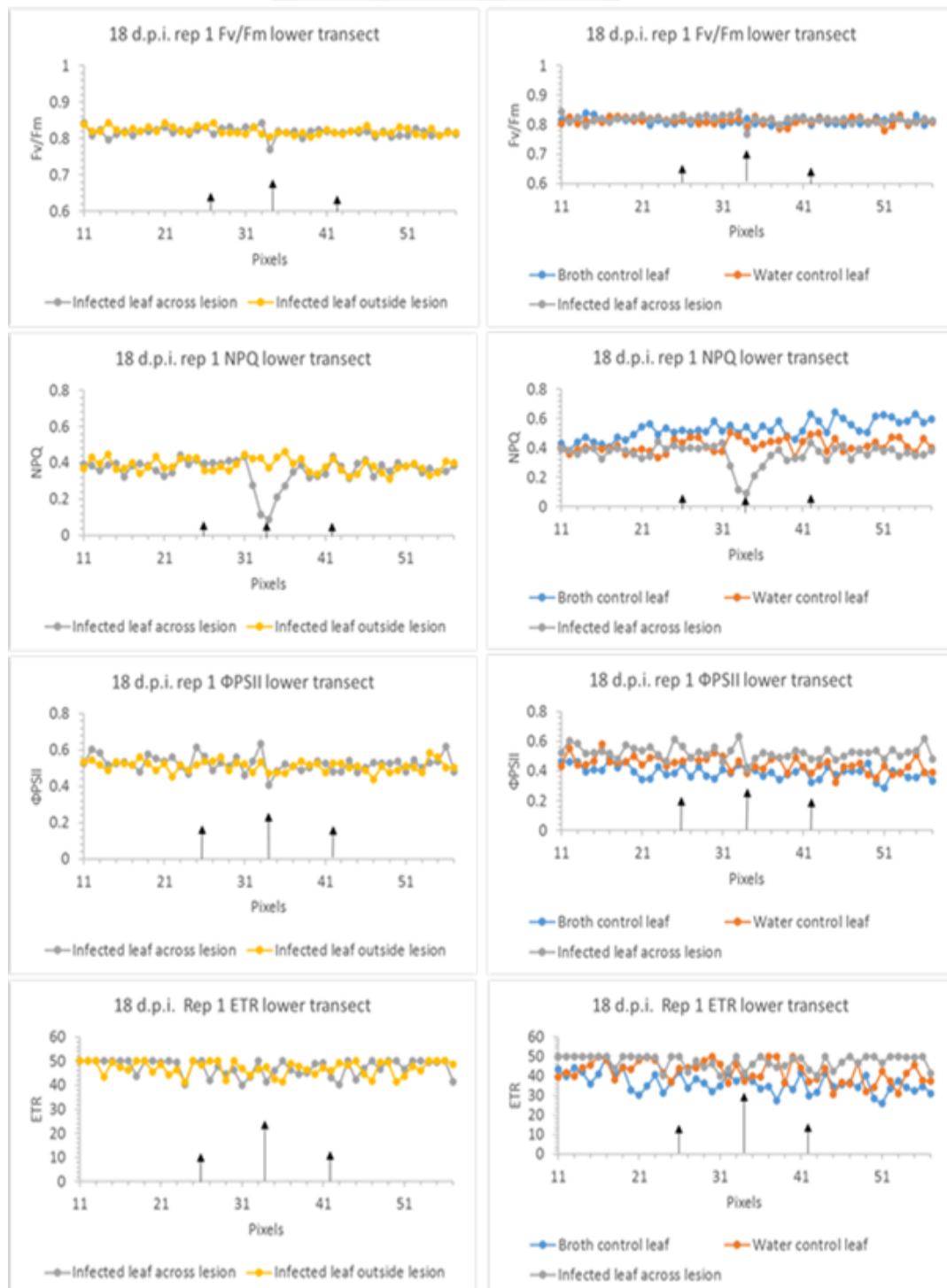
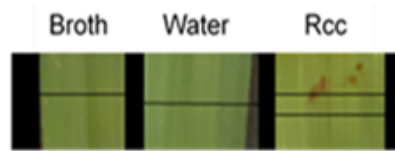
## Appendix 1

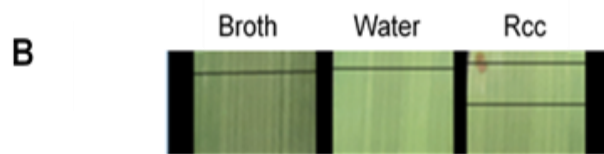
The images and graphs in Appendix 1 expand on the information shown in exemplary Figure 25 in Chapter 2, depicting chlorophyll fluorescence measured across leaf transects. The photographs show the location of upper and lower leaf transects. The graphs show chlorophyll fluorescence parameter values along the transects. The left-hand panels show parameters for transects across lesions and across nearby non-symptomatic areas of infected leaves. The right-hand panels show parameters for transects across lesions and across equivalent areas of control leaves. Measurements were taken at 18 and 26 days after inoculation. Replicates categorised as group A = small, developing lesion. Replicates categorised as Group B = lesion at more advanced stage of development.

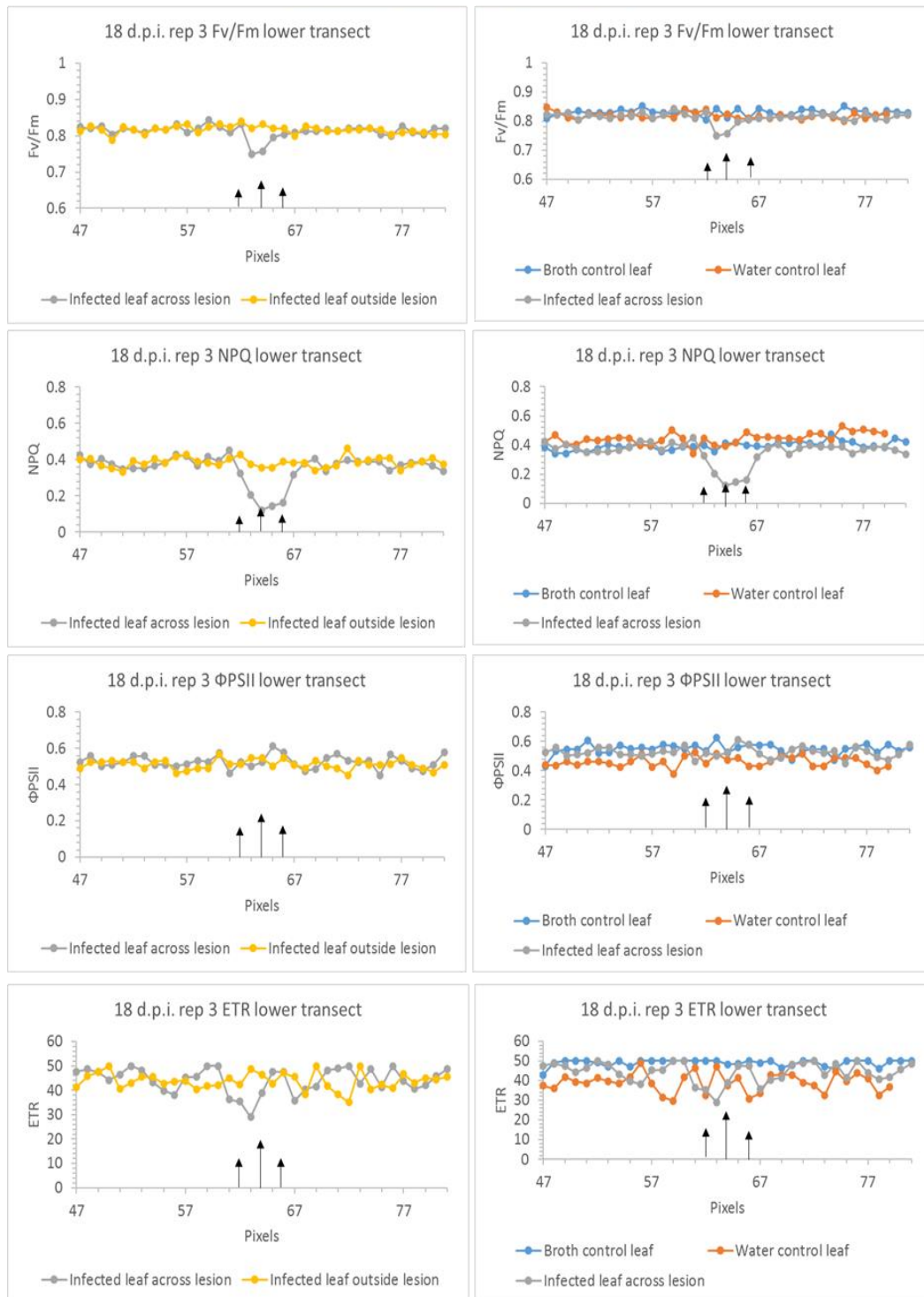
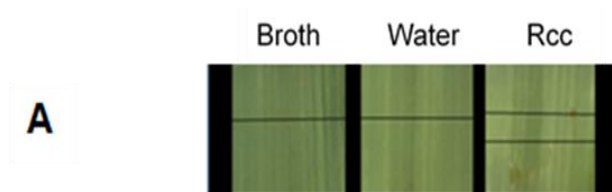
A

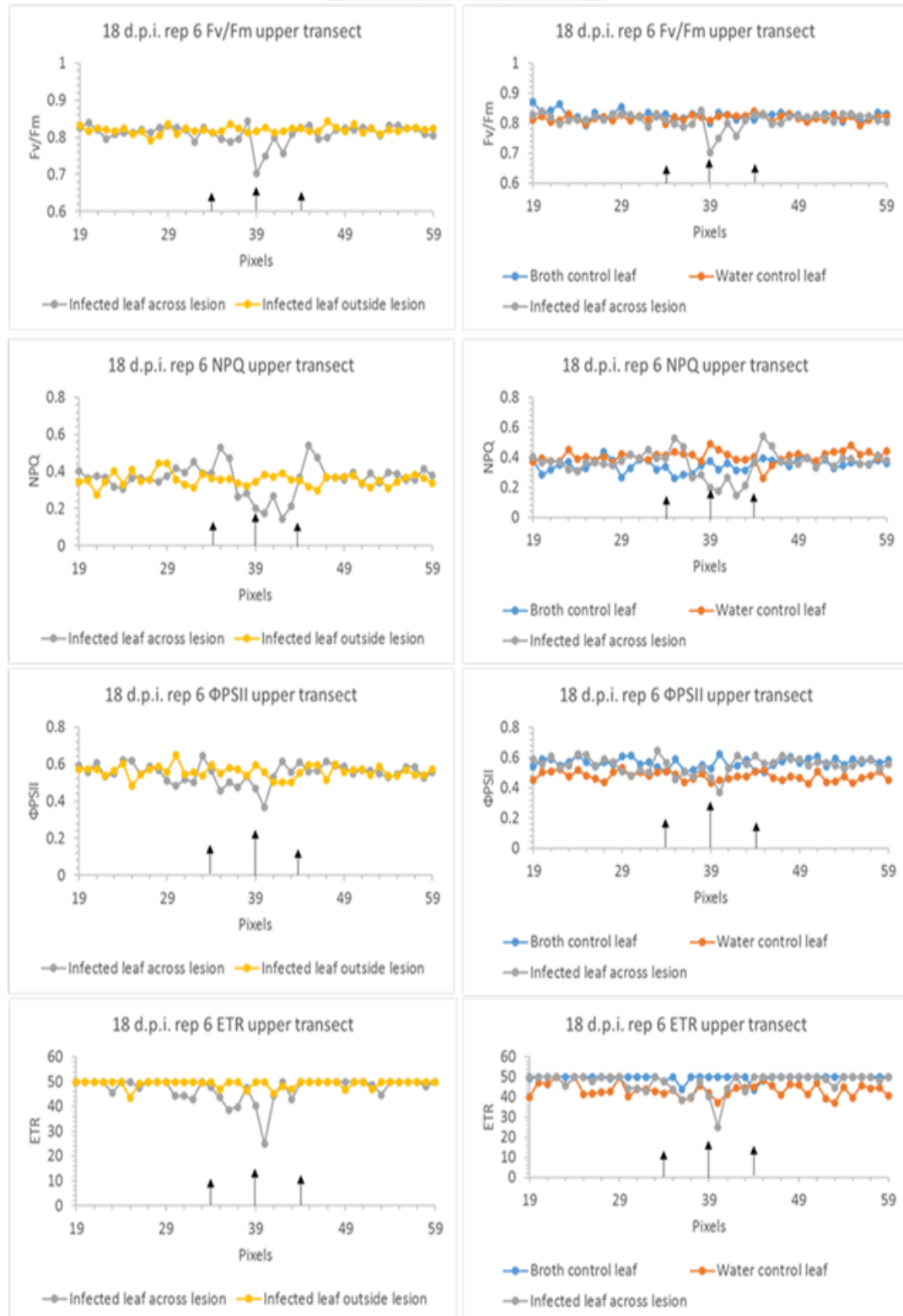
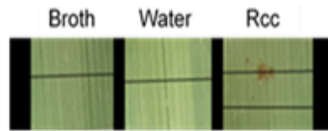


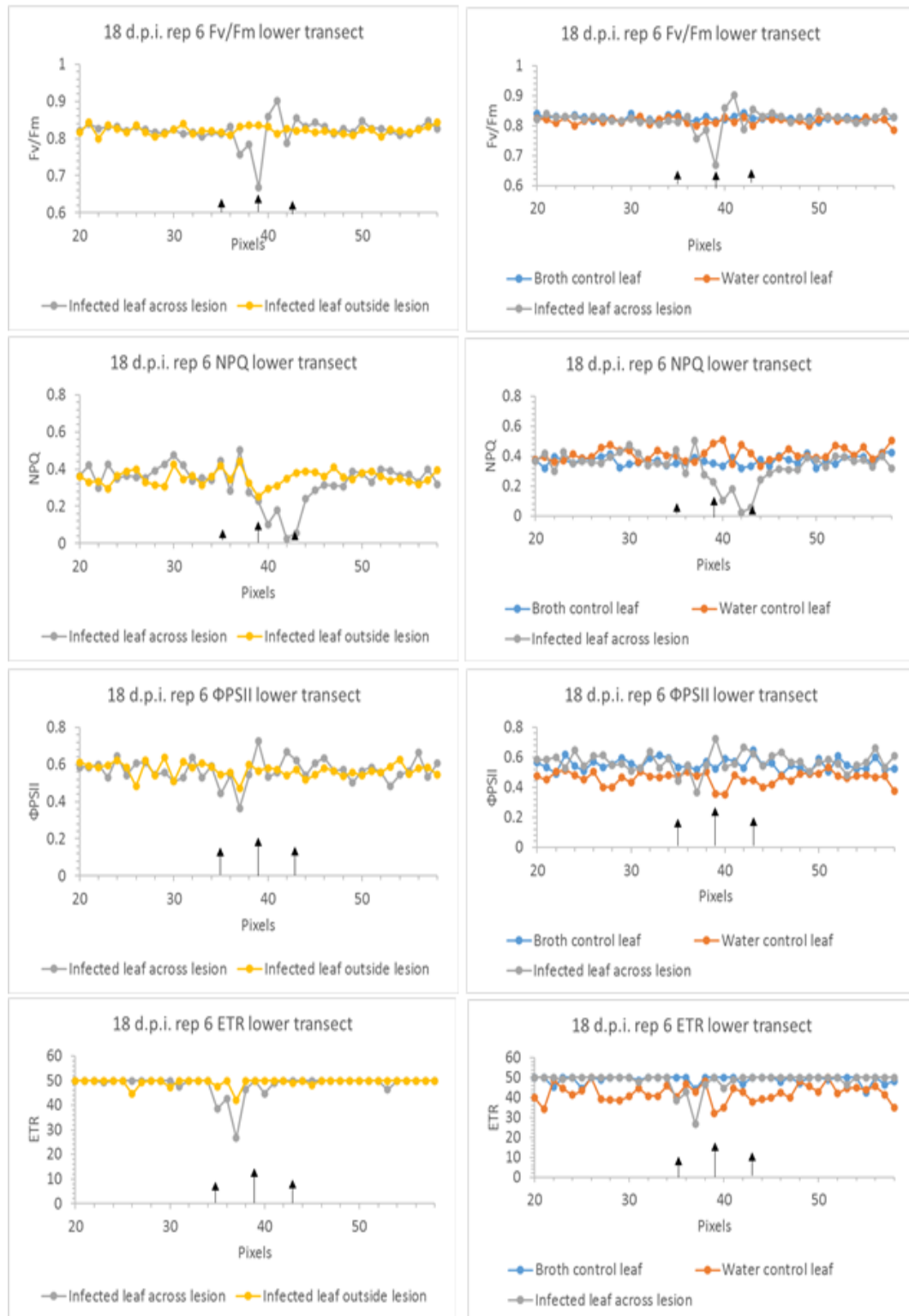
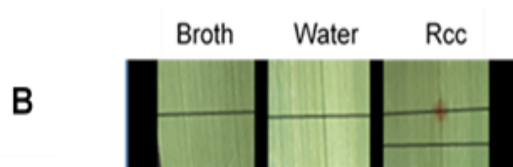
**A**



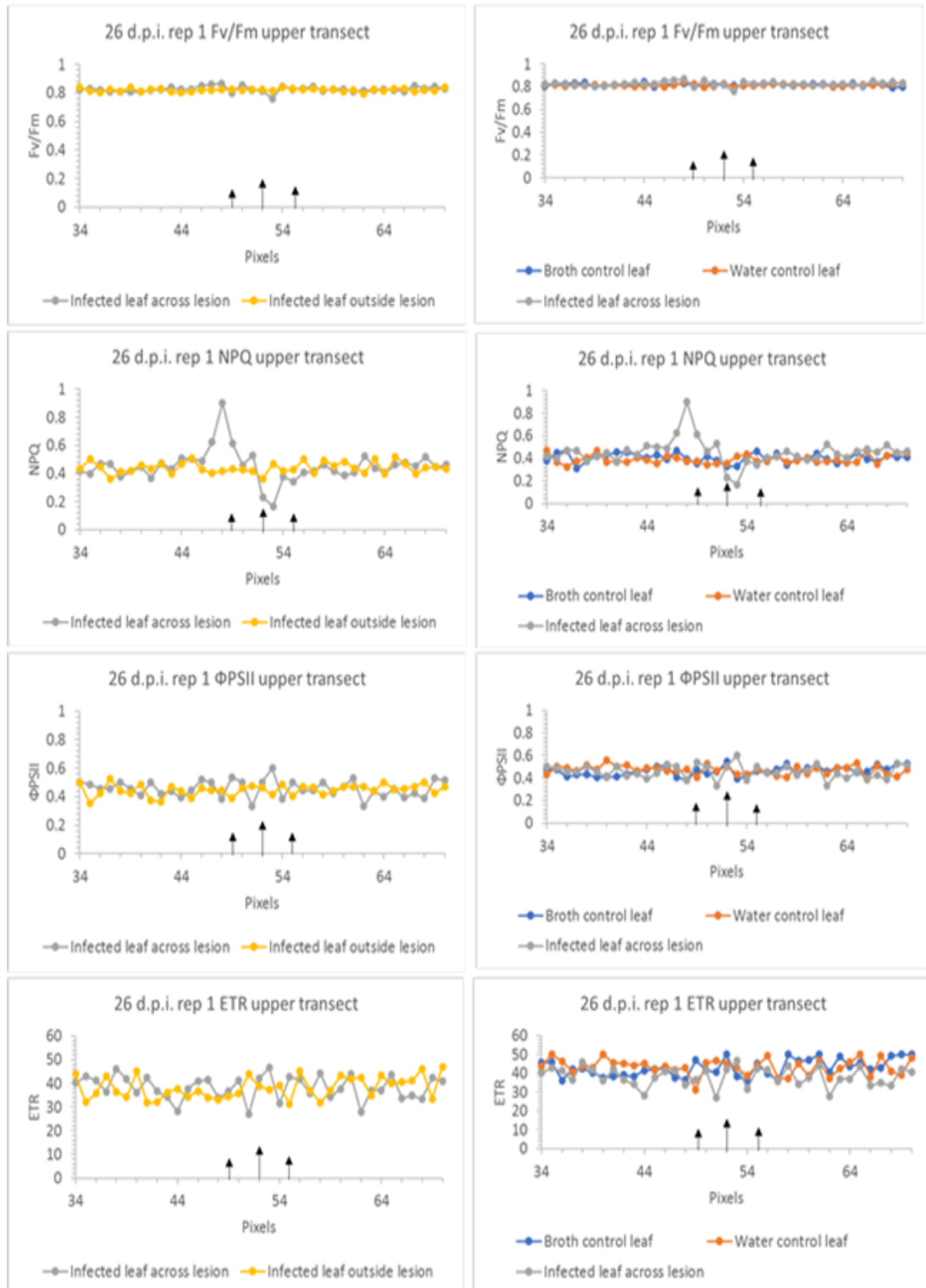
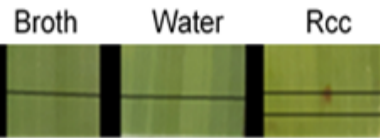




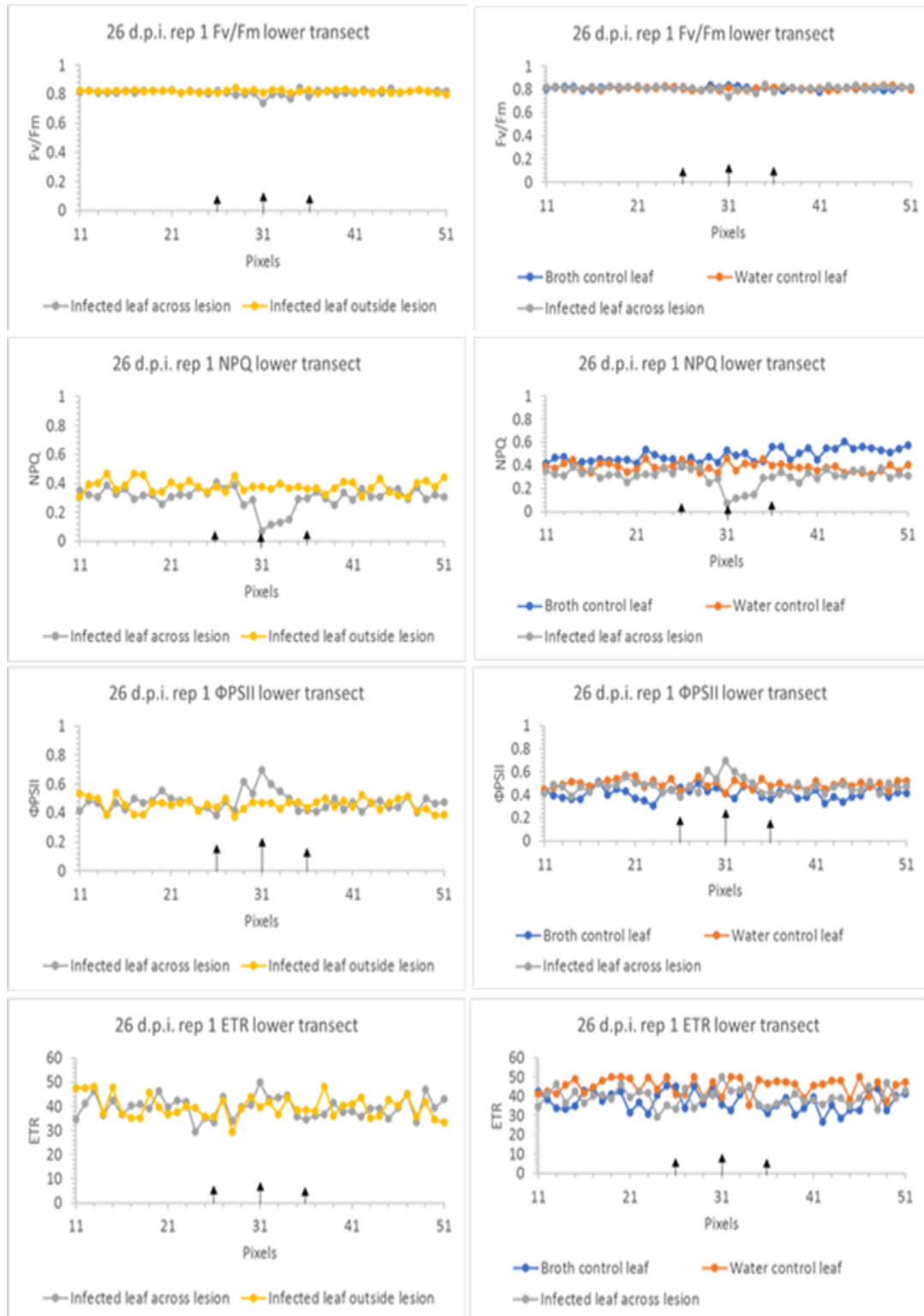
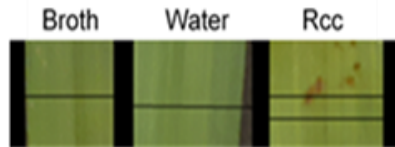
**B**

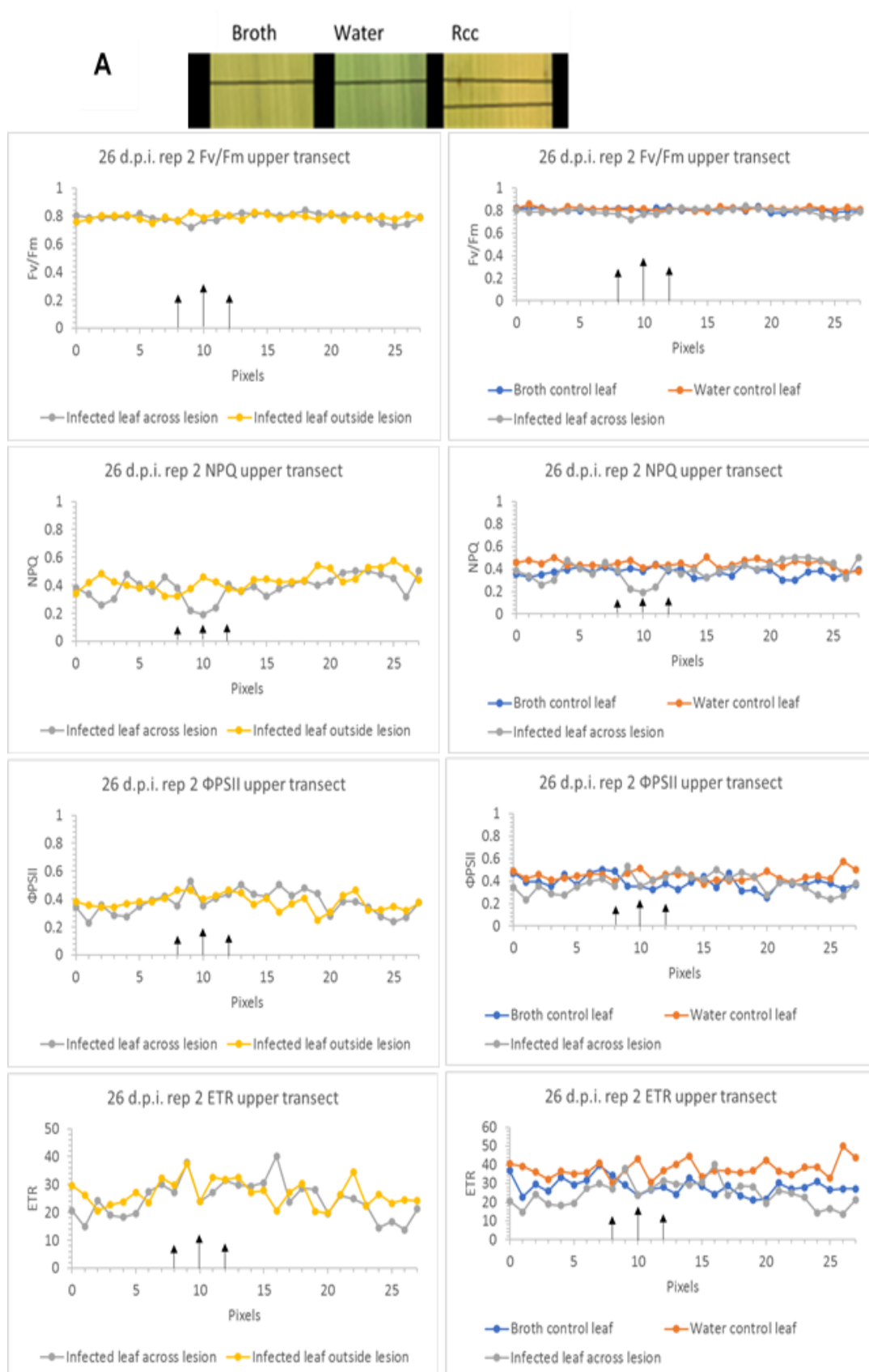


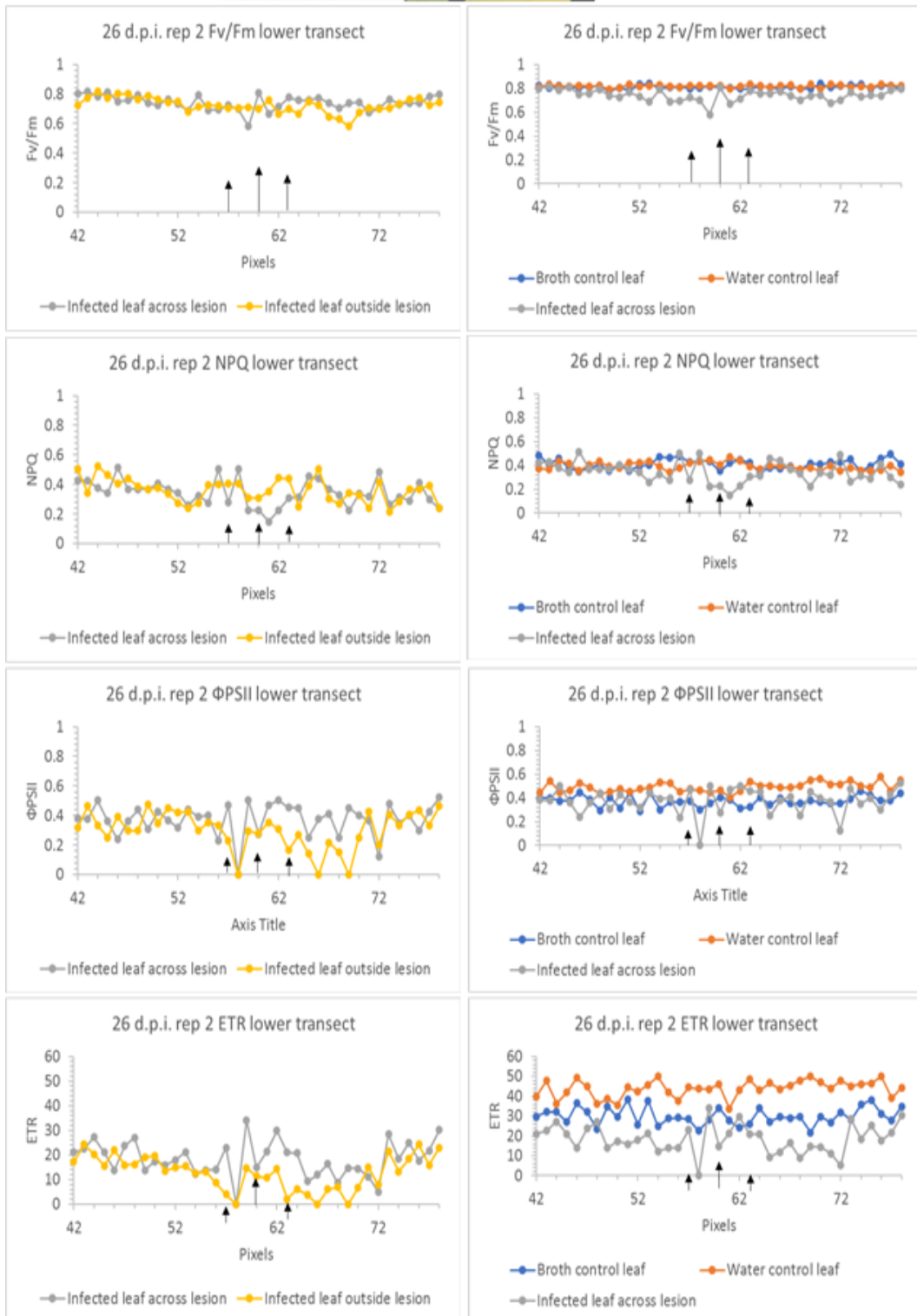
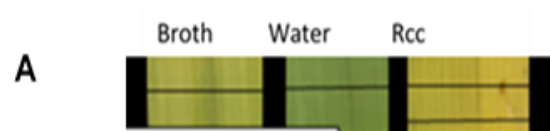
**B**



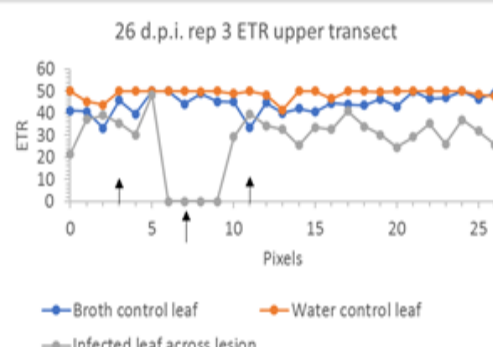
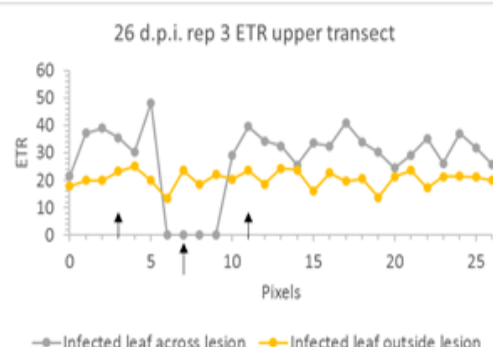
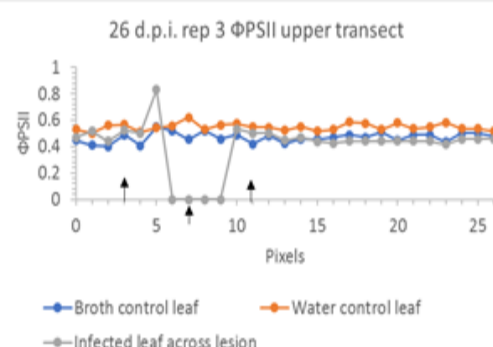
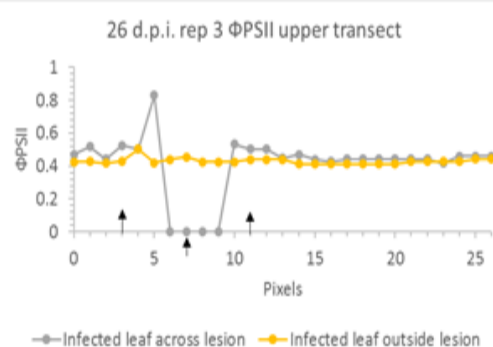
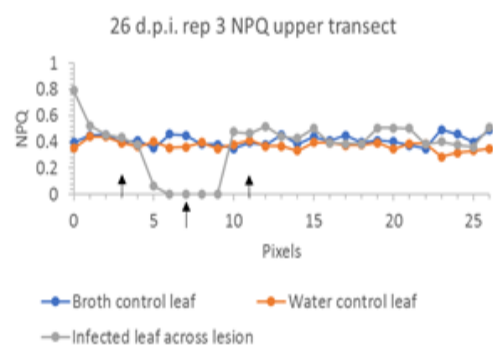
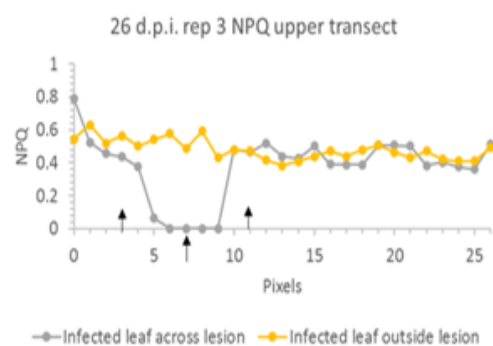
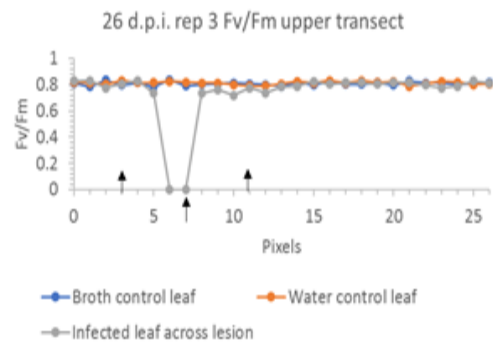
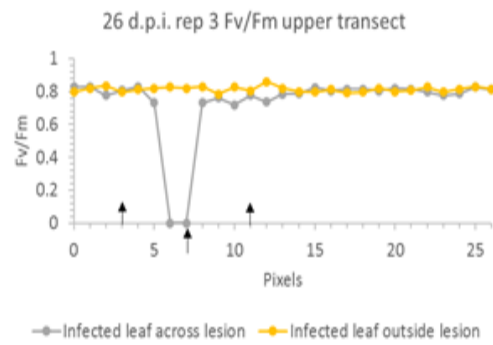
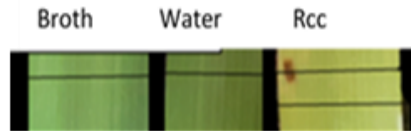
A

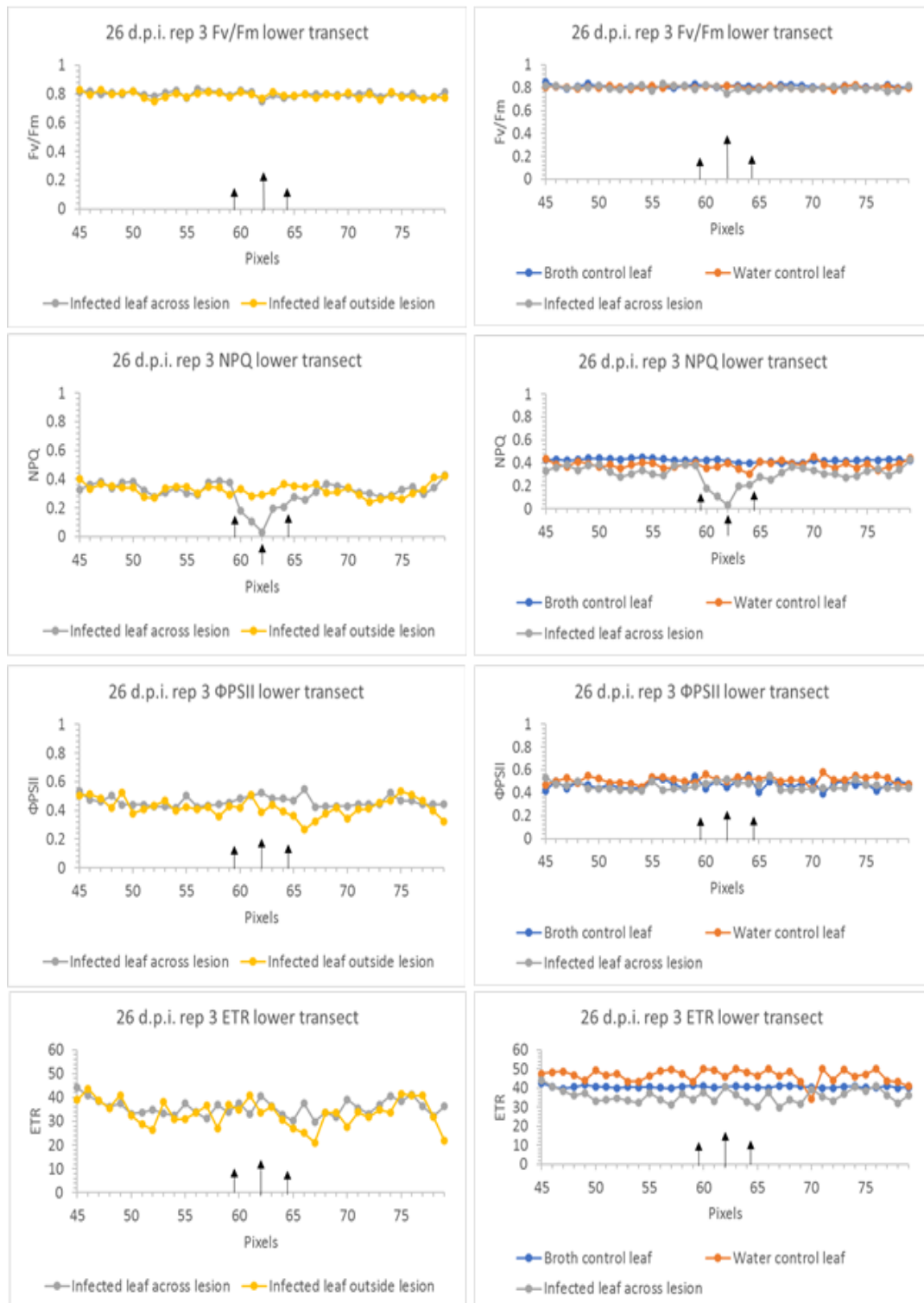
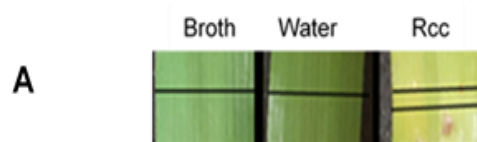


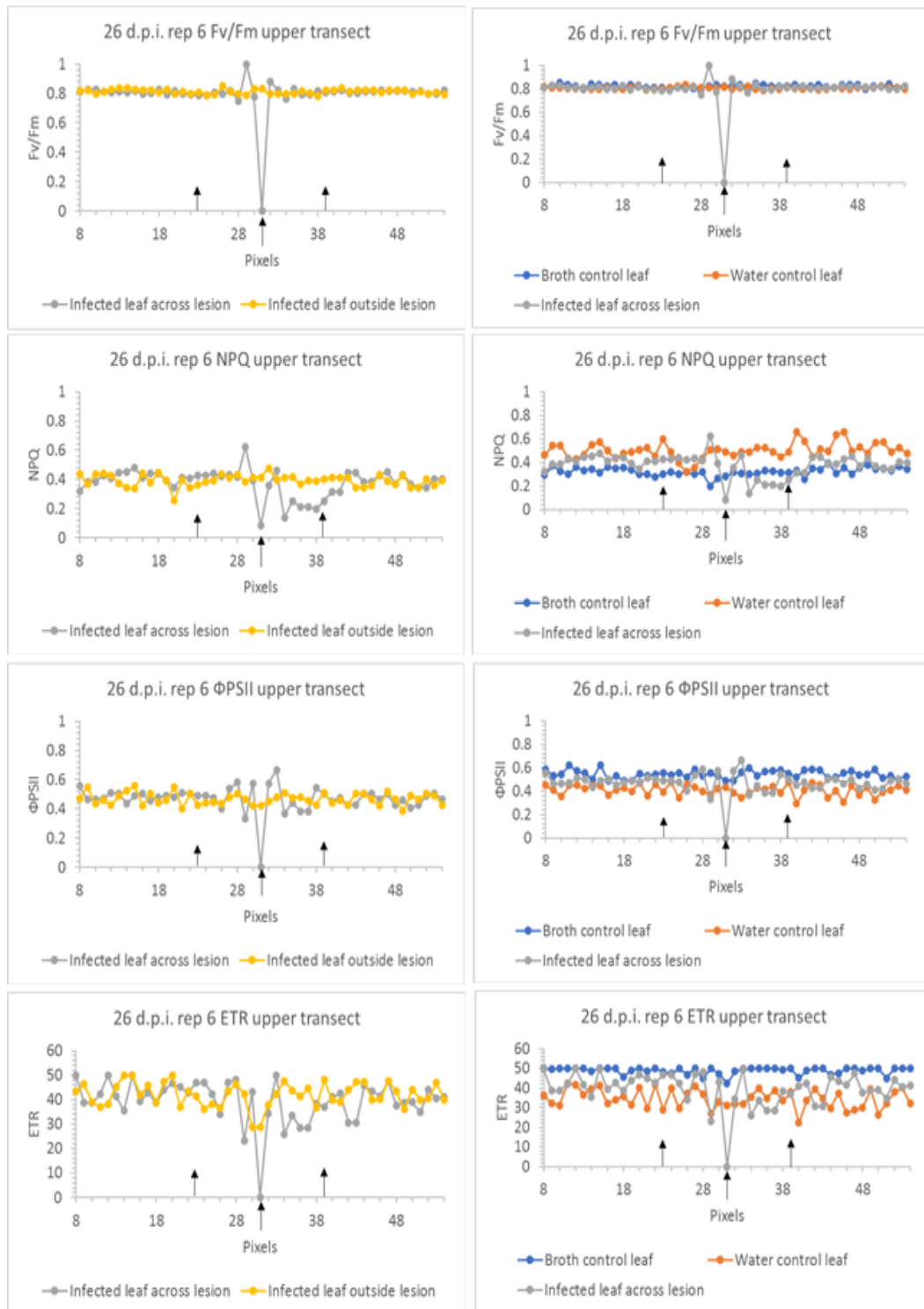
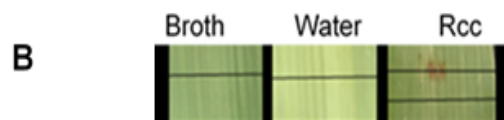




**B**







**B**

Broth      Water      Rcc

